INTERACTIONS OF CHLOROQUINE AND/OR ETHANOL ON RENAL MORPHOLOGY OF NORMAL OR LOW PROTEIN FED MALE SPRAGUE DAWLEY RATS

Abdurrahman Abdulkadir

Supervisor – Prof E.F Mbajiorgu

A Dissertation submitted to the Faculty of Health Sciences, University of the Witwatersrand, in fulfilment of the requirement for the degree of Master of Science in Medicine.

Johannesburg, 2018

Declaration

I Abdurrahman Abdulkadir declare that this Dissertation is my own, unaided work. It is being submitted for the degree of Master of Science in Medicine at the University of the Witwatersrand, Johannesburg. It is not been submitted before for any degree or examination at any other University.

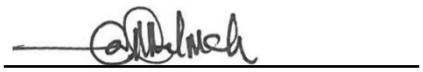

30th July 2018

For my Mother, Wife and Daughters

Hajiya Salamah

Aisha

Ramlah & Salamah-Ihsan

Presentations arising from the study

1. Volumetric analysis of kidney in protein-malnourished rats administered chloroquine and alcohol: a microfocus computed tomography and stereology study.

Abdurrahman Abdulkadir, Trust Nyirenda, EF Mbajiorgu

Oral presentation at the 3rd National Imaging with Radiation (Imgrad2017) Conference, Wits Education Campus, School of Public Health, University of the Witwatersrand, 14-15 September 2017.

2. Interaction of chloroquine and ethanol causes upregulation of AQP2 water channel and reduced urine output in protein malnourished rats.

Abdurrahman Abdulkadir, Trust Nyirenda, EF Mbajiorgu

Poster presented at the 8th cross-faculty postgraduate symposium of the University of the Witwatersrand, at the auditorium of School of Public Health, Wits University, 25-26 October 2017.

Publication arising from the study

1. Abdulkadir, A., Mbajiorgu, E. F. and Nyirenda, T. (2018). Effects of concurrent chloroquine and ethanol administration on the rat kidney morphology. *Pan Afr Med J*, 29(49). [doi:10.11604/pamj.2018.29.49.12471]

Abstract

The aim of this study was to investigate the renal morphometric and histopathological changes, arising from the hazard of concurrent administration of chloroquine and alcohol on a background protein malnourished state using rat as experimental animal model.

Sixty-four (64) rats were randomly distributed into eight groups of eight rats each as follows: control groups that received 0.9% saline and plain drinking water while on either normal or low protein diets (NPC, LPC). Chloroquine treatment groups while on either normal or low protein diets (NPQ, LPQ). Alcohol treatment groups while on either normal or low protein diets (NPE, LPE). Chloroquine and Alcohol treatment groups on normal or low protein diets (NPQE, LPQE). Chloroquine in 0.9% normal saline was administered once weekly to NPQ, LPQ, NPQE, and LPQE. While NPE, LPE, NPQE and LPQE received 6% ethanol in drinking water *ad libitum*. NPC and LPC received 0.9% normal saline and plain drinking water. After 8 weeks (60 days), the rats were terminated, kidneys were harvested and fixed for analyses. Routine H&E histology, Masson's trichrome for collagen, kidney volume estimation, relative medullary thickness measurements, renal cortical thickness measurements, microscopic morphometry, glomeruli count and immunofluorescence for aquaporin 2 (AQP2) were conducted. Urine volume estimation, serum urea and creatinine were also assessed.

The results showed a decreased mean body weight ($p=0.0001$), relative kidney weight ($p=0.0001$) and kidney volume ($p=0.0001$) in all low protein treated rats group compared to NPC and compared to their cohorts in normal protein group. The urine output decline with derangements of serum urea and creatinine in the low protein treated rats compared to NPC and compared to their cohorts in the normal protein group. There was upregulation of AQP2 water channel with increased collagen fibre deposition and distortion of normal renal histology in the experimental rat groups both within the normal protein and the low protein groups compared to NPC.

In conclusion, concurrent administration of chloroquine and alcohol causes distortion of kidney histology and derangements of renal function in low protein fed rats and has the potential to cause kidney failure.

Acknowledgements

All praises and thanks are due to Allah the sovereign creator of all life on lands and in the sea; it is with His infinite mercy that I was able to complete this work.

The boundless love, prayers and sacrifices of my mother, wife and daughters: Hajiya Salamah, Aisha, Ramlah and Salamah-Ihsan, is what kept me going on to accomplish this work.

Heartfelt salutation and appreciation to my humble supervisor, Prof Felix Mbajiorgu for sparing time to supervise, guide and support me in this endeavour.

All members of my family from the two houses of Dr Abdulkadir and Muhammad Lawal that helped me in any way with prayers, moral and financial support, I deeply appreciate all that you have done. I must mention Bashir, Mubarak, Sulaiman, Maryam, Dan Aba, Bilyaminu and A'I Benin, not that I forget the others; it is just that the list will go on forever.

I acknowledge Prof Kennedy Erlwanger, Mrs Hasiena Ali, and Mrs Alison Mortimer for unflinching support and never complaining. The most amazing CAS family never cease to surprise me with their ways of solving little and big problems, thank you for being there. I thank Federal University Birnin Kebbi for providing study sponsorship through TETFund, the Faculty of Health Sciences University of the Witwatersrand for research funding (MFREF) and School of Anatomical sciences for funding through Prof EF Mbajiorgu. I am overwhelmed by the generosity of Dr Tanya Augustine for allowing me to use the fluorescence microscope and words of encouragement. I also thank Mr Pilani Nkomozepi for all the guidance and support. Mr Kudakwashe Jakata you did save me a lot of stress with the µCT and VGStudio training, thank you. My colleagues Hassan, Nura, Trust and Lynette thank you for all your support. I will conclude with the Gentlemen and Ladies of the 'fishbowl' you have made the process worthwhile and I will never regret knowing you people in this life.

Table of contents

List of abbreviations

µA	Microampere
µm	Micrometre
µCT	Microfocus computed tomography
ABC	ATP-Binding cassette
ADH	Antidiuretic hormone
ALDH	Acetaldehyde dehydrogenase
AMPA	a-amino-3-hydroxy-5-methyl-4-isoxazole propionate
APC	Antigen-presenting cells
AQP2	Aquaporin 2
CE	Coefficient of error
CT	Cortical thickness
DAPI	Diamidino-2-phenylindole, dihydrochloride
FAS	Foetal alcohol syndrome
IM	Inner medulla
ISOM	Inner strip of outer medulla
LP	Low protein
LPC	Low protein control
LPE	Low protein with ethanol
LPQ	Low protein with chloroquine
LPQE	Low protein with chloroquine and ethanol
MMV	Medicine for malaria venture
MT	Medullary thickness
NMDA	N-methyl-D-aspartate
NP	Normal protein

NPC	Normal protein control
NPE	Normal protein with ethanol
NPQ	Normal protein with chloroquine
NPQE	Normal protein with chloroquine and ethanol
OSOM	Outer strip of outer medulla
PBS	Phosphate buffered saline
pH	Potential of hydrogen
RMT	Relative medullary thickness
SSF	Section sample fraction
SURS	Systematic uniform random sampling
TIF	Tagged image format
v/v	Volume per volume
vgi	Volume graphics image
VGStudio	Volume graphics studio
w/w	Weight per weight

List of figures

List of tables

1 CHAPTER ONE: INTRODUCTION

Malaria is a worldwide public health problem, especially in sub-Saharan Africa (Khosa et al., 2013; WHO, 2017). Recent world health organisation (WHO) report, showed 212 million new malaria cases and 429 000 deaths due to malaria globally. Africa has the highest malaria burden with 90% and 92% of malaria incidence and mortality respectively (WHO, 2017). Malaria is caused by *Plasmodium* species notably the *P. falciparum, P. ovale, P. malariae, P. vivax* (Rougemont et al., 2004) transmitted by a vector female *Anopheles gambiae* mosquito (CDC, 2015). The use of chloroquine in treatment and prophylaxis of malaria reduced the disease progression and decreased the global mortality (Wellems and Plowe, 2001). Malaria eradication with chloroquine was imminent until resistance to the drug spread from SouthEast Asia to different parts of the world in the late 1950s (Wellems and Plowe, 2001). The emergence of chloroquine-resistant malaria led to the development of artemisinin combination therapy for malaria treatment (Ashley et al., 2014). However, chloroquine was not completely replaced as an anti-malaria drug and was available in most part of Africa (Frosch et al., 2011), because of its affordability. Furthermore, re-emergence of chloroquine-sensitive malaria (Mwanza et al., 2017) and the emergence of artemisinin-resistant malaria in Asia (Ashley et al., 2014) and recently in Africa (Lu et al., 2017) rejuvenate chloroquine use as an antimalarial drug. Additionally, chloroquine is used on a long time basis in the treatment of rheumatoid arthritis and a host of many inflammatory diseases (Al-Bari, 2015) which may ultimately lead to cumulative renal toxicity as previously reported (Mũller-Hõcker et al., 2003; Albay et al., 2005). In most of the developing countries where malaria is endemic (figure 1.1), chloroquine is freely accessible across the counter without prescription and is abused (Oluleye et al., 2015) malaria endemic regions of the world.

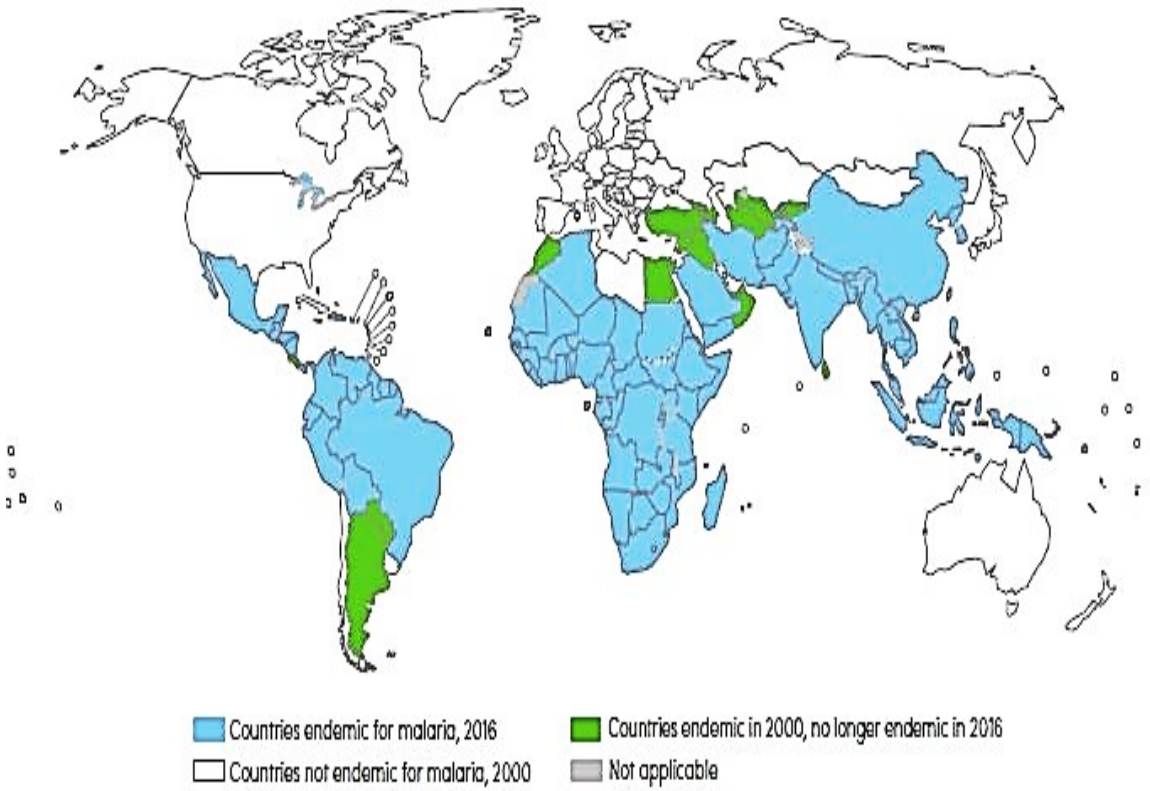

Figure 1.1: WHO world malaria map 2016

Source: World Malaria Report 2016 (WHO, 2017).

Alcohol consumption has been steadily on the increase in Africa (Pisa et al., 2010) especially in countries where malaria is endemic (figure 1.2). Commonly, people consume alcohol while on chloroquine treatment for malaria or rheumatoid arthritis without considering the health implication of such combination. In light of this problem, Musabayane et al. (2000a) reported on the physiological implications (renal toxicity) arising from the concomitant chronic administration of chloroquine and alcohol in rats without considering the protein intake and the possible effects of inadequate dietary protein intake on drug effects (Mbajiorgu et al.,2008)

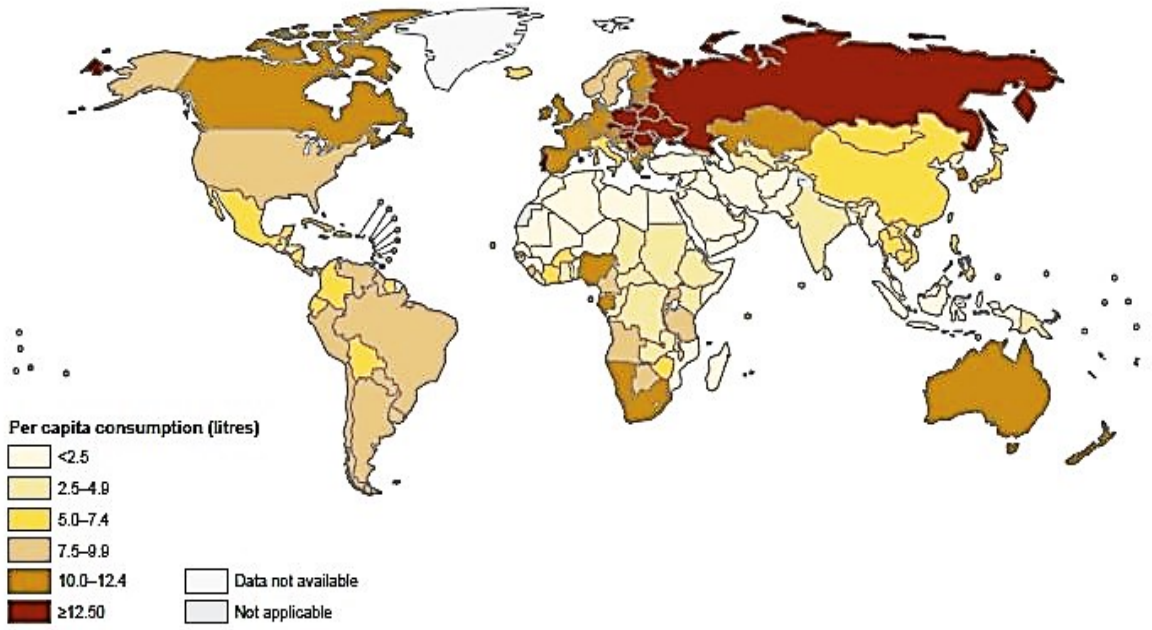

Figure 1.2: WHO Alcohol per capita consumption map 2010

Source: Global status report on alcohol and health 2014 (WHO, 2014).

Protein malnutrition is a condition in which the amount of protein required by the body for homeostatic processes is inadequate or poorly utilized (Dos Santos et al., 2017). It is a common form of malnutrition affecting millions of people in developing countries especially sub-Saharan Africa (Temba et al., 2016; Dos Santos et al., 2017). Protein malnutrition is worsened by insufficient food intake due to poverty,

inequity and illiteracy (Schönfeldt and Hall, 2012). The health implications of chloroquine and alcohol abuse under such prevailing poor nutritional status in these malaria endemic communities have not received much attention from researchers. Hence, the need for this study, which is to bring insight into the potential renal problem/injury that might be associated with the concomitant ingestion of chloroquine and alcohol on a background protein malnutrition, to help prevent the overwhelming increase of kidney failure in sub-Saharan Africa.

Renal disease is increasingly becoming one of the public health problems with a prevalence of 8-16% worldwide (Jha et al., 2013). Reports on the global burden of diseases show that chronic kidney disease cases increased by 48.1% from 1990 to 2013 (Glassock et al., 2017). Moreover, it is an increasing burden in most African countries especially sub-Saharan Africa (Naicker, 2013). However, lack of national and regional registries makes the statistics of kidney disease difficult in Africa and is highly under-reported (Naicker, 2013; Stanifer et al., 2014). Hypertension and glomerulonephritis are the commonest causes of chronic kidney disease in these regions (Naicker, 2013). One of the main features of chronic kidney disease is the fibrosis and organ shrinkage that develop regardless of the initial cause (Hewitson, 2012).

The function of the kidneys is central to the proper function of the body being responsible for the removal of waste products and excess fluids from the body through the production of urine and maintenance of a stable balance of body chemicals (Young et al., 2006). This involves complex steps of excretion and reabsorption, regulation of the body's salt, potassium and acid content and the production of hormones that affect the function of other organs (Young et al., 2006). Thus, the effects of the concurrent presence of chloroquine and alcohol in protein malnutrition, on the function of the kidney is critical to understanding the pattern of renal failure in Africa as disruption of these functions could lead to several homeostatic imbalance in the body.

The lack of quantitative data on the impact and/or interactive effects of combined administration of chloroquine and alcohol on renal morphology and function in the face of protein malnutrition necessitated this study, using the rat as a model.

1.1 Problem statement

The increased kidney failure in Africa in which, administration of chloroquine and alcohol have contributory role, is evident in the literature and can be worsen by protein malnutrition, another indigenous African problem, necessitated this study. The contribution of protein malnutrition (a common poverty related factor in Sub-Saharan Africa) has not been explored and may give more insight to the increased renal problems in these communities.

1.2 Broad Aim

To investigate renal morphological changes associated with the interaction of chloroquine and ethanol administration in low and normal protein diet.

1.3 Specific Objectives

- To examine the morphological changes (gross and microscopic) in the kidney of treated and control rats using morphometry techniques.
- To quantify kidney volume (absolute) changes in the treated rats and compare such with the controls using μCT scan, volume analysis and stereology.
- To determine the effects of the treatment on aquaporin 2 (AQP2) water channel in the kidney collecting ducts of the experimental rats using immunofluorescence technique.
- To measure 24 hours urinary output (urine volume) in experimental animals using a metabolic cage.
- To assess kidney function by determining the serum levels of urea and creatinine in the experimental animals.

1.4 Hypothesis

Concomitant administration of alcohol and chloroquine adversely affects renal morphology and function in protein malnourished male rats.

2 CHAPTER TWO: LITERATURE REVIEW

2.1 CHLOROQUINE

Chloroquine is a synthetic antimalarial drug used in the treatment and prophylaxis of malaria infection (Bijker et al., 2013), but also used in the treatment of other medical condition such as rheumatoid arthritis (Bhalekar et al., 2015) and systemic lupus erythematosus (Rainsford et al., 2015).

Hans Andersag, a German chemist working in Bayer pharmaceutical company, first synthesized chloroquine in 1934 (Krafts et al., 2012), and is characterized as 7-chloro-4(-4-diethylamino-1-methylbutylamino) quinolone ($C_{18}H_{26}ClN_3$) (figure 2.1) (Cooper and Magwere, 2008; Browning, 2014), derived from the bark of cinchona tree (Meshnick and Dobson, 2001). Chloroquine is colourless, bitter and soluble in both fat and water (Browning, 2014). Chloroquine is a weak base and dissolves more in acidic solutions than neutral and basic solutions (Cooper and Magwere, 2008). At a high pH > 7.0, chloroquine is monoprotonated and can cross the lipid bilayer of lysosomal food vacuole of cells after which chloroquine is biprotonated and trapped due to low pH <4.0 in the vacuole (Browning, 2014).

Chloroquine is administered orally, intramuscularly, subcutaneously (Cooper and Magwere, 2008), rectally (Minker and Ivan, 1990) and intraperitoneal (Farahna et al., 2010; Unekwuojo et al., 2011; Harhaji-Trajkovic et al., 2012). Chloroquine is rapidly and completely absorbed from the gut when taken orally and has a bioavailability of 75-80% (Browning, 2014). Chloroquine reaches peak plasma concentration within 1-2 hours (Augustijns and Verbeke, 1993; De Vries et al., 1994) and has a wide tissue distribution at a volume of 160-800 l/kg (Browning, 2014).

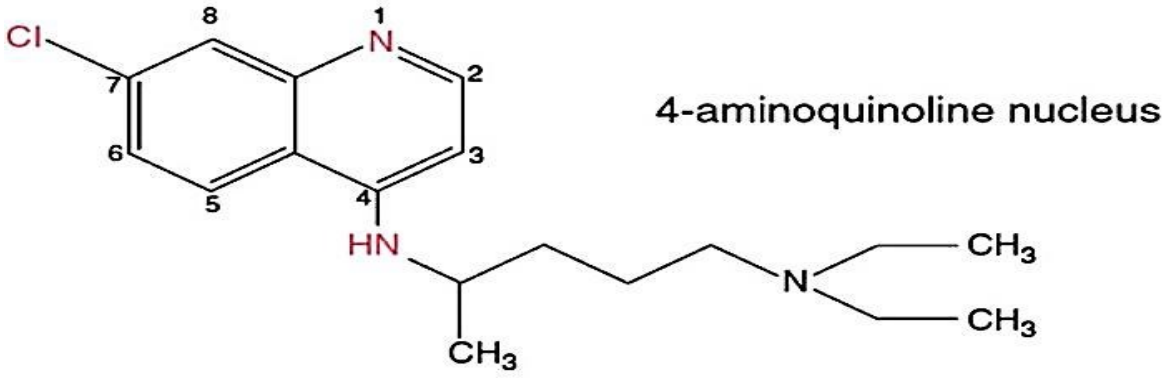

Figure 2.1: Chloroquine structure

Chloroquine structure with 4-aminoquinoline nucleus (Browning, 2014).

2.2 Antimalarial use of chloroquine

Over the years, malaria has an overwhelming effect on human lives and continues to be one of the most life-threatening transmittable disease. Malaria is mostly caused by *P. falciparum* and *P. vivax* with humans being the main hosts and is transmitted through the bite of infected female *Anopheles* mosquitoes during a blood meal to nourish its eggs (Webb, 2011).

Chloroquine has remained the most effective single anti-malaria drug for many decades and successfully used in malaria control programs worldwide (Wellems and Plowe, 2001). Until the emergence of chloroquine-resistant strains of malaria parasite in Southeast Asia and South America, malaria became widespread between 1958 through 1970 (Slater, 1993; Ridley, 1998; Trape, 2001; Wellems and Plowe, 2001). Consequently, combination therapies such as artemisinin-based combination therapies were developed to treat drug-resistant malaria parasites (Ashley et al., 2014). Other new combination therapies for the efficacious treatment of drug-resistant malaria parasites are in clinical development that could be used as single-dose regimens to ensure compliance (Phillips et al., 2017). Artemisinin became the first line antimalarial drug in 2005, and recorded great success in reducing mortality due to malaria infection, until artemisinin-resistance was reported in Asia and recently in Africa (Ashley et al., 2014; Lu et al., 2017).

Meanwhile, chloroquine re-emerged efficacy against malaria resistance parasite has also been reported in Malawi (Frosch et al., 2014), Ethiopia (Mekonnen et al., 2014), Zambia (Mwanza et al., 2016; Mwanza et al., 2017), Cameroon (Ndam et al., 2017) amongst others. The above suggest that chloroquine may remain the dependable drug of choice for malaria treatment for years to come. Hence, the need to study the toxicity of chloroquine in some organs such as renal system in the light of increasing renal diseases (Glasssock et al., 2017).

2.2.1 Life cycle of the malaria parasite

The malaria cycle begins with sporozoites release into human circulation during a blood meal, which rapidly enters the liver cells. In the liver, the sporozoites produce schizonts, which ruptures the infected hepatocyte and release merozoites. The merozoites immediately attack the red blood cells and replicate (Cowman et al., 2016). The merozoites are responsible for clinical symptoms and signs of malaria and are the target of chloroquine action (Ginsburg et al., 1998). Some of the merozoites differentiate into male and female gametocytes, which are taken up by the female *Anopheles* mosquito during a blood meal (MMV, 2010). In the mosquito, the gametocytes fuse to form a zygote, which in turn become ookinete. The ookinete migrates to the insect's mid-gut and transforms into oocyst, which finally become sporozoites and the cycle continue in human (MMV, 2010) (figure 2.2).

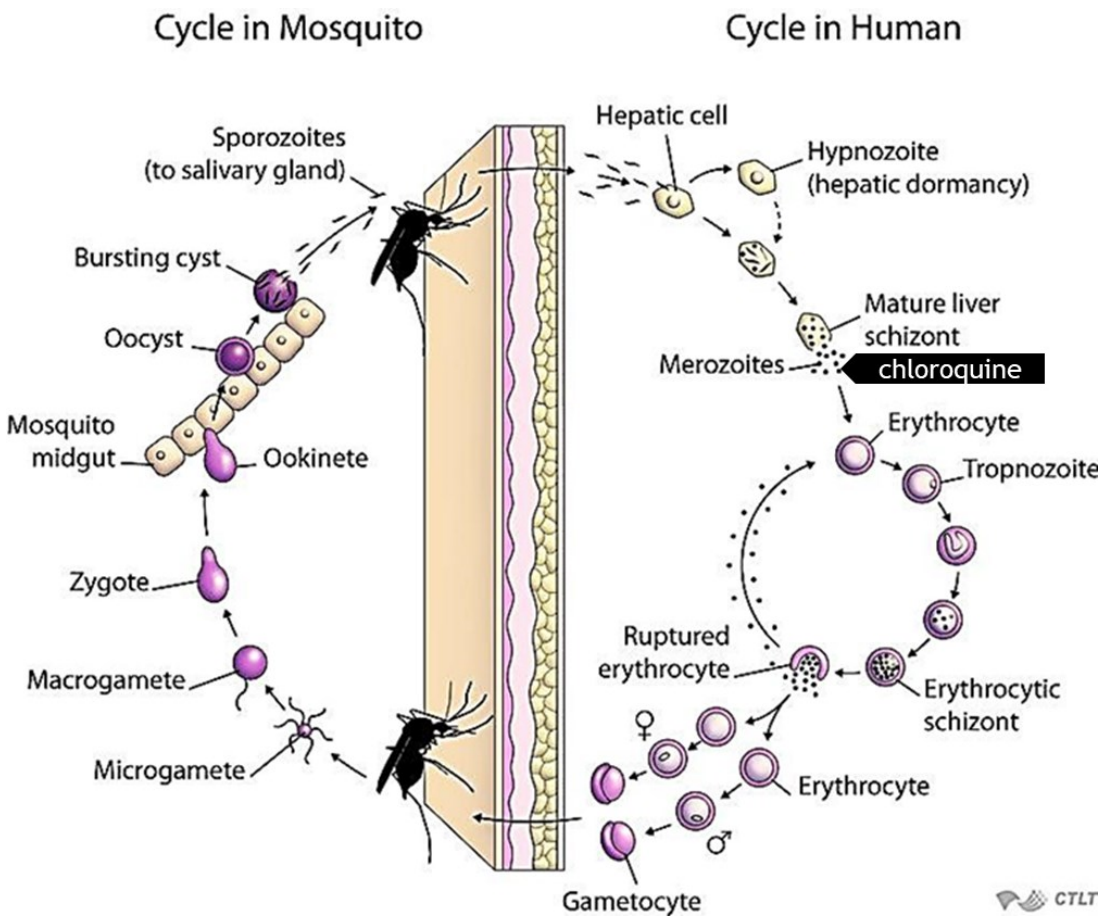

Figure 2.2: Life cycle of the malaria parasite

Source: "Lifecycle of the malaria parasite" from Epidemiology of Infectious Diseases. Available at: http://ocw.jhsph.edu. (Date accessed 16/02/2018).

2.2.2 Mechanism of Chloroquine action in malaria

Chloroquine is able to accumulate in the lysosomal food vacuole of the malaria parasite and inhibit the activity of heme polymerase (figure 2.2), which leads to accumulation of heme to toxic levels within the parasite (Slater, 1993; Foley and Tilley, 1997). Heme polymerase is an enzyme specific to the malaria parasite, which polymerises heme to haemozoin, a detoxified insoluble heme crystal (Sullivan, 2002). Understanding of the enzyme heme polymerase will provide prospects to develop newer drugs targeting the inhibition of heme polymerase (Sullivan, 2002; Olafson et al., 2015).

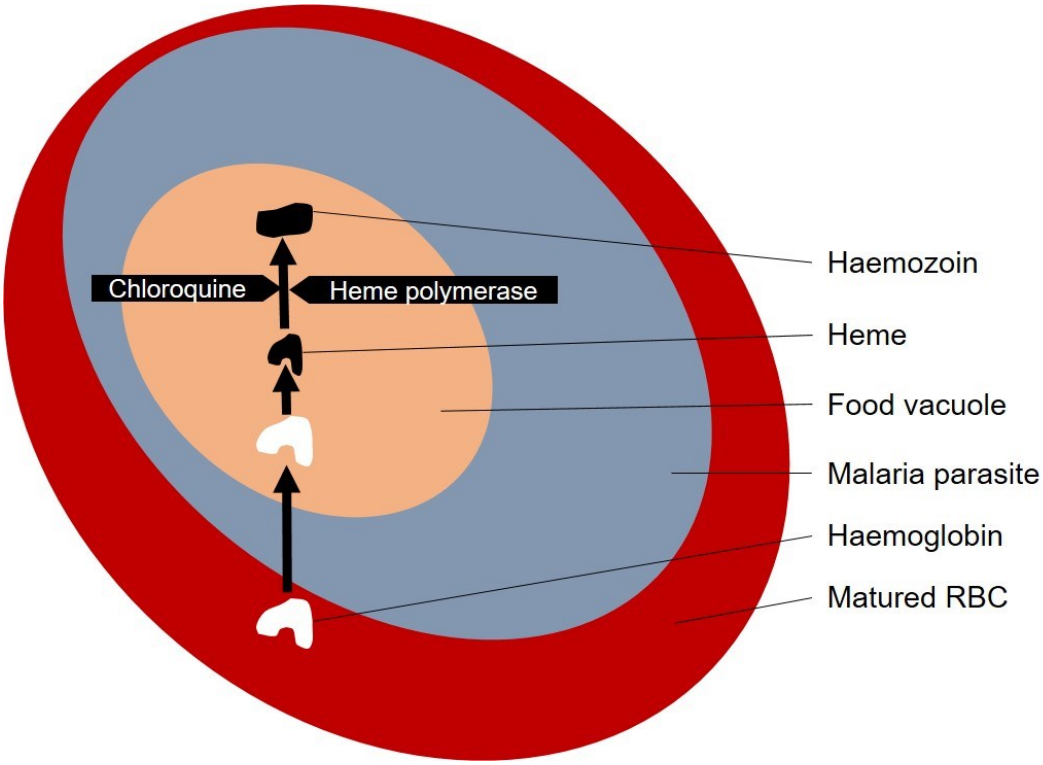

Figure 2.3: Mechanism of chloroquine action in malaria

Diagram of chloroquine action, inhibiting heme polymerase in the malaria parasite food vacuole. Key: RBC – red blood cell.

2.3 Other uses of chloroquine

Apart from the anti-malaria use of chloroquine, the drug is also used in other disease conditions such as rheumatoid arthritis, systemic lupus erythematosus, chronic ulcerative stomatitis, viral diseases and cancer chemotherapy amongst others (Al-Bari, 2015). In these conditions, chloroquine accumulates in the lysosomal food vacuole of cells and brings about its effects through an entirely different mode of action.

In inflammatory conditions, for example ulcerative stomatitis, because chloroquine is a weak base, it has a high affinity for the lysosome acidic environment (Wallace et al., 2012). Accumulation of chloroquine in the T-lymphocyte decreases the acidity of the lysosomes, which affects degradation of endocytosed materials and the function of the antigen presenting cells (APCs) (Wallace et al., 2012). These mechanisms lead to an impaired immune response, which includes but not limited to inhibition of

antigen presentation and production of cytokines IL-1, IL-6 and TNF (Wallace et al., 2012). Although these mechanisms contribute to the anti-inflammatory effect of chloroquine, the understanding of the mechanism continues to evolve to date (Wallace et al., 2012).

Furthermore, the lysosomal actions of chloroquine changes the pH from acidic to basic in viruses target cells, thereby interrupting virus entry into the cell and consequently the replication cycle (Savarino et al., 2003). Some viruses require a pH-dependant step to enter a cell while others require a pH-dependant step for post-translational modification (Savarino et al., 2003). Most viruses are attracted to the lysosome acidic environment for continued replication, interfering with the process inhibits the virus replication cycle. Some of the virus reported to be affected by chloroquine include Flaviviridae virus family including Zika virus (Shiryaev et al., 2017), Borna virus, hepatitis A virus and HIV-1 (Savarino et al., 2003). In the case of HIV-1, viral load was reported to be lower when lamivudine and hydroxyurea were given in combination with chloroquine than when lamivudine and hydroxyurea were given alone (Savarino et al., 2006).

Also, in cancer chemotherapy and/or radiotherapy, accumulation of chloroquine in the cancer cell lysosome, alters the lysosomal pH and increase the lysosome membrane permeability. This will lead to release of proteolytic enzymes into the cell, which damages the intracellular proteins including the membrane repair proteins. Chloroquine also blocks the action ATP-binding cassette (ABC) transmembrane proteins family, which are believed to contribute to multidrug resistance in cancer by expelling the chemotherapeutic drugs (Al-Bari, 2015). These mechanisms of chloroquine make the target cancer cell more susceptible to chemotherapy and radiotherapy.

2.4 Chloroquine metabolism and excretion

Chloroquine is metabolised in the liver by oxidative deamination, N-oxidation and the removal of the side chain from the rings (Houzé et al., 1992) (figure 2.4). The specific cytochrome P450 enzymes involved in chloroquine metabolism are CYP3A, CYP2C8

and CYP2D6 isoforms (Ducharme and Farinotti, 1996; Projean et al., 2003). The enzyme CYP3A has extrahepatic distribution and contribute to the extrahepatic metabolism of chloroquine (Cooper and Magwere, 2008). Chloroquine is metabolised to active molecules desethylchloroquine and bis-desethylchloroquine, which are subsequently eliminated (Ducharme and Farinotti, 1996). The elimination half-life of chloroquine is 20-60 days in human (Ducharme and Farinotti, 1996; Krishna and White, 1996). However, chloroquine has been detected in human urine about 120 days after a single dose of 300mg (Gustafsson et al., 1983). More than 60% of chloroquine is excreted via the kidney (Kalia and Dutz, 2007), with about 70% of the urinary chloroquine unmetabolised (Mackenzie, 1983). Other routes of excretion are through faeces (8-25%), and skin (Mackenzie, 1983), while more than 30% is deposited in the tissues (Titus, 1989).

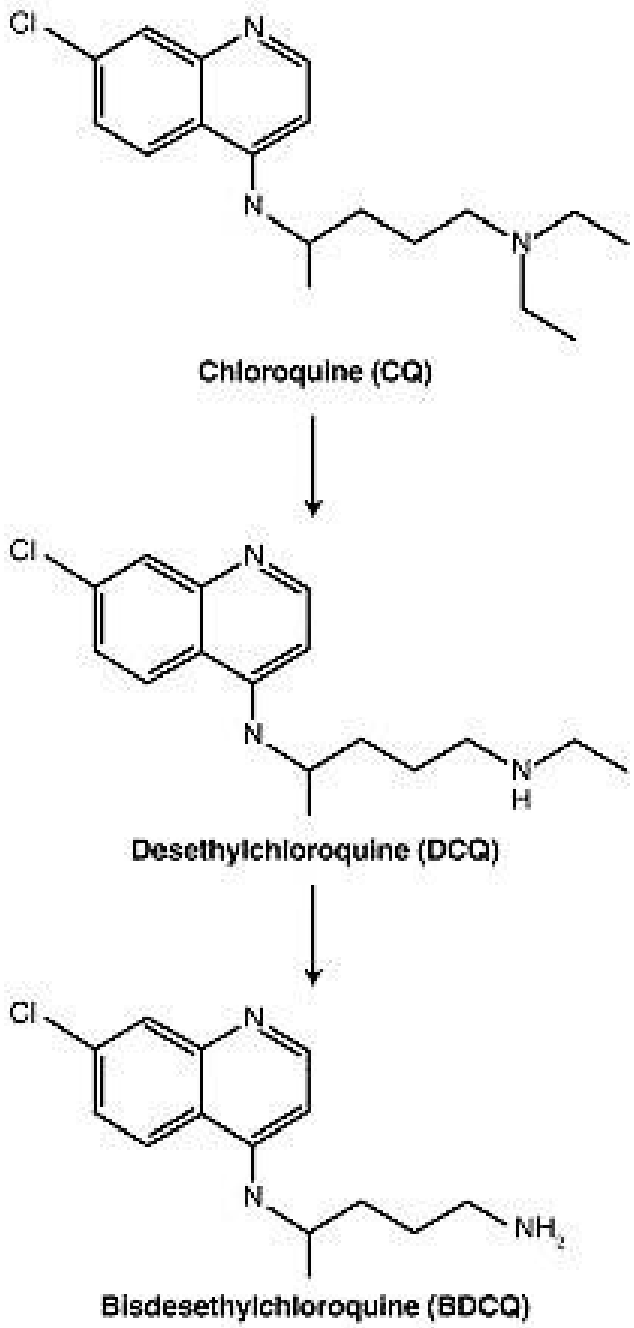

Figure 2.4: Metabolism of chloroquine

Metabolism of chloroquine by removal of the side chain, DCQ and BDCQ are subsequently eliminated (Browning, 2014).

2.5 Toxicity and Side effects of chloroquine

Chloroquine use is associated with certain minor side effects, which include pruritus, nausea, vomiting, buccal mucosa ulceration (Al-Bari, 2015) and soft tissue abscess

from an intramuscular injection (Adam and Elbashir, 2004). However, major organ toxicities of chloroquine arise because of prolonged usage/abuse of the drug due to unregulated use (Oluleye et al., 2015). The reported toxicity includes retinopathy (Oluleye et al., 2015), hepatotoxicity (Kumar Mishra et al., 2013), cardiotoxicity (Tönnesmann et al., 2013) and nephrotoxicity (Albay et al., 2005).

In the kidney, which is the organ of concern in this study, evidence suggestes chloroquine toxicity in both human and rats (Musabayane et al., 2000b; Albay et al., 2005). A previous report have shown that patients on chloroquine therapy for rheumatoid arthritis were disposed to renal problems (Albay et al., 2005). The reported renal chloroquine toxicities include glomerular and tubular cells vacuolation, cellular inclusions, mild tubular atrophy, interstitial fibrosis proteinuria, increased serum blood urea nitrogen and creatinine and increased glomerular filtration rate resulting from chronic chloroquine administration (Mũller-Hõcker et al., 2003; Albay et al., 2005). Furthermore, animal (rats) experiments reports increased sodium excretion, urine flow rate and glomerular filtration rate following chloroquine administration (Musabayane et al., 2000a; Ahmed et al., 2003). Chloroquine is a nitric oxide stimulator, which mediates some of its renal actions (Ahmed et al., 2003). Some of the morphological changes caused by chloroquine administration in rats include renal tubular cells degeneration and vacuolation, luminal debris, inflammation and glomerular atrophy (Musabayane et al., 2000b; El Shishtawy et al., 2015).

2.6 ALCOHOL

Alcohol (i.e., ethanol, figure 2.5) also is one of the social drugs, which has been in existence and used widely in ceremonies since the ancient times (Gately, 2008).

Figure 2.5: Chemical structure of ethanol

In modern times, both men and women of all ages commonly abuse alcohol as suggested by the amount of alcohol consumption reported by WHO (2014). The world average of total adult per capita consumption is 6.31 litres of pure alcohol while African average stands at 6.15 litres (WHO, 2014; Ferreira-Borges et al., 2015). The total adult per capita alcohol consumption is the litres of pure alcohol consumed by an adult (15 years and above) in a given population (WHO, 2014; Ferreira-Borges et al., 2015).

Moderate alcohol consumption boost self-confidence, sociability, produce euphoria and reduce anxiety (Eckardt et al., 1998). In excess, alcohol causes lethargy, sedation, impaired judgement, blurred vision and even unconsciousness and death (Mukherjee, 2013). Hence, Long-term excessive consumption of alcohol leads to alcohol dependence (Hingson et al., 2006). Alcohol dependence also called alcoholism can lead to serious physiological problem in the brain such as shrinkage of striatum, amygdala and hippocampus, which are connected to memory problems. In addition, psychological conditions such as depression and schizophrenia are also associated with alcoholism (Pinheiro et al., 2015). Other problems of alcoholism include impairment of motor function, decreased absorption of essential vitamins and nutritional deficiencies such as thiamine deficiency, which is associated with cognitive dysfunction (Rundio, 2013).

2.7 Mechanism of action of alcohol

Alcohol is primarily a central nervous system (CNS) depressant through its action on several central nervous system neurotransmitters (Costardi et al., 2015). Alcohol stimulates gamma-aminobutyric acid (GABA), which is the main CNS inhibitory neurotransmitter via $GABA_A$ receptor and causes sedation, loss of inhibition and relaxation (Costardi et al., 2015). Other neurotransmitters stimulated by alcohol are dopamine and serotonin, which cause a feeling of well-being, mood elevation, pleasure and satisfaction (Costardi et al., 2015). Furthermore, alcohol inhibits glutamate, which is the main excitatory neurotransmitter of the CNS via its receptors a-amino-3-hydroxy-5-methyl-4-isoxazole propionate (AMPA) and N-methyl-D-aspartate (NMDA); and cause reduced cognitive function, attention deficit, and

impaired sleep-wake regulation (Costardi et al., 2015). Others include endocannabinoid pathway inhibition leading to motor incoordination and difficulty in logical reasoning (Costardi et al., 2015). Alcohol also inhibits Mitogen-Activated Protein Kinases (MAPK) involved with explicit memory, leading to loss of the function and it inhibits the cerebellum calcium channels leading to unsteady gait and loss of spatial orientation (Costardi et al., 2015).

2.8 Metabolism and excretion of alcohol

Alcohol metabolism is achieved via oxidative and non-oxidative pathways (Pisa et al., 2010). The oxidative pathways are the enzymes system in the hepatocytes and the first-pass metabolism. The non-oxidative pathway is the production of fatty acids from alcohol in the absence of oxygen (Pisa et al., 2010).

2.8.1 Oxidative metabolism of alcohol

The oxidative metabolism of alcohol involves the addition of oxygen or removal of hydrogen from alcohol involving an intermediate electron carrier nicotinamide adenine dinucleotide (NAD). These processes deplete liver oxygen leading to hypoxia and leaving the hepatocytes vulnerable to injury (Pisa et al., 2010).

The first-pass metabolism is the oxidation of alcohol involving the gastric alcohol dehydrogenase situated in the gastric mucosa, however, some researchers also demonstrated first pass metabolism occurring in the liver (Zakhari, 2006; Pisa et al., 2010). The significance of the first-pass metabolism is the reduction of unmetabolised alcohol reaching systemic circulation.

The hepatocyte oxidative systems are the alcohol dehydrogenase and CYP2E1 located in the cytosol, the microsomal ethanol oxidising system (MEOS) located in the endoplasmic reticulum and the catalases located in the peroxisomes (Pisa et al., 2010). All the oxidative pathways produce acetaldehyde (Pisa et al., 2010), which is a highly reactive and toxic product quickly oxidised by the acetaldehyde dehydrogenase (ALDH) to acetate in the hepatocyte mitochondria. The acetate

produced is further oxidised in the peripheral tissues to produce water, fatty acids and carbon dioxide (Pisa et al., 2010). Furthermore, the liver metabolises only a certain amount of alcohol at a time and excess unmetabolised alcohol reached the lungs through the systemic circulation, at this point alcohol breath can be tested in heavy drinkers (Hlastala, 1998).

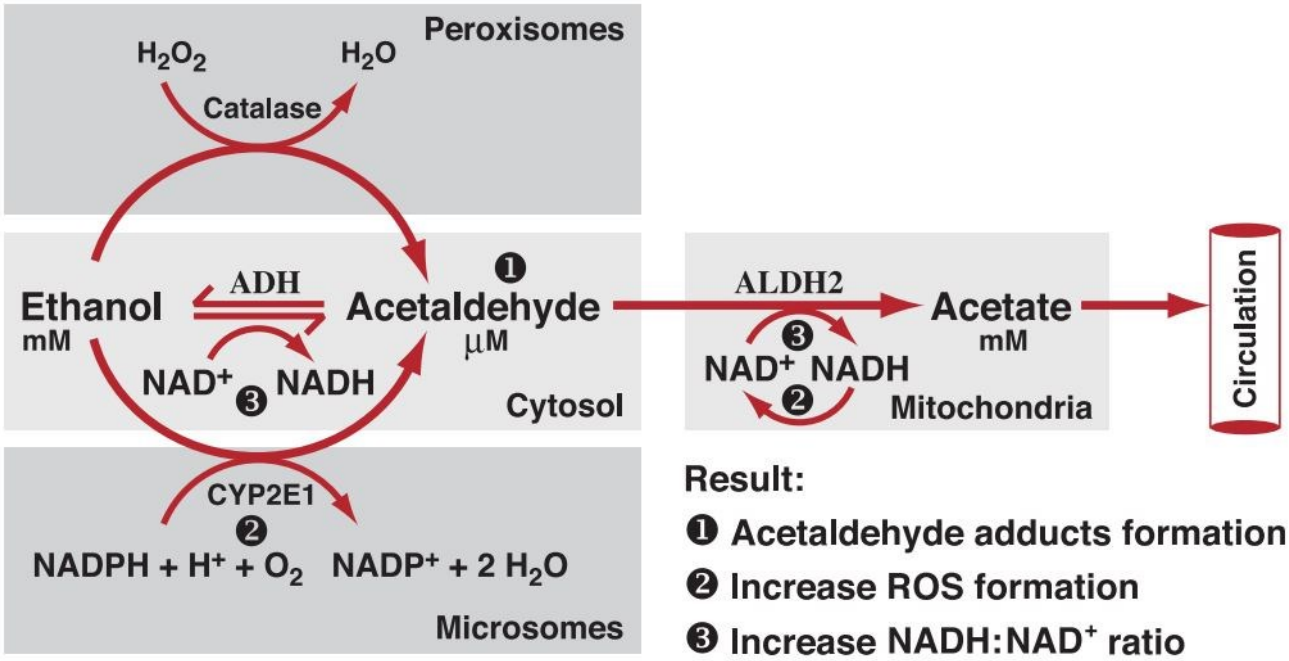

Figure 2.6: Oxidative metabolism of alcohol

ADH-alcohol dehydrogenase, $ALDH_2$-acetaldehyde dehydrogenase, H_2O-water, H_2O_2-hydrogen peroxide, MEOS-microsomal ethanol oxidizing system, NAD-nicotinamide adenine dinucleotide, NADH-reduced nicotinamide adenine dinucleotide, NADP-nicotinamide adenine dinucleotide phosphate, NADPH-reduced nicotinamide adenine dinucleotide phosphate, H-hydrogen, O_2-oxygen, ROS-reactive oxygen species (Zakhari, 2006).

2.8.2 Non-oxidative metabolism of alcohol

The non-oxidative metabolism of alcohol follows two main pathways (figure 2.4). The first pathway occurs because of the reaction between an alcohol molecule and fatty acids leading to the production of fatty acid ethyl esters (FAEEs). These by-products have pathological and diagnostic value because FAEEs can be detected in serum and tissues long after alcohol has been eliminated from the body (Zakhari, 2006;

Pisa et al., 2010). The second pathway requires phospholipase D (PLD), an enzyme responsible for the breakdown of phospholipids to produce phosphatidic acid (Zakhari, 2006). Phosphatidic acid is vital to cellular communications. At a high level of circulating alcohol, PLD has a high affinity for alcohol leading to the production of phosphatidyl ethanol (Zakhari, 2006). Although the effects of this by-product are yet to be established, the reaction occurs at the expense of phosphatidic acid leading to inhibition of its production and disruption of cell signalling pathways (Zakhari, 2006).

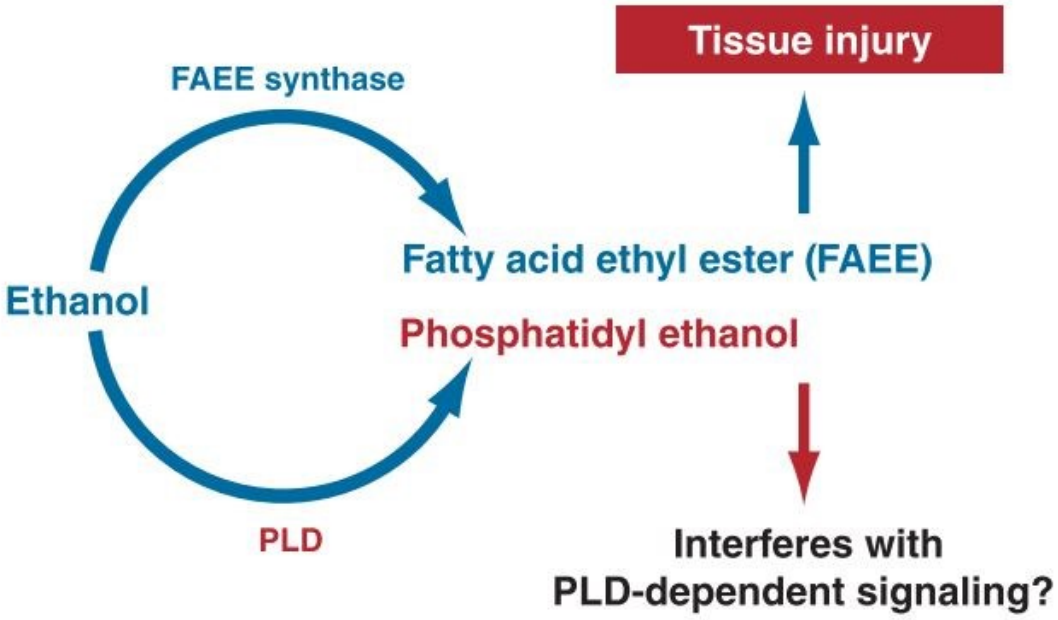

Figure 2.7: Non-oxidative metabolism of alcohol

The non-oxidative metabolism of alcohol occur in two pathways depicted above. PLD-phospholipase D. (Zakhari, 2006).

2.8.3 Alcohol excretion

Alcohol is completely oxidised to water and carbon dioxide, some amount is exhaled through lungs unchanged and very minute quantity in the urine and sweat (Ramchandani et al., 2001; Pisa et al., 2010).

2.9 Health effects of alcohol

The number of deaths associated with alcohol consumption reported in 2012 was about 3.3 million, which translates to 5.9% of all global mortality (WHO, 2014). This alcohol-attributable mortality is due to alcohol-induced chronic diseases and neuropsychiatric disorders in about 58.3% of the cases, while about 41.6% are due to injuries (both intended and unintended) (WHO, 2014).

At safe limits (24 standard alcohol drink per week for men and 16 drinks for women) of alcohol intake (Niemelä et al., 2017), alcohol generates production of high-density lipoprotein cholesterol, improve endothelial function and reduce inflammation in the blood. These benefits of alcohol reduces the risk of heart attack, stroke and emboli formation (O'keefe et al., 2014). However, chronic excessive ingestion can cause cardiomegaly, cardiac arrhythmias, cardiomyopathy and even cardiac death (Spies et al., 2001).

Excessive alcohol consumption causes hepatitis, fatty liver and cirrhosis, which can lead to hepatocellular carcinoma (Kirpich et al., 2016). This is because excess alcohol is metabolised by CYP2E1, which generates oxidative stress and disrupt hepatocyte function (Seki, 2016).

In the brain, excessive alcohol consumption is associated with brain atrophy, impairment of cognitive and memory capabilities. Some of these associated neurocognitive problems of alcohol can be reversed with prolonged abstinence. The reversal depends on the demographic and genetic factors, alcohol use pattern and nutritional status (Oscar-Berman and Marinković, 2007).

Excessive consumption of alcoholic beverages in pregnancy exposes the foetus to teratogenic effects of alcohol, this leads to foetal alcohol syndrome (FAS) and foetal alcohol spectrum disorders (Tenenbaum et al., 2016). Annual estimate of 119 000 children born with FAS worldwide is reported (Popova et al., 2017). In South Africa, the prevalence continues to increase (May et al., 2017). FAS cause physical and behavioural development retardation, intellectual disability and organs malformations (Tenenbaum et al., 2016).

In the kidney, short-term alcohol ingestion causes much damage to the kidney as the long-term intake does. Long-term excessive alcohol consumption is a risk factor for renal failure and end-stage renal disease (Singh et al., 2013). It promotes the formation of interstitial oedema, renal hypertrophy and inhibits antidiuretic hormone action in the kidney tubules (Singh et al., 2013) leading to renal dysfunction affecting the urine concentrating ability amongst others.

2.10 PROTEIN MALNUTRITION

Protein malnutrition is a condition in which an individual is having nitrogen imbalance (lack of nitrogen equilibrium) due to insufficient protein necessary for normal body metabolic function, commonly resulting from insufficient intake of nitrogen-containing food (inadequate protein intake) (Bain et al., 2013; Dos Santos et al., 2017). Other reasons for protein malnutrition besides dietary insufficiency could be from gastric surgeries (Motamedi et al., 2017) and renal medical conditions (Zha and Qian, 2017).

Protein malnutrition continues to be a major health problem worldwide, the current report indicates that about a billion people (145 million children) in the world had long-term insufficient dietary protein intake, mostly in Africa and South Asia (Wu, 2016) where malaria is endemic. Due to high level of poverty and hunger in the African continent, most of the populace depend mainly on cereals and legumes (a low-quality protein source) as their only protein source in addition to the low protein intake (Schönfeldt and Hall, 2012). Additionally, because of the low quality of plant proteins, widespread protein deficiency is common in these African communities (Manary, 2013). Though, the adverse effects of protein deficiency and imbalance on normal physiological processes in the body has been reported in animal studies (Carrillo et al., 2014; Campisano et al., 2017), the contributory effects of protein deficiency to the efficacy or inefficacy of drug therapies have been highly understudied and reported, especially in poverty-stricken African societies. Some health problems caused by protein malnutrition in humans include but not limited to skeletal muscle wasting, physical fatigue, impaired immune response, frequent infections, cardiac failure, cardiovascular abnormalities, hypertension, Loss of libido, reduced fertility, bone fragility and kidney injury (Wu, 2016).

2.11 DRUG METABOLISM IN THE PRESENCE OF ALCOHOL AND PROTEIN MALNUTRITION

2.11.1 Drug Metabolism

Drugs (e.g. chloroquine) are one of many foreign compounds (xenobiotics) entering the human body intentionally, unintentionally or coincidentally, and requires elimination. Drugs elimination involve absorption into systemic circulation, distribution to various body organs, metabolism and elimination. Absorption of drugs is mainly through the gut, but also occur through skin and lungs. During absorption, certain drugs can be metabolised by the gut mucosal enzymes in a process called first-pass elimination (Caldwell et al., 1995). Drugs reaching body tissues via systemic circulation can be eliminated unchanged such as pancuronium, which is easily cleared into urine and bile, or some volatile drugs that can be easily eliminated through lungs. Some drugs mostly lipophilic are retained in the tissues unchanged, while others undergo a spontaneous chemical transformation, which is the breakdown of drugs without enzymatic action (Caldwell et al., 1995). The predominant pathway is the enzymatic metabolism (figure 2.4) through the action of the phases I and II drugs metabolizing enzymes (Caldwell et al., 1995).

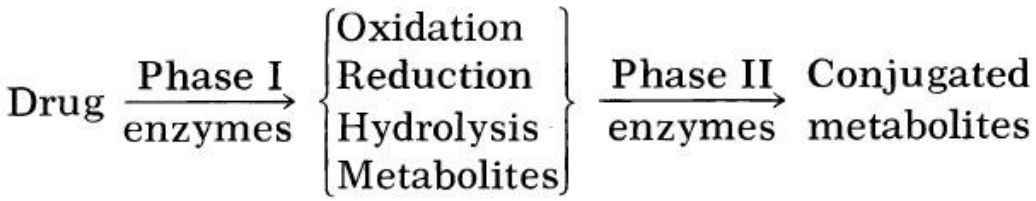

Figure 2.8: Pathway of drug metabolism in human

Simple flow chart of the predominant pathway of drug metabolism (Drayer, 1974)

2.11.2 Phase I metabolism of drugs

Drug metabolising enzymes are enzyme systems predominantly in the liver, but also present in the kidney and gut (Mackenzie et al., 2017). The oxidative or phase I enzymes include the cytochrome P450 enzymes, flavin-containing monooxygenases and alcohol dehydrogenases (Hines and Mccarver, 2002). The phase I enzymes are

involved with the biotransformation of drugs to active intermediate metabolites usually by oxidation. These intermediate metabolites are highly active and are conjugated with endogenous molecules such as glutathione to inactive metabolites for subsequent excretion (Park, 2001), (Figure 2.8).

2.11.3 Phase II metabolism of drugs

The conjugating or phase II enzymes are the glutathione *S*-transferase, *N*-acetyltransferase, uridine 5'-diphospho-glucuronosyltransferase, epoxide hydrolase and sulfotransferases (Mccarver and Hines, 2002). These enzymes are involved with the conjugation of certain intermediate active metabolites of drugs for subsequent elimination. However, some drugs like morphine are metabolised directly by phase II enzymes without undergoing phase I metabolism (Park, 2001), (Figure 2.8).

2.11.4 Drugs interaction

Drug-drug interactions occur during drug absorption, distribution, and metabolism or at the receptor site of action and excretion. Example of interaction during absorption following oral administration is that proton pump inhibitors increase gastric pH affect gastric absorption of many drugs that require low pH to be dissolved and absorbed. During distribution, drugs requires protein (such as albumin) binding, competing for the same binding site ensue between drugs and lead to the displacement of the one with low affinity. This will affects its distribution, subsequent elimination and perhaps its action (Caterina et al., 2013). Furthermore, majority of the drug interactions are due to inhibition/induction of drug metabolizing enzymes (Caterina et al., 2013). Inhibition of the enzymes could lead to delayed breakdown and accumulation of the drugs, while induction accelerates the breakdown and decrease the concentration of the drugs (Snyder et al., 2012; Berg et al., 2017).

Although drug-drug interactions are the major cause of adverse drug interaction (Snyder et al., 2012), clinically, drug interaction is employed for some benefits (Caterina et al., 2013). For example, potentiation drug interaction in which certain

drug or adjuvant enhance the action of another drug or an adjuvant, but the enhancing drug or adjuvant has no direct action, is often used as a beneficial drug interaction (Caterina et al., 2013). However, side effects of the drug might also be potentiated in the process (Caterina et al., 2013). In synergism, two drugs act simultaneously on one target resulting in more effect greater than individual drug acting alone, this is common in combination therapy (Caterina et al., 2013). Whereas antagonism is the diminishing effect of a certain drug by another drug, a clinical example is an antidote against poisoning (Caterina et al., 2013). These modes of drug interaction can occur at any level of drug-drug interaction from absorption to elimination depending on the drugs involved and there point of interaction (Caterina et al., 2013).

2.11.5 Alcohol and drug metabolism

Alcohol affects drugs absorption and metabolism, the drugs as well affect alcohol absorption and metabolism. Alcohol is shown to affect gastric emptying thereby affecting absorption and bioavailability of most drugs administered orally (Fraser, 1997). This suggests alcohol might affect the absorption and bioavailability of oral chloroquine. Furthermore, high doses of alcohol induce CYP2E1, an enzyme involved in the metabolism of other drugs. Therefore, higher doses of alcohol may inhibit this enzyme and affect the metabolism of drugs such as rifampicin (Fraser, 1997) and even chloroquine. However, alcohol causes reduction of protein synthesis by decreasing enzyme production (and ultimately drugs metabolism) including alcohol dehydrogenase, which leads to slow alcohol clearance and increased blood alcohol concentration and its toxicity in the organs (Lieber, 2002; Santolaria and González-Reimers, 2013).

2.11.6 Protein deficiency and drug metabolism

Several researchers have shown that deficiency of dietary protein, prevalent in protein malnutrition affects both the oxidative and conjugation pathways of drug metabolism (Wood and Woodcock, 1970; Kato, 1977; Hamberg et al., 1990) by

diminishing the synthesis of the drug metabolizing enzymes, because of the diminished synthesis of the protein required for enzyme production. For example, Ezzeldin (2012) suggested that there is a risk of metronidazole accumulation in the presence of protein malnutrition. Another study on cancer-related protein malnutrition, the authors find altered metabolism increased the toxicity of chemotherapeutic drugs due to protein malnutrition (Motawi et al., 2013).

The study by Adelusi and Salako (1982) indicated that protein malnutrition delayed absorption of chloroquine from the site of intraperitoneal injection into systemic circulation, causes slow uptake and elimination by the liver, due to the reduced synthesis of the cytochrome enzymes responsible for chloroquine metabolism. In addition, to confirm their observation, normal protein diet was restored to previously low protein fed rats, which shows the return of normal chloroquine metabolism.

In summary, alcohol and protein malnutrition alter drugs metabolism and elimination, which lead to accumulation and increased toxicity of the drug. Thus, chloroquine and/or alcohol administration with low protein possibly cause increased organ (kidney) toxicity.

2.12 Anatomy and function of the kidney

2.12.1 Gross anatomy of the kidney

The kidney is bean-shaped organ located in the upper retroperitoneal space in the abdomen, one on each side of the vertebrae. Normally, the right kidney is lower than the left kidney owing to the presence of the liver in the right hypochondrium. In rats, the right kidney is cranial compared to the left. Each kidney has the adrenal gland located above it invested in a fascia with the kidney. The left kidney is related to the stomach, spleen, pancreas, jejunum and the descending colon. The right kidney is separated from the liver by the hepato-renal recess. Fresh kidney is reddish-brown colour (Ross and Pawlina, 2011) with convex lateral surface and a concave medial surface, the medial surface has the renal hilum a point where the renal vessels, renal pelvis and nerves enter and leave the kidney. The renal sinus is the space within the kidney occupied by the renal vessels, nerves, renal pelvis and some fat (Moore and

Dalley, 2006). An outer fatty capsule and an inner fibrous capsule covers both the left and right kidney.

Sagittal section of the kidney revealed the inner morphological structure of the kidney showing the renal cortex and medulla, which are vividly distinguishable on gross section (figure 2.9). On histological section (H&E stained), the cortex is the outer dark stained area beneath the capsule while medulla is the inner light stained area consisting of the renal pyramids (figure 2.10). The apex of the pyramid is the renal papilla. A part of the cortex extending between the pyramids are the renal columns. The renal pelvis is a flattened, upper funnel-shaped expansion of the ureter, it receives two or three major calyces, each of which bifurcates or trifurcate into minor calyces. Each of the minor calyces is indented by the renal papilla (Moore and Dalley, 2006). Rat kidney is unipapillate having only one calyx (Hofstetter et al., 2005).

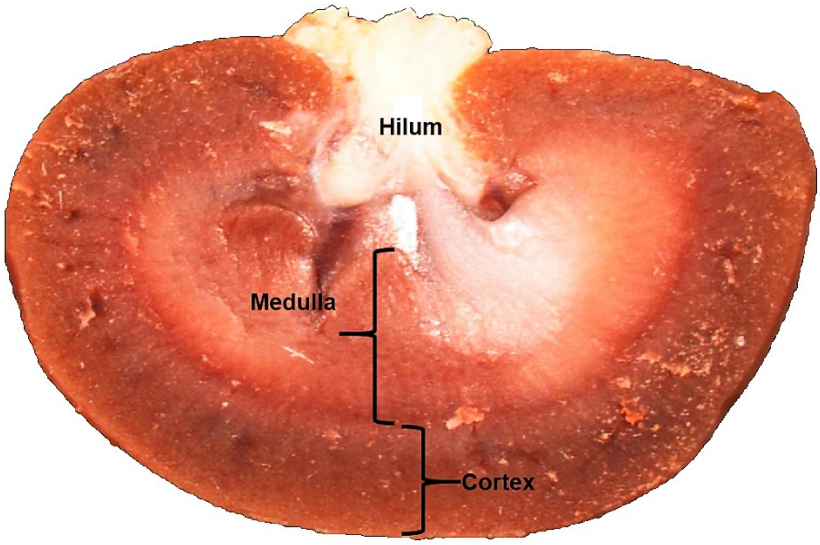

Figure 2.9: Sagittal section of rat kidney

This sagittal section of male Sprague-Dawley rat kidney reveals the renal cortex and medulla (labelled therein) and the renal hilum. Photographed with a digital camera.

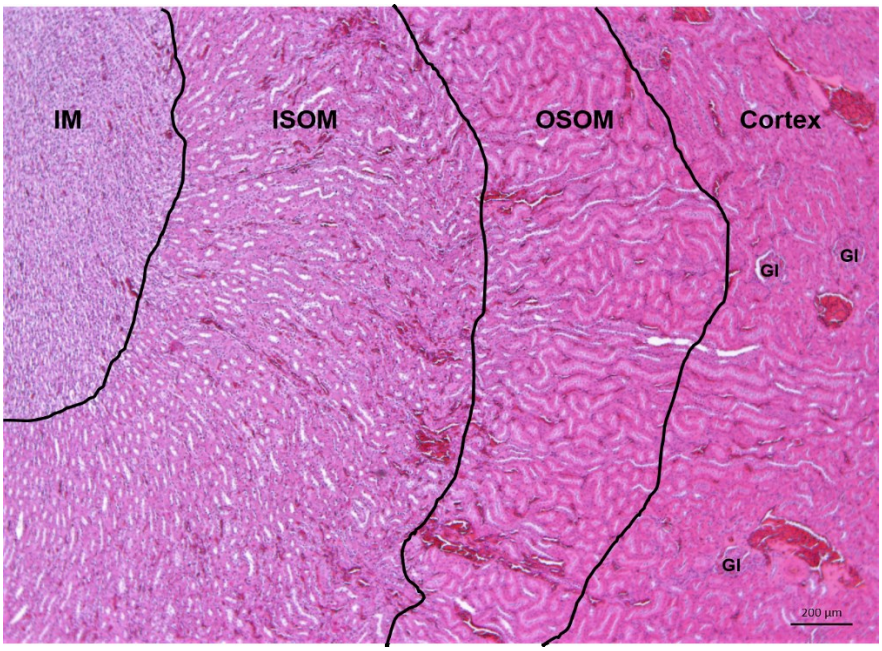

Figure 2.10: Histological cross-section of rat kidney

In this H&E stained section of rat kidney renal cortex and medulla can be easily identified as dark and light stained areas respectively. Gl – glomeruli, IM – inner medulla, OSOM – an outer strip of outer medulla, ISOM – an inner strip of outer medulla. Scale bar - 200µm.

The nephron (figure 2.11) is the functional unit of the kidney and comprises of the uriniferous tubule and collecting duct. It begins at the vascular pole of the glomerulus, continues with the tubules to make uriniferous tubule and then connect to the collecting duct via a connecting tubule. Collecting duct empties the urine into the minor calyx (Young et al., 2006). The interstitium of the kidney surrounds the nephron, blood vessels, ducts and lymphatic vessels.

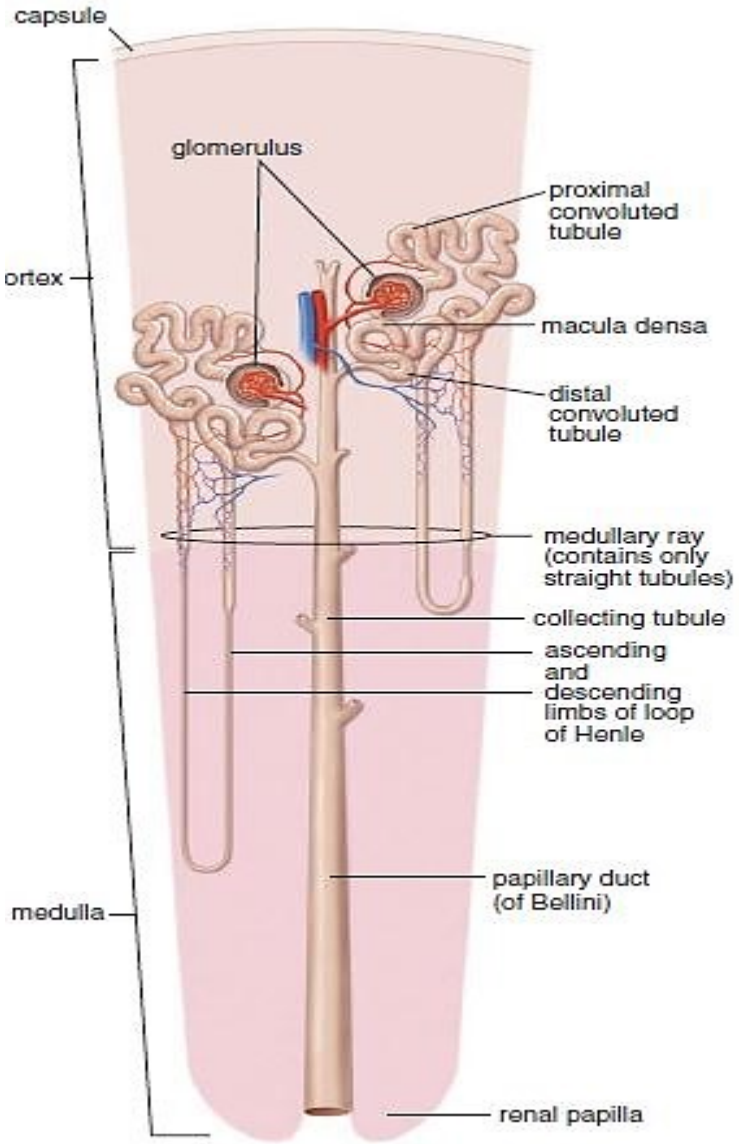

Figure 2.11: Diagram of the nephron

This diagram depicts the various parts of the human nephron (Ross and Pawlina, 2011).

2.12.2 Histology of the kidney

The glomeruli are a tuft of capillaries where ultrafiltration of blood occurs; it is notched on the Bowman’s capsule creating the renal corpuscle. The visceral epithelial layer of the Bowman's capsule invested the glomerulus. It is a specialised epithelium called the podocytes. The glomerular endothelial cells and glomerular basement membrane together with the podocytes formed the filtration apparatus. The space between the visceral layer of the Bowman's capsule and the parietal layer

is the urinary space where the ultrafiltrate drain into to reach the proximal convoluted tubule (Ross and Pawlina, 2011). The proximal convoluted tubule is lined by cuboidal epithelium with apical specialisations. It exhibits surface brush border and basal striations. These features help to distinguish proximal convoluted tubule cells in histological sections. Other features are the tight junction that closes the intercellular space, the presence of lateral folds and the interdigitations of the basal processes (Ross and Pawlina, 2011).

The loop of Henle has a descending limb and an ascending limb with a loop at the middle. The thick descending limb of the loop of Henle is the proximal straight tubule and it has lower cuboidal epithelia with less apical brush border. It is not specialised in absorption as the convoluted proximal tubule. The thin limb of Henle epithelium is lined by squamous. The thick ascending limb of the loop of Henle is the distal straight tubule and lined by cuboidal epithelium. The distal convoluted tubule has a simple cuboidal epithelium, like the proximal convoluted tubule although slightly lower with the absence of the brush border and a more prominent tubular lumen (Ross and Pawlina, 2011). The loop of Henle is involved in the concentration of the urine, by the countercurrent multiplier system. It creates and maintains osmotic gradient in the medullary interstitium, which increases ion concentration from the corticomedullary junction to the papilla. This is because the ascending limb is permeable to NaCl and impermeable to water. Solutes that leak back into the loop of Henle through the descending limb go back into interstitium at the ascending limb. The peritubular capillary network forms the vasa recta parallel to the loop of Henle with descending arteriolae rectae and an ascending venulae rectae (Ross and Pawlina, 2011).

The vasa recta serve as the countercurrent exchange system supplying blood to the medulla without affecting the ion gradient. Because the interstitium is hyperosmotic from above downward, blood in the arteriolae rectae loses water, gain salt and becomes hyperosmotic as it descends, while as it ascends in the venulae rectae it loses salt to gain water to become isosmotic (Ross and Pawlina, 2011). With regard to the urine, the ultrafiltrate reaching the descending loop of Henle becomes hyperosmotic, because as noted above the descending loop of Henle is permeable to water and impermeable to salts, however, as the urine ascends the loop of Henle the process is reversed and the ultrafiltrate reaching the distal convoluted tubule and

collecting duct is hypoosmotic. The collecting duct under ADH influence is highly permeable to water and adds salt to the urine, thereby concentrating the urine and equilibrating the osmolality (Ross and Pawlina, 2011).

The collecting duct begins with a small lumen and continues to enlarge as it advances to the renal papilla and terminate into the minor calyx of the renal pelvis. The connecting tubule line by simple squamous epithelium gradually changes to cuboidal in the collecting duct with a transition to columnar towards the papillary collecting duct. The collecting duct has two cell types, the principal cells and the intercalated cells. The principal cells are more abundant and contain the ADH-regulated AQP2 water channels, which are responsible for water reabsorption in the collecting duct (Ross and Pawlina, 2011). Musabayane et al. (2000a) suggested chloroquine and alcohol concurrent administration elevates serum levels of ADH, which might affect the regulation of AQP2.

2.12.3 Regulation of aquaporin 2 water channel

The ADH-regulated aquaporin 2 water channel (AQP2) is abundant within the cytoplasm of the principal cells of the collecting ducts. However, when the channels are activated by the binding of ADH to V_2 receptors on the basolateral membrane of the principal cells, the AQP2 are translocated to the apical membrane of the principal cells to increase water reabsorption of the collecting ducts (Wilson et al., 2013; Park and Kwon, 2015). Antidiuretic hormone regulates the activity of the AQP2 via a short term and long term regulatory pathways (Kwon et al., 2013; Park and Kwon, 2015). The short-term involves the trafficking of the AQP2 protein to the apical membrane, while the long-term involves the increase in the abundance AQP2 proteins in the principal cells of the collecting ducts (Park and Kwon, 2015).

3 CHAPTER THREE: MATERIALS AND METHOD

3.1 Ethics approval

The Animal Ethics Screening Committee of the University of the Witwatersrand approved this study. Approval number AESC 2015/11 /54C (Appendix 2).

3.2 Animals

Sixty-four adult (9 weeks old) male Sprague-Dawley rats, average weight 420±50g were used in the study.

3.3 Housing and caging

The rats were individually housed in Perspex cages lined with sawdust and paper shreds. The ambient temperature of the central animal services was maintained at 21±1°C and a 12-hour light cycle.

3.4 Chloroquine and alcohol preparation

Chloroquine phosphate salt (Sigma-Aldrich, PHR1258) was reconstituted in our lab with 0.9% saline to make 10mg/ml solution, which is the safe dose used in malaria treatment and in research (Mbajiorgu et al., 2008). The drug solution was freshly prepared every week just before administration. Ethanol stock solution of 100% ethanol was diluted to make 6% ethanol in drinking water v/v. The ethanol concentration (6%) is approximate of the alcohol content in beer (Nogueira et al., 2017).

3.5 Feed preparation

To prepare the 6% low protein diet, the standard (21%) rat chow (Nutrition hub, South Africa) in powder form was mixed weight by weight with six parts of cassava powder. This mixture is then moisturised to a dough form, which is then shaped exactly as the commercial rat feed and dried in an oven at 30°C, and was used to feed the rats in the low protein subgroups. Cassava powder was purchased from Yeoville market, Johannesburg (coordinates, 26°10′S 28°3′E). Analysis of the standard rat chow and the low protein diet was done at nutrition laboratories (ARC, Irene and University of Free State) (Table 3.1 and Appendix 4).

Table 3.1: Proximate analyses of the feed samples

Components	**Unit**	**Control diet (23% of protein)**	**Low protein diet (6% of protein)**
Dry Matter	%	91.11	92.78
Moisture	%	8.89	7.22
Ash	%	6.99	3.35
Fat (ether extraction)	%	3.34	3.25
Crude fibre	%	2.60	3.74
*Protein (N x6.25)	%	22.75	5.73
Calcium	%	1.32	2.95
Phosphorous	%	0.62	0.15
Total energy	MJ/kg	16.58	**15.97

* For the conversion of nitrogen content to protein content a factor 6.25 was used.

** The test of this result was conducted at the department of animal, wildlife and grassland sciences, University of Free State.

3.6 Experimental design

The rats were weighted and then randomly assigned into two groups of 32 rats each (normal and low protein groups: NP and LP respectively) based on the dietary protein content (figure 3.1). Each dietary group comprise of four randomly assigned subgroups of eight rats each: (1) Control subgroups that received neither chloroquine nor alcohol treatments while on either normal or low protein diets (NPC, LPC). (2) Chloroquine treatment subgroups while on either normal or low protein diets (NPQ, LPQ). (3) Alcohol treatment subgroups while on either normal or low protein diets (NPE, LPE), and (4) chloroquine and alcohol treatment subgroups while on normal or low protein diets (NPQE, LPQE). All rats in LP group were fed on a low protein diet, one week prior to the chloroquine and alcohol administration.

Chloroquine was administered intraperitoneal once weekly at 0.1ml/100g (equivalent of 1mg/100g) body weight to subgroups NPQ, LPQ, NPQE and LPQE while subgroups NPC, NPE, LPC and LPE received 0.1ml/100g of 0.9% saline intraperitoneal injections weekly. Alcohol was supplied in drinking water at 6% v/v *ad libitum* to the subgroups NPE, LPE, NPQE and LPQE whereas subgroups NPC, NPQ, LPC and LPQ received plain drinking water *ad libitum*.

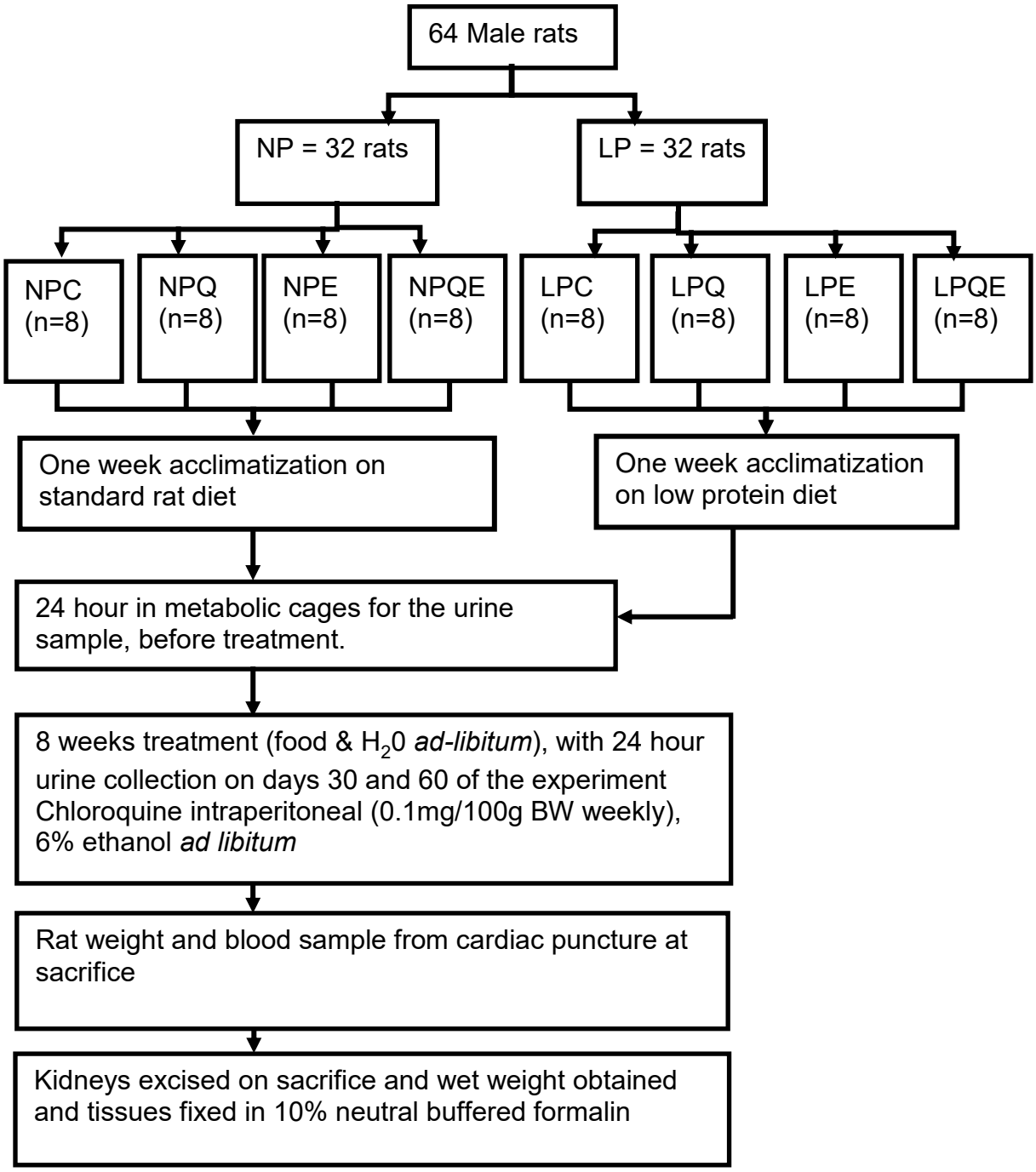

Figure 3.1: Diagram of the experiment

NP – Normal protein, LP – Low protein, NPC – Normal protein control, NPQ – Normal protein with chloroquine, NPE – Normal protein with alcohol, NPQE – Normal protein with chloroquine and alcohol, LPC, Low protein control, LPQ – Low protein with chloroquine, LPE – Low protein with alcohol, LPQE – Low protein with chloroquine and alcohol. BW – Body weight.

3.7 Urine volume estimation

To estimate the 24-hour urine volume, the rats were placed individually in a metabolic cage for a 24-hour duration on days 0, 30 and 60 of the experiment. The metabolic cages are designed with two chambers, an upper rat-holding chamber and the lower urine and faeces collection unit. Rats are placed in the upper chamber with food and water supplied *ad libitum*, and a fenestrated floor allowing free passage of the faeces and urine to the lower chamber. The lower chamber has funnel pathways allowing perfect separation and collection of the urine and faeces into different containers (Appendix 6A). Finally, the urine volume was measured using calibrated measuring cylinder and measurements were recorded.

3.8 Termination of the experiment

The animals were weighed using Snowrex electronic scale (Clover scales, South Africa), at the end of 8 weeks treatment, their weights recorded and then euthanised with an overdose of sodium pentobarbitone (Euthanaze®) at 20mg/100g body weight intraperitoneal injection. Weight gain/loss was calculated by subtracting initial body weight from the terminal body weight.

3.9 Tissue and blood collection

Blood samples were also immediately collected using 5ml syringes with 21G needles via cardiac puncture into plain blood sample tubes. The blood collected was centrifuged with Rotofix 32 A (Hettich Zentrifugen, Germany) centrifuging machine at 1067 x g for 10 minutes at room temperature. Serum was then collected into a 1 ml Eppendorf tubes and stored in the deep freezer (-80°C) for further analyses.

Kidneys were removed through midline abdominal incision, weighed immediately using RADWAG sensitive electronic scale (Wagi Elektroniczne, Poland) and their wet weights recorded and thereafter immersed in 10% neutral buffered formalin for fixation for routine histology processing. The right kidney was used for relative

medullary thickness (RMT) measurements while the left kidney was used for microfocus computer tomography scans and volume analysis in addition to histology.

3.10 Laboratory and other analysis

3.10.1 Blood analyses

Serum obtained from the blood was sent to Idexx Laboratories, Johannesburg for serum urea and creatinine analyses. Serum urea and creatinine were determined using Idexx Vettest® Chemistry Analyser based on the conductivimetric urease assay as described by Horak and Sunderman (1972) and the Jaffe method (Delanghe and Speeckaert, 2011) respectively.

3.10.2 Relative medullary thickness (RMT) measurements

The kidney gross length, breadth and width were measured using a dial vernier calliper (Mauser Inox 0-150mm, 0.05mm accuracy) as the first step of RMT measurement. Furthermore, the right kidney was bisected into two mid-sagittal halves, and photographs of the sagittal sections were taken with Nikon DSfi1 digital camera attached to Nikon SMZ1500 dissecting microscope (Nikon, Japan) at 4x magnification. The images were imported into ImageJ image analysis software version 1.50i (National Institutes of Health, USA). On ImageJ, the scale was set properly and standardised by comparing the length of the kidney measured with a vernier calliper to the length measured with the ImageJ software, and the two results perfectly correlated. Medullary thickness was measured on ImageJ software from the corticomedullary junction to the tip of the papilla, cortical thickness was also measured from underneath the renal capsule to the corticomedullary junction in three directions (Casotti et al., 2006) (Appendix 6B) and the results were exported from the ImageJ into Microsoft Excel for further analyses. RMT is calculated using the formula:

$$\mathrm{RMT} = \frac{10 \times \text{medullary thickness}}{\sqrt[3]{\text{length} \times \text{width} \times \text{thickness}}}$$

3.10.3 Micro-focus tomography scan

The formalin-fixed left kidney was scanned with a Nikon X TH 225/320 microfocus computed tomography machine (Nikon, UK) at the voltage of 50KV and the current of 100μA to achieve the ideal contrast at 5μ resolution. The kidneys were removed from the formalin and exposed to air for the scanning period (approximately eight minutes). The scanned images were reconstructed to a three-dimensional vgi file and imported into VGStudio Max software version 3.0 (Volume Graphics GmbH, Germany) for analysis.

3.10.4 Three-dimensional kidney volume estimation

The reconstructed image was imported into the VGStudio image analysis software, surface determination option was used to separate the kidney tissue material from the air background because the kidneys were scanned in the air, and then the region growing option was used to select only the kidney material from the background for 3D volume analysis. Volume analyser option was executed to get the result of the volume analysis. In addition, 2D serial sections were exported from the VGStudio in TIF format, at a distance of 10μm, which enabled us to conduct stereological volume estimation using the volumest plugin on ImageJ.

3.10.5 Sampling procedure for stereology

Firstly, a pilot study was conducted to determine the number of sections required for the efficiency of the stereological method, in which ten sections were determined to provide a significant coefficient of error, efficient for the volume estimation. Gundersen and Jensen (1987) provide a detailed explanation of the efficiency of the volume estimation using stereology and calculation of the coefficient of error.

Systematic uniform random sampling (SURS), which combines the efficiency of systematic sampling and the unbiasedness of random sampling was used to sample the ten sections for volume estimation. Using SURS, the first section was selected randomly and the remaining nine sections were systematically selected in a sequence of a certain interval. This interval is determined by the section sampling fraction (SSF), which is the number of sections from which only one section will be selected (figure 3.2). This way each of the kidney section has an equal chance of being selected and in addition, completely remove bias in the selection process, this idea was adopted from Nyengaard (1999).

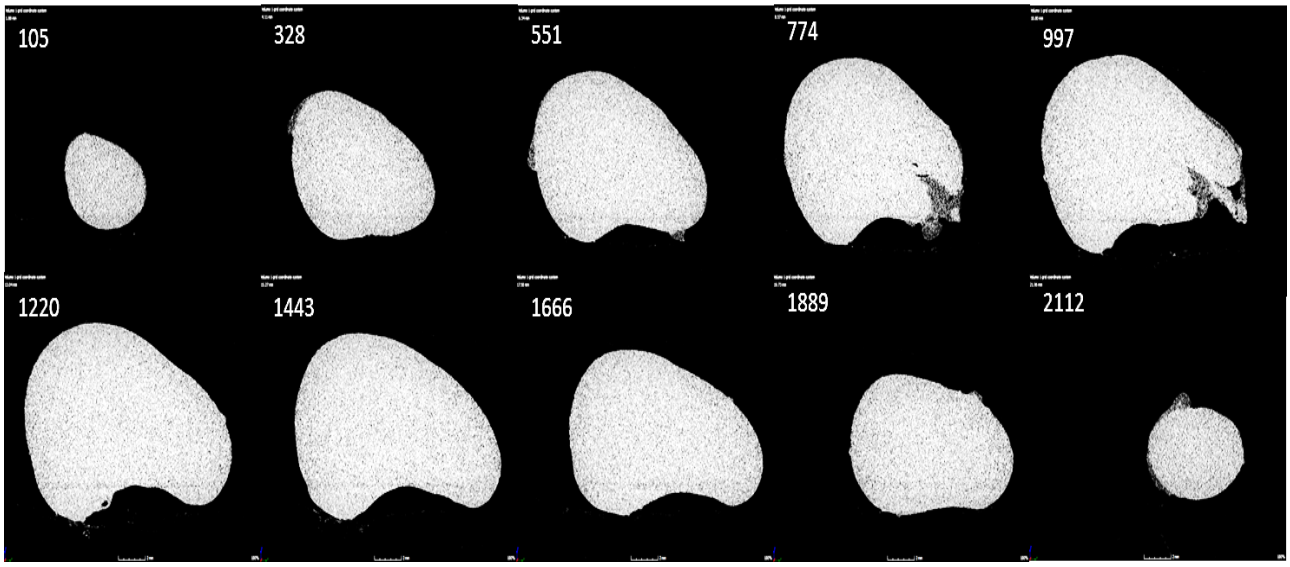

Figure 3.2: 2D serial sections for volume estimation of kidney

The representative kidney in the above figure had the total serial sections of 2227 sections and the section sample fraction is one in every 223 sections. The first section (105th) randomly selected and subsequently every 223rd section chosen until ten sections selected.

3.10.6 Stereological volume estimation

The ten selected serial sections were imported as image sequence into ImageJ and the scale was set to get the result in mm^3 and standardise the procedure. Volumest plugin immediately prompts for section thickness and the total number of sections for the volume estimation.

Volumest plugin uses the Cavalieri principle of point counting. In this principle, a grid is superimposed on the tissue slide and points hitting the region of interest on the slide are counted (∑p) then multiplied by area per point (a/p) to get the area of the section. The area of the section is then multiplied by section thickness (t) to get the volume of the tissue section as in the first equation below. Section volume is then multiplied by SSF to get the total organ volume as in the second equation below. In addition, the volumest plugin automatically estimates the coefficient of error (CE) for each kidney volume estimated.

Equation 1: $\mathrm{Volume}_{\mathrm{section}} = \mathrm{t} \times \mathrm{a} / \mathrm{p} \times \sum \mathrm{p}$

Equation 2: $\mathrm{Volume}_{\mathrm{total}} = \mathrm{Volume}_{\mathrm{section}} \times \mathrm{SSF}$

3.10.7 Histology

The fixed left kidney was dissected into three blocks; the middle block (in all the samples for consistency) was routinely processed using Citadel 1000 (Shandon, England) automatic tissue processor, embedded in paraffin wax and 5 µm thick sections were cut using a rotary microtome (Jung Biocut 2035, Leica, Germany).

3.10.8 H&E and Masson's trichrome staining techniques

The tissue sections, on gelatine-coated slides, were stained with haematoxylin and eosin (H&E), and light microscopic analysis and morphometric measurements were carried out. In addition, some sections were stained with Masson's trichrome stain for collagen fibre profile. (Appendices 5D and 5E for H&E and Masson's trichrome procedures respectively).

3.10.9 Glomeruli counting method

On the H&E stained sections, random non-overlapping fields in the cortex were photographed using Axiocam HRc2 camera attached to Axioskop 2 microscope

(Zeiss, Germany GmbH) and imported into ImageJ, a grid was superimposed and the glomeruli that were completely within the field were counted, while any of the glomeruli cut by the field edge were not counted. In each of the experimental group and control, ten fields were examined and the average was calculated. The result of the counting is the number of glomeruli in a single camera field at x10 magnification (5.78 mm^2 area).

3.10.10 Renal corpuscular and tubular diameter measurements

Photomicrographs of the most circular profiles were taken at x63 magnification using Axiocam HRc2 camera attached to Axioskop 2 (Zeiss, Germany GmbH) microscope. The photomicrographs were then analysed with Zen Lite image analysis software. Glomeruli tuft diameter, renal corpuscle diameter and urinary space diameter were measured. In addition, diameters and epithelial cell heights of proximal convoluted and distal convoluted tubules were also measured. In each of the treatment groups and control and for each parameter, 30 measurements were taken.

3.10.11 Collagen fibre quantification method

Masson's trichrome sections were photographed using Axiocam HRc2 camera attached to Axioskop 2 (Zeiss, Germany GmbH) microscope and imported into ImageJ. A grid was overlayed, the area fraction of the collagen fibre was calculated as the area of collagen deposition per single camera field at x10 magnification (5.78mm^2 area) in ten fields, and the average was taken. Points of grid intersection on the collagen deposition were counted, and then the points were multiplied by area per point (0.07mm^2) to get the collagen deposition area. The area fraction of the collagen fibres is defined as the area of the collagen deposition divided by 5.78mm^2.

3.10.12 Immunofluorescence of the aquaporin 2 water channel

The tissue sections on silane-coated slides were dewaxed, hydrated, and then washed in tap water for immunofluorescence procedure. Heat antigen retrieval was done in a microwave oven at 720-watt power for ten minutes, using citrate buffer at pH 6.0. Then, the sections were washed in phosphate buffered saline (PBS) and then incubated with 10% normal goat serum in PBS for one hour to block endogenous peroxidase. Sections were then incubated with rabbit anti-aquaporin 2 (Abcam, ab15116) primary antibody in PBS overnight at 4°C.

On the second day, sections were washed in PBS and incubated with goat anti-rabbit Alexa flour 488 (Abcam, ab150077) secondary antibody in PBS for 1 hour in the dark at room temperature. Then washed with PBS and incubated with 4', 6-diamidino-2-phenylindole, dihydrochloride (DAPI) nuclear stain for 5 minutes and then washed, coverslipped with fluoromount®, allowed to dry and kept at 4°C until viewing and analysis (Appendix 5F).

Fluorescence images were captured using XC10 digital camera attached to Olympus IX51 inverted fluorescence microscope (Olympus, Japan). Images of Alexa fluor channel were acquired at 300 ms exposure time, while images of DAPI channel were acquired at 70 ms exposure time. CellSens dimension 1.11 image analysis software was used to overlay the Alexa fluor channel and DAPI channel. Alexa fluor channel represents the aquaporin 2 expression while DAPI channel represents the nuclear expression. All images in both channels and in all the experimental groups were taken at x20 magnification.

3.11 Data management, presentation and analysis

Data management and visualization were done with Microsoft Excel 2016 version. Statistical analysis was done with STATA 13.1 statistical package at 5% level of significance. Bar charts were used in the graphical presentation of the data and were presented as a mean ± standard error of the mean (Mean±SEM). The data were tested for normality with Shapiro-wilk test, and normally distributed data were analysed with one-way analysis of variance (ANOVA) while data not normally

distributed were analysed with Kruskal-Wallis test. Bonferroni post-hoc (corrected for significant one-way ANOVA) was used for multiple mean pairwise comparisons and Dunn multiple mean pairwise comparisons for significant Kruskal-Wallis test. Spearman correlation in RStudio program was used to estimate the correlation between the VGStudio kidney volume estimation method and the stereological kidney volume estimation method.

All experimental groups compare to NPC, then all LP-treated groups compare to their cohort in NP. LP-treated groups also compare to LPC, which is a sub-control group.

4 CHAPTER FOUR: RESULTS

4.1 General findings

All rats were in good health before the experiment and at termination, no mortality or signs of any adverse change in behaviour was recorded. Body weight at termination was significantly lower in the entire LP-treated groups compared to NPC and compared to their cohorts in NP (p=0.0001) (table 4.1).

Table 4.1: Body weight in experimental rats

	NPC	NPQ	NPE	NPQE	LPC	LPQ	LPE	LPQE
Initial body weight (g)	392.3±11	422.8±16	439.8±25	427.5±15	434.5±12	440.3±17	423.8±12	440.5±19
Terminal body weight (g)	557.3±14	575.0±11	594.3±22	565.3±15	431.6±10*	434.0±20*#	418.0±13*#	422.8±21*#
Weight gain/loss (g)	165.0±9	153.3±10	156.5±10	139.8±10	-3.8±5*	-6.3±4*#	-5.8±5*#	-18.8±8*#

Body weight changes in experimental rats. Values with asterisks indicate significant difference from the control group (i.e. NPC), while values with hashtag indicate significant difference comparing cohorts (i.e. NP-groups compared to LP-groups). Absent of asterisk or hashtag indicate no significant difference. The data are presented as Mean±SEM (n=8). Key: NPC & LPC– Normal and Low protein controls, NPE & LPE- Normal and Low protein alcohol only, NPQ & LPQ- Normal and Low protein chloroquine only, NPEQ &LPQE –Chloroquine and alcohol concurrent treatment.

There were increases and decreases in body weight amongst the NP-treated and LP-treated rat groups respectively. While the percentage weight gain of rats in NPC, NPQ, NPE and NPQE were 42.43 %, 37.31 %, 36.63 % and 33.09 % respectively, the percentage weight loss in LP-treated rats, LPC, LPQ, LPE and LPQE were 0.53 %, 1.56 %, 1.13 % and 4.08 % respectively.

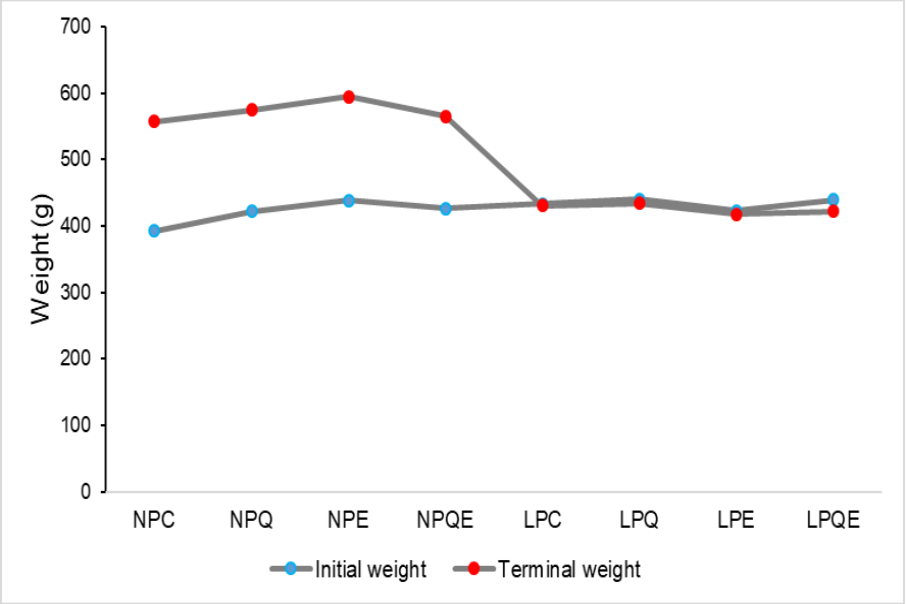

Figure 4.1: Body weight changes in experimental groups

The changes in body weight of the experimental rats, by comparing initial body weight before the experiment and the body weight at the termination of the experiment (see text above for percentage weight changes). Key: NPC & LPC– Normal and Low protein controls, NPE & LPE- Normal and Low protein alcohol only, NPQ & LPQ- Normal and Low protein chloroquine only, NPEQ &LPQE –Chloroquine and alcohol concurrent treatment.

The average food consumption was essentially the same, with a slight reduction in all the experimental groups compared to control, with no statistical significant difference (p=0.4618).

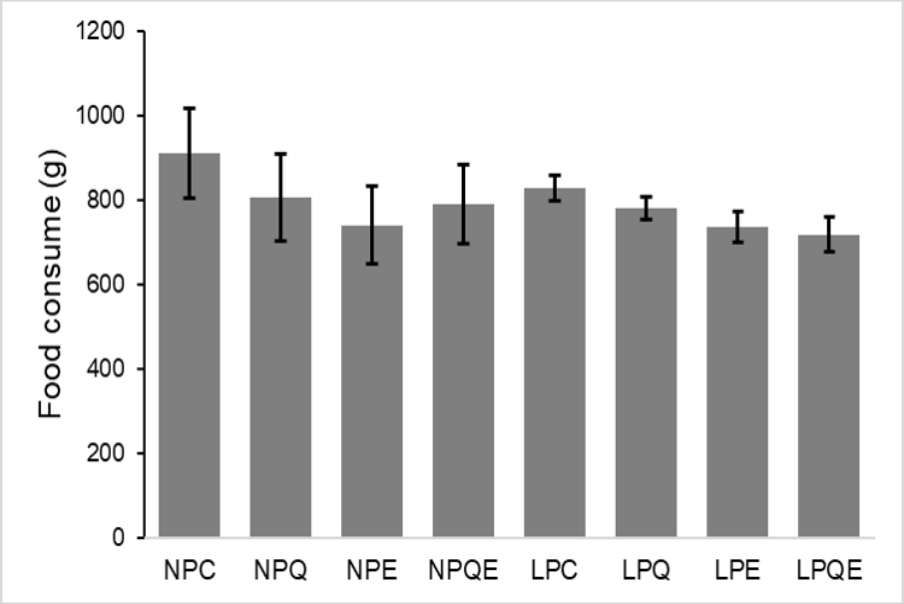

Figure 4.2: Estimated food consumption

The mean estimated food consumption in the experimental rat groups. However, no statistically significant difference (n=8). Key: NPC & LPC– Normal and Low protein controls, NPE & LPE- Normal and Low protein alcohol only, NPQ & LPQ- Normal and Low protein chloroquine only, NPEQ &LPQE –Chloroquine and alcohol concurrent treatment.

4.2 Urine volume

The urinary output values are shown in table 4.2. The result showed 24-hour urine volume before the commencement of treatment, was not significantly different in all the experimental groups compared to NPC, except LPQ compared to its cohort, NPQ (p=0.0003). After 30 days of treatment (i.e. Mid-treatment analysis), 24-hour urine production significantly decreases (p=0.0001) in the entire LP-treated groups compared to NPC and compared to their cohorts in NP. At termination, the 24-hour urine production again significantly decrease (p=0.00001) in the LP-treated groups compared to NPC and compared to their cohorts in NP, but no significant difference within the LP-treated groups or within the NP-treated group.

Table 4.2: 24 hours urine production in experimental rats

	NPC	NPQ	NPE	NPQE	LPC	LPQ	LPE	LPQE
Pre-treatment 24 hours urine production (ml)	17.3±1.46	19.0±1.77	19.2±1.78	15.8±1.46	10.6±1.13	11.4±1.70$^{\#}$	13.4±1.79	12.0±1.38
Mid-treatment 24 hours urine production (ml)	20.0±1.82	23.1±4.65	21.4±1.41	13.3±1.63	11.5±3.12*	10.4±1.0$^{*\#}$	5.9±1.09$^{*\#}$	6.4±1.21$^{*\#}$
Terminal urine production(ml)	22.4±2.12	23.4±3.31	21.1±1.58	14.6±1.40	9.7±1.68*	12.8±1.05$^{*\#}$	5.0±0.78$^{*\#}$	4.5±0.85$^{*\#}$

Urine production over 24 hours in the experimental rats. Values with asterisks indicate significant difference from the control group (i.e. NPC), while values with hashtag indicate significant difference comparing cohorts (i.e. NP-groups compared to LP-groups). Absent of asterisk or hashtag indicate no significant difference. The data are presented as Mean±SEM (n=8). Key: NPC & LPC– Normal and Low protein controls, NPE & LPE- Normal and Low protein alcohol only, NPQ & LPQ- Normal and Low protein chloroquine only, NPEQ &LPQE –Chloroquine and alcohol concurrent treatment.

4.3 Biochemical Analyses

Serum creatinine was significantly higher in NPE (p=0.0485), LPC (p=0.0025), LPE (p=0.0133) and LPQE (p=0.0024) compared to NPC (figure 4.6). In addition, NPQ, NPQE and LPQ have slightly increase creatinine compared to NPC. However, no significance recorded within the LP-treated or within the NP-treated.

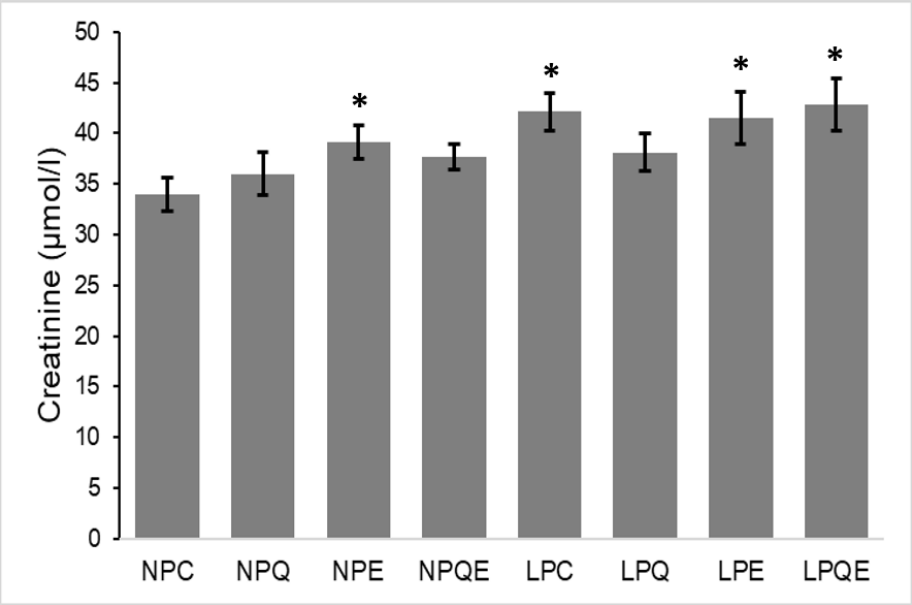

Figure 4.3: Serum creatinine level

The serum creatinine level in all the experimental animals Values with asterisks indicate significant difference from the control group (i.e. NPC). Absent of asterisk indicate no significant difference (n=7). Key: NPC & LPC– Normal and Low protein controls, NPE & LPE- Normal and Low protein alcohol only, NPQ & LPQ- Normal and Low protein chloroquine only, NPEQ &LPQE –Chloroquine and alcohol concurrent treatment.

Serum urea was significantly (p=0.0001) lower in LP-treated groups compared to NPC and their cohorts in NP (figure 4.7). There were no significant difference in urea in the NP-treated groups.

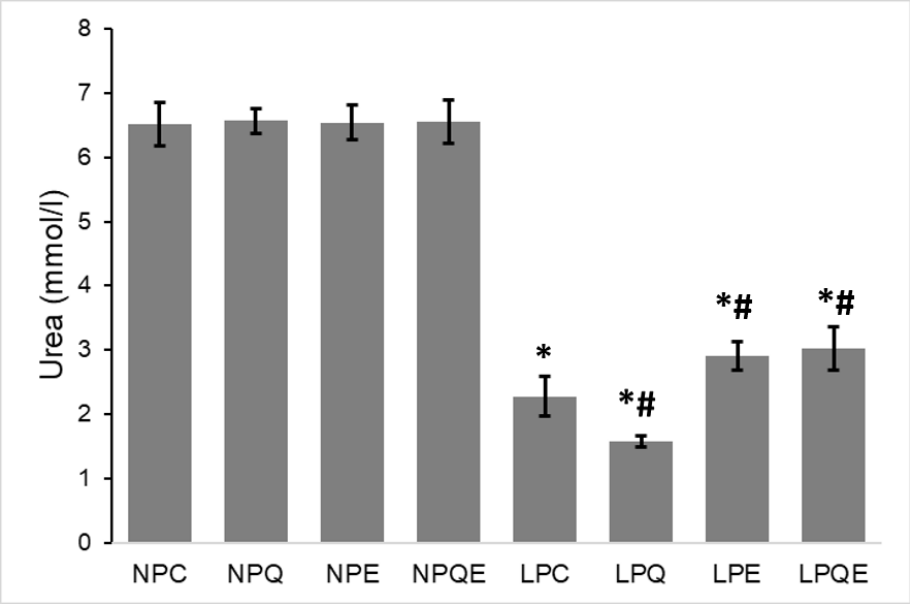

Figure 4.4: Serum urea level

The serum urea level in all the experimental animals. Values with asterisks indicate significant difference from the control group (i.e. NPC), while values with hashtag indicate significant difference comparing cohorts (i.e. NP-groups compared to LP-groups). Absent of asterisk or hashtag indicate no significant difference (n=5). Key: NPC & LPC– Normal and Low protein controls, NPE & LPE- Normal and Low protein alcohol only, NPQ & LPQ- Normal and Low protein chloroquine only, NPEQ &LPQE –Chloroquine and alcohol concurrent treatment.

4.4 Relative kidney weight

The relative kidney weight values shown in table 4.3, was significantly decreased in the LPC (p=0.0158), LPQ (p=0.0125) and LPE (p=0.0048), but only slightly low in LPQE (p=0.1988) compared to NPC. Furthermore, in comparison to their cohorts in NP, only LPQ (p=0.031) and LPE (p=0.0187) significantly decreased. However, no significance recorded within the LP-treated or within the NP-treated.

Table 4.3: Absolute and relative kidney weights

	NPC	NPQ	NPE	NPQE	LPC	LPQ	LPE	LPQE
Absolute kidney weight (g)	3.4±0.12	3.5±0.13	3.6±0.21	3.5±0.09	2.4±0.07*	2.4±0.08*#	2.3±0.06*#	2.5±0.13*#
Relative kidney weight (% body weight)	0.61±0.01	0.61±0.01	0.60±0.01	0.62±0.01	0.57±0.01*	0.56±0.01*#	0.55±0.01*#	0.60±0.01

Absolute kidney weight and the relative kidney weight of the experimental rats. Values with asterisks indicate significant difference from the control group (i.e. NPC), while values with hashtag indicate significant difference comparing cohorts (i.e. NP-groups compared to LP-groups). Absent of asterisk or hashtag indicate no significant difference. The data are presented as Mean±SEM (n=8). Key: NPC & LPC– Normal and Low protein controls, NPE & LPE- Normal and Low protein alcohol only, NPQ & LPQ- Normal and Low protein chloroquine only, NPEQ &LPQE –Chloroquine and alcohol concurrent treatment.

4.5 Kidney volume

Kidney volume measured using VGStudio max 3.0 software is significantly (p=0.0001) lower in LP-treated groups compared to NPC and compared to their cohorts in NP (figure 4.4). In addition, the kidney volume measured by stereology is also lower significantly (p=0.00001) in the LP-treated groups compared to NPC and compared to their cohorts in NP (figure 4.5), but no significance recorded within the LP-treated or within the NP-treated. However, chloroquine alone slightly increase the kidney volume in the NP- treated groups compared to control (p=0.2667).

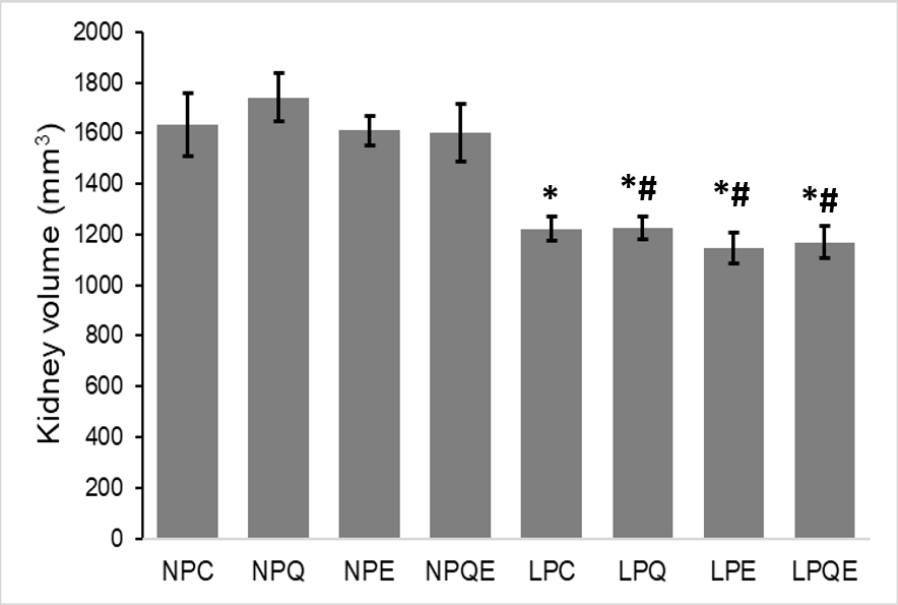

Figure 4.5: Kidney volume estimation using VGStudio software

Automated kidney volume using VGStudio max 3.0 in all the experimental animals. Values with asterisks indicate significant difference from the control group (i.e. NPC), while values with hashtag indicate significant difference comparing cohorts (i.e. NP-groups compared to LP-groups). Absent of asterisk or hashtag indicate no significant difference (n=7). Key: NPC & LPC– Normal and Low protein controls, NPE & LPE- Normal and Low protein alcohol only, NPQ & LPQ- Normal and Low protein chloroquine only, NPEQ &LPQE –Chloroquine and alcohol concurrent treatment.

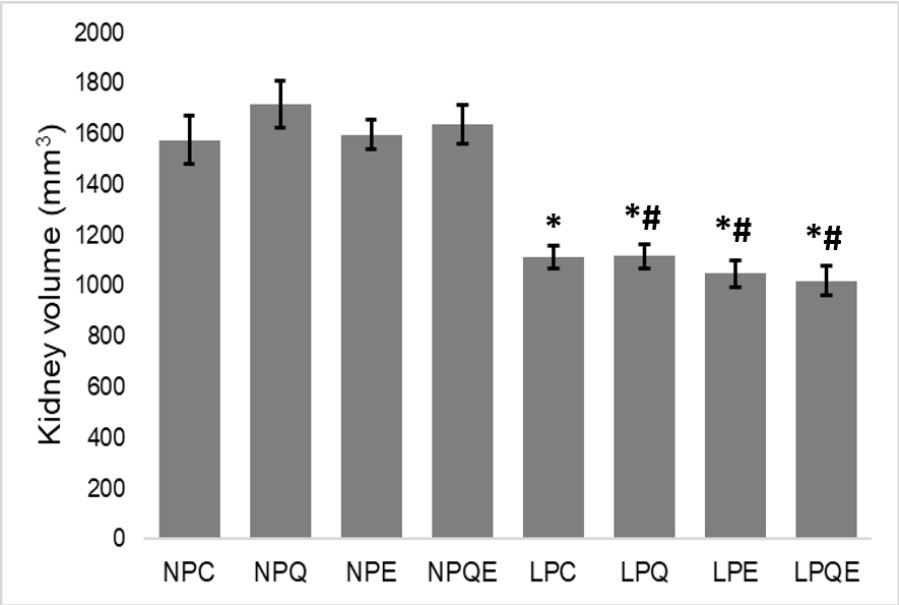

Figure 4.6: Kidney volume estimation using stereology

Stereological kidney volume estimated using 2D sections in the experimental animals. Values with asterisks indicate significant difference from the control group (i.e. NPC), while values with hashtag indicate significant difference comparing cohorts (i.e. NP-groups compared to LP-groups). Absent of asterisk or hashtag indicate no significant difference (n=7). Key: NPC & LPC– Normal and Low protein controls, NPE & LPE- Normal and Low protein alcohol only, NPQ & LPQ- Normal and Low protein chloroquine only, NPEQ &LPQE –Chloroquine and alcohol concurrent treatment.

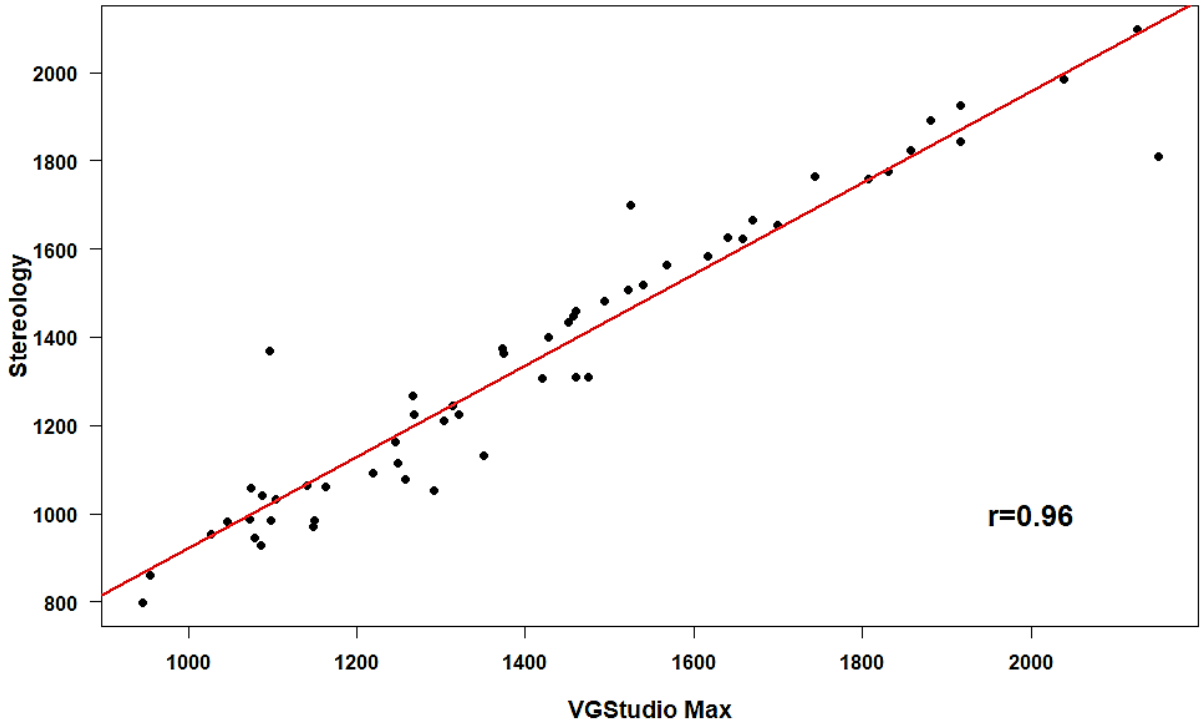

Figure 4.7: Relationship of the methods of kidney volume estimation

This correlation was done in RStudio using Spearman's correlation. It shows that both methods are good and hence achieved similar and comparable results. Both are reliable methods and can be used.

4.6 Renal morphometry

4.6.1 Relative medullary thickness (RMT)

The RMT (shown in figure 4.8) was slightly increased in all the LP-treated groups compared to NPC and compared to their cohorts except a decrease in LPQ compared NPQ, which is also not significant (p=0.2912).

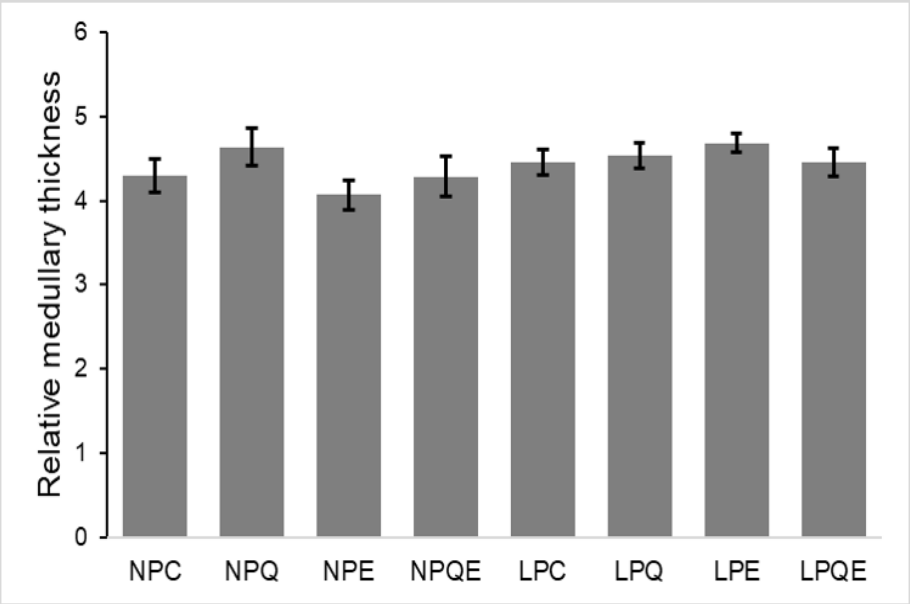

Figure 4.8: Relative medullary thickness

The relative medullary thickness in all the experimental animals. However, no statistically significant difference (n=8). Key: NPC & LPC– Normal and Low protein controls, NPE & LPE- Normal and Low protein alcohol only, NPQ & LPQ- Normal and Low protein chloroquine only, NPEQ &LPQE –Chloroquine and alcohol concurrent treatment.

4.6.2 Cortical thickness

The results of the mean cortical thickness is shown in Figure 4.9. The mean renal cortical thickness tapered significantly (p=0.0004), in all LP-treated groups compared to NPC and compared to their cohorts in NP, however, no significance recorded within the LP-treated or within the NP-treated.

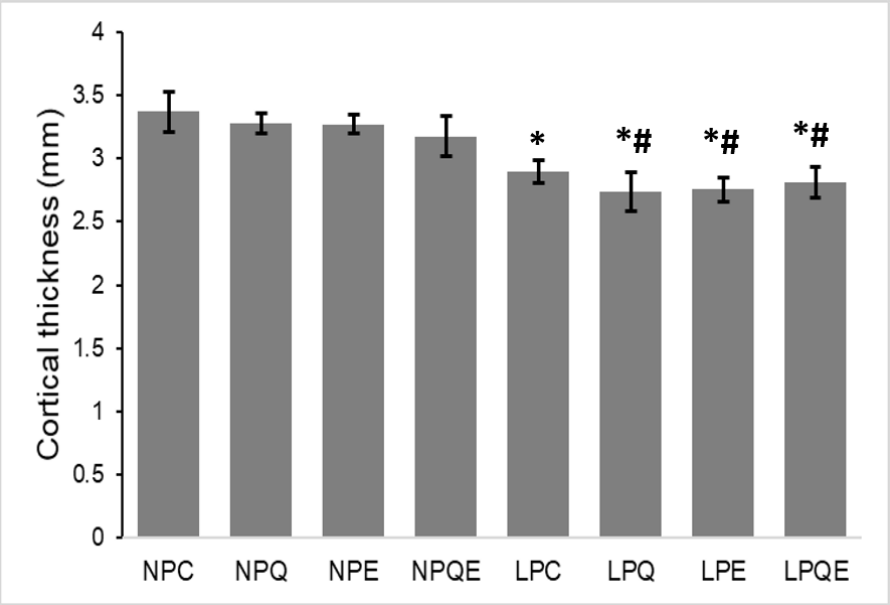

Figure 4.9: Renal cortical thickness

The renal cortical thickness in all the experimental animals. Values with asterisks indicate significant difference from the control group (i.e. NPC), while values with hashtag indicate significant difference comparing cohorts (i.e. NP-groups compared to LP-groups). Absent of asterisk or hashtag indicate no significant difference (n=8). Key: NPC & LPC– Normal and Low protein controls, NPE & LPE- Normal and Low protein alcohol only, NPQ & LPQ- Normal and Low protein chloroquine only, NPEQ &LPQE –Chloroquine and alcohol concurrent treatment.

4.6.3 Morphometry parameters examined in kidney sections

Further morphometric measurements were carried out on the kidney sections after standard H&E processing. The parameters measured were glomerular and renal corpuscular diameters including the urinary (Bowman's) space diameter, the diameter and epithelial heights of the proximal and the distal tubules. In addition, the glomeruli number was counted and the collagen fibre quantified using Masson's trichrome slides.

The mean values from the morphometric evaluation are summarised in table 4.4. The results show a significant decrease of renal corpuscular diameter in LPQ (p=0.0099), LPE (p=0.0253) and LPQE (p=0.0077) compared to NPC, but only significantly decreases in LPE (p=0.0212) and LPQE (p=0.0299) compared to their cohorts in NP. In the LP-treated groups, the renal corpuscular diameter significantly decrease in LPQ (p=0.0139), LPE (p=0.0339) and LPQE (p=0.0109) compared to LPC, but no significance recorded within the NP-treated group.

The Bowman's space significantly (p=0.00001) decreased in NPQ, NPE, NPQE and all the LP-treated groups compared to NPC. Furthermore, a significant decrease was recorded in LPC (p=0.00001), LPE (p=0.00001) and LPQE (p=0.00001) compared to their cohorts in NP. Comparison within LP-treated groups shows a significant decrease of the Bowman's space in the LPE (p=0.0113) and LPQE (p=0.0052) compared to LPC, however no significance seen within the NP-treated groups.

The results of the glomerular diameter recorded show no statistically significant difference in all the pairwise mean comparison of the treated groups with the control and cohorts. However, only a slight decrease of the diameter was seen in all the experimental groups compared to NPC (p=0.4612) except the LPC.

The diameter of the proximal convoluted tubules was significantly decreased (p=0.0224) in LPQE compared to NPC, compared to its cohort (p=0.00001) and compared to LPC (p=0.0288). All NP-treated groups show a slight increase in the proximal tubule diameter, while LPQ and LPE show a slight decrease.

Distal tubule diameter significantly decreased in all the LP-treated groups compared to NPC and compared to their cohorts in NP (p=0.0001). In addition, LPQ (p=0.0462)

and LPQE (p=0.0059) showed a significant decrease compared to LPC. No significant difference within the NP-treated groups.

Proximal convoluted tubules epithelial cell height showed no significant (p=0.2172) change in both the NP-treated and LP-treated groups except a slight increase in NPQ compared to NPC. In the distal convoluted tubules, the epithelial cells height was not significantly (p=0.3284) different in both the NP-treated and LP-treated groups except a slight increase in NPQ and LPQ.

Table 4.4: Morphometry parameters examined in kidney sections

	NPC	NPQ	NPE	NPQE	LPC	LPQ	LPE	LPQE
Glomerular diameter (mm)	0.088±0.002	0.086±0.002	0.086±0.002	0.086±0.002	0.089±0.002	0.087±0.002	0.086±0.002	0.085±0.002
Renal corpuscular diameter (mm)	0.099±0.003	0.095±0.002	0.097±0.002	0.096±0.002	0.096±0.002	0.092±0.002*&	0.093±0.002*#&	0.091±0.002*#&
Urinary space diameter (mm)	0.008±0.0004	0.005±0.0003*	0.006±0.0004*	0.006±0.0004*	0.005±0.0003*	0.005±0.0002*	0.004±0.0002*#&	0.004±0.0002*#&
Proximal tubule diameter (mm)	0.040±0.0006	0.042±0.0008	0.042±0.0006	0.042±0.0006	0.040±0.0006	0.039±0.0007	0.039±0.0006	0.038±0.0007*#&
Proximal tubule epithelial height (mm)	0.007±0.0002	0.008±0.0002	0.007±0.0002	0.007±0.0002	0.007±0.0002	0.007±0.0002	0.007±0.0002	0.007±0.0002
Distal tubule diameter (mm)	0.037±0.0009	0.037±0.0007	0.038±0.0008	0.036±0.0007	0.033±0.0008*	0.032±0.0011*#	0.032±0.0007*#	0.030±0.0006*#&
Distal tubule epithelial height (mm)	0.009±0.0003	0.010±0.0003	0.009±0.0003	0.009±0.0002	0.009±0.0002	0.010±0.0004	0.009±0.0003	0.009±0.0002

Table above shows the morphometry parameters in all the experimental animals. Values with asterisks indicate significant difference from the control group (i.e. NPC), values with hashtag indicate significant difference comparing cohorts (i.e. NP-groups compared to LP-groups), while values with ampersand indicate significance difference from LPC. Absent of asterisk, hashtag or ampersand indicate no significant difference. Mean±SEM (n=5). Key: NPC & LPC– Normal and Low protein controls, NPE & LPE- Normal and Low protein alcohol only, NPQ & LPQ- Normal and Low protein chloroquine only, NPEQ &LPQE –Chloroquine and alcohol concurrent treatment.

4.6.4 Number of glomeruli in section

The number of glomeruli counted in a single camera field (5.78 mm^2 area) was significantly lower (p=0.0195) in the NPQ, NPQE and the entire LP-treated groups (figure 4.10). However, as noted above the glomerular diameter did not significantly change in the experimental groups compared to the control group (p=0.4612).

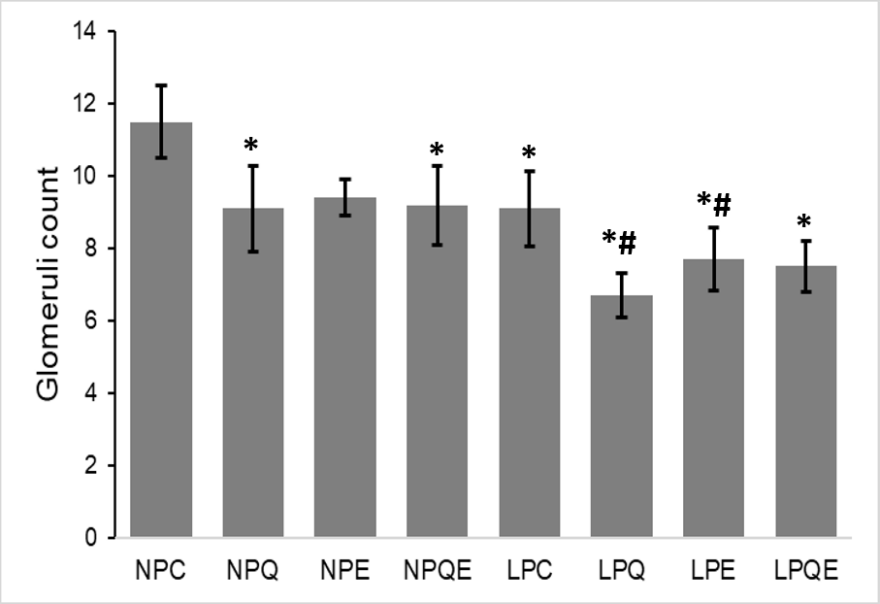

Figure 4.10: Number of glomeruli in section

The number of glomeruli in all the experimental animals. Values with asterisks indicate significant difference from the control group (i.e. NPC), while values with hashtag indicate significant difference comparing cohorts (i.e. NP-groups compared to LP-groups). Absent of asterisk or hashtag indicate no significant difference (n=5). Key: NPC & LPC– Normal and Low protein controls, NPE & LPE- Normal and Low protein alcohol only, NPQ & LPQ- Normal and Low protein chloroquine only, NPEQ &LPQE –Chloroquine and alcohol concurrent treatment.

4.6.5 Collagen fibre quantification

The Masson's trichrome stain qualitatively allow appreciation of the increased collagen fibre deposition in all the LP-treated groups compared to the NPC and their cohorts (figure 4.12). Furthermore, a semi-quantitative grid system was used to effectively quantify the amount of collagen fibre deposited; non-significant (p=0.2099) increase collagen fibre deposition was recorded in all the LP-treated groups compared to control (figure 4.11).

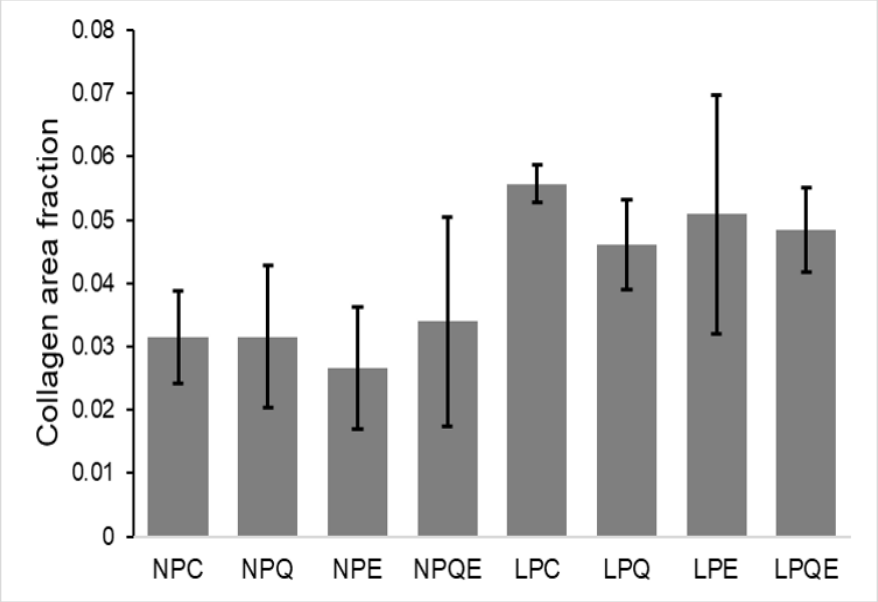

Figure 4.11: Collagen area fraction quantification

The collagen fibre quantification in all the experimental animals. No significant difference recorded (n=5). Key: NPC & LPC– Normal and Low protein controls, NPE & LPE- Normal and Low protein alcohol only, NPQ & LPQ- Normal and Low protein chloroquine only, NPEQ &LPQE –Chloroquine and alcohol concurrent treatment.

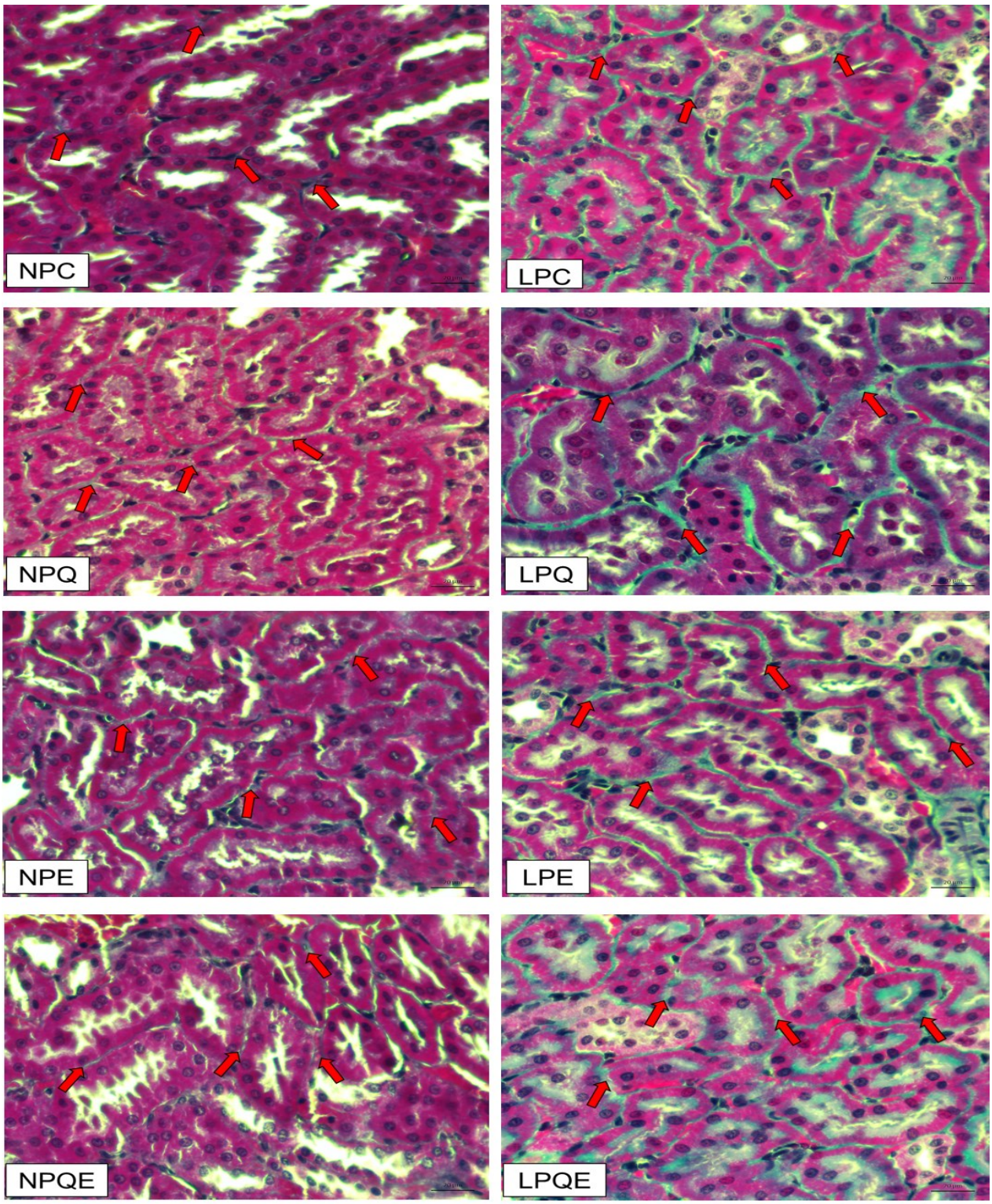

Figure 4.12: Masson's trichrome stain

This plate shows Masson's trichrome stain comparing NP-treated (left panel) and LP-treated (right panel) groups. Light green was used to demonstrate the collagen fibre in this method (red arrow). Scale bar=20µm. Key: NPC & LPC– Normal and Low protein controls, NPE & LPE- Normal and Low protein alcohol only, NPQ & LPQ- Normal and Low protein chloroquine only, NPEQ &LPQE –Chloroquine and alcohol concurrent treatment.

4.7 Histological evaluation

The histological evaluation results (H&E) as shown in figure 4.13 below are as follows:

(**A)** Normal kidney section from the control group (NPC). The proximal tubule (Pt) shows normal low columnar cells with apical brush border intact (white arrow points at Pt cell nucleus). The distal tubule (Dt) shows normal cuboidal cells with a paler cytoplasm (black arrow points at Dt cell nucleus) compared to the proximal tubule (Pt). The renal corpuscle shows an intact glomerular tuft (Gl, Insert) surrounded with clearly visible urinary space (red arrowhead).

(B) Kidney section of rat treated with chloroquine alone in the normal protein group (NPQ). Shows degeneration of the apical brush border (Bb) (light green arrow), the presence of vacuolation (blue arrows) and necrosis (blue asterisk) in some of the proximal tubule (Pt) cells. Degeneration of some distal tubule (Dt) cells (light green arrow) and widening of its lumen. Narrowing of the urinary space (indicated with red arrowhead; Insert) in the renal corpuscle.

(C) Kidney section of rat treated with alcohol alone in the normal protein group (NPE). Narrowing of the urinary space in the renal corpuscle (red arrowhead). Normal proximal tubule (Pt) and mild degeneration of some distal tubule (Dt) cells (light green arrow).

(D) Kidney section of rat treated with chloroquine and alcohol in the normal protein group (NPQE). Degeneration of the apical brush border (Bb) (light green arrow) in some of the proximal tubule (Pt). Degeneration of some distal tubule (Dt) cells (light green arrow) and widening of its lumen. Narrowing of the urinary space in the renal corpuscle (red arrowhead, distortion of Bowman's capsule and glomerular tuft (Gl)).

(E) Kidney section of rat fed low protein only (LPC). Narrowing of the urinary space in the renal corpuscle (red arrowhead). Normal proximal tubule (Pt) cell with normal apical brush border (Bb) and normal distal tubule (Dt) cells.

(F) Kidney section of rat treated with chloroquine alone in the low protein group (LPQ). Shows degeneration of the apical brush border (Bb) (light green arrow) in some of the proximal tubule (Pt) and luminal deposits (black arrowhead). Degeneration of some distal tubule (Dt) cells (light green arrow). Narrowing of the

urinary space in the renal corpuscle (red arrowhead, distortion of Bowman’s capsule and glomerular tuft (GI)).

(G) Kidney section of rat treated with alcohol in the low protein group (LPE). Narrowing of the urinary space in the renal corpuscle (red arrowhead, distortion of Bowman’s capsule and glomerular tuft (GI)). Mild degeneration of the apical brush border (Bb) in some proximal tubule (Pt) (light green arrow) and necrosis of some proximal tubule (Pt) cells (Blue asterisk). The distal tubule (Dt) cells show mild degeneration (light green arrow).

(H) Kidney section of rat treated with chloroquine and alcohol in the low protein group (LPQE). Degeneration of some distal tubule (Dt) cells (light green arrow) and widening of its lumen, nuclei appear bare (black arrow). Narrowing of the urinary space in the renal corpuscle (red arrowhead, distortion of Bowman’s capsule and glomerular tuft (GI)). Degeneration of the apical brush border (Bb) (light green arrow) and luminal debris (black arrowhead; (Insert)) in some of the proximal tubule (Pt).

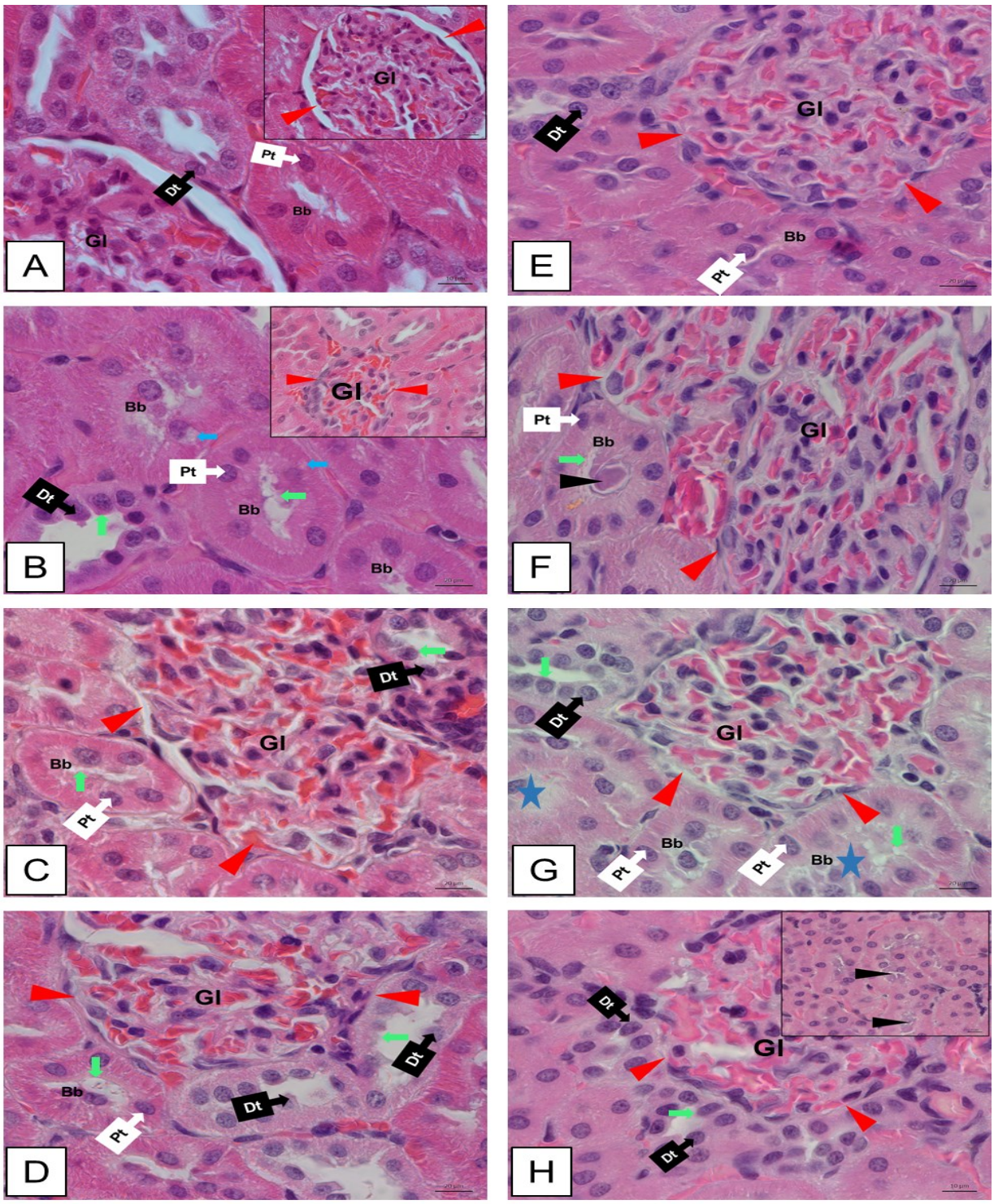

Figure 4.13: Sections of kidney stained with H&E

This plate shows the histological changes in NP-treated (left panel) and LP-treated (right panel) groups. A-NPC, B-NPQ, C-NPE, D-NPQE, E-LPC, F-LPQ, G-LPE, H-LPQE. Scale bar in A-H and the insert = 10µm. Key: Blue asterisk-shows necrosis; Blue arrow-shows vacuolation; Light green arrow-shows degeneration; Red arrowhead-shows the urinary space; Pt-proximal tubule; Dt-distal tubule; Gl-glomerulus; Bb-brush border.

4.8 Immunofluorescence of the AQP2 water channel

The activated AQP2 water channels are located in the apical membrane of the principal cells of collecting duct as shown by comparing the negative control and a positive control (figure 4.14). Immunofluorescence technique allows the qualitative visualisation of the level of activation of the AQP2 water channels in the experimental groups compared to the control (NPC).

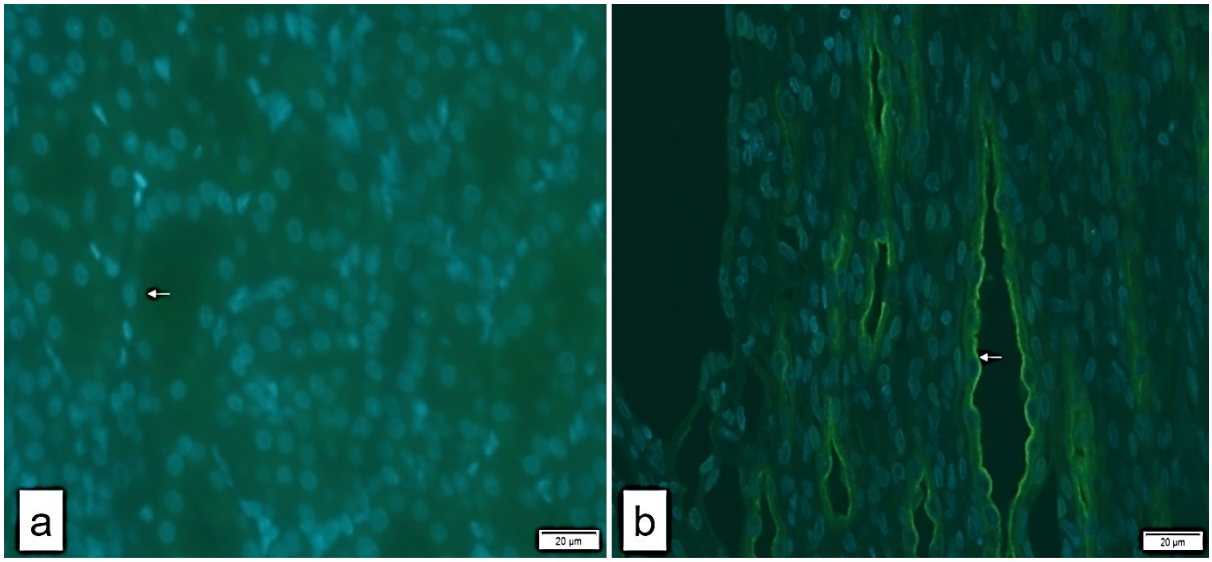

Figure 4.14: Immunolocalization of the AQP2 water channels in kidney tissues

Immunolocalization of the AQP2 water channels. (a) Negative control, (b) Positive control. The white arrow indicates the apical membrane of the collecting duct cells. Scale bar=20µm.

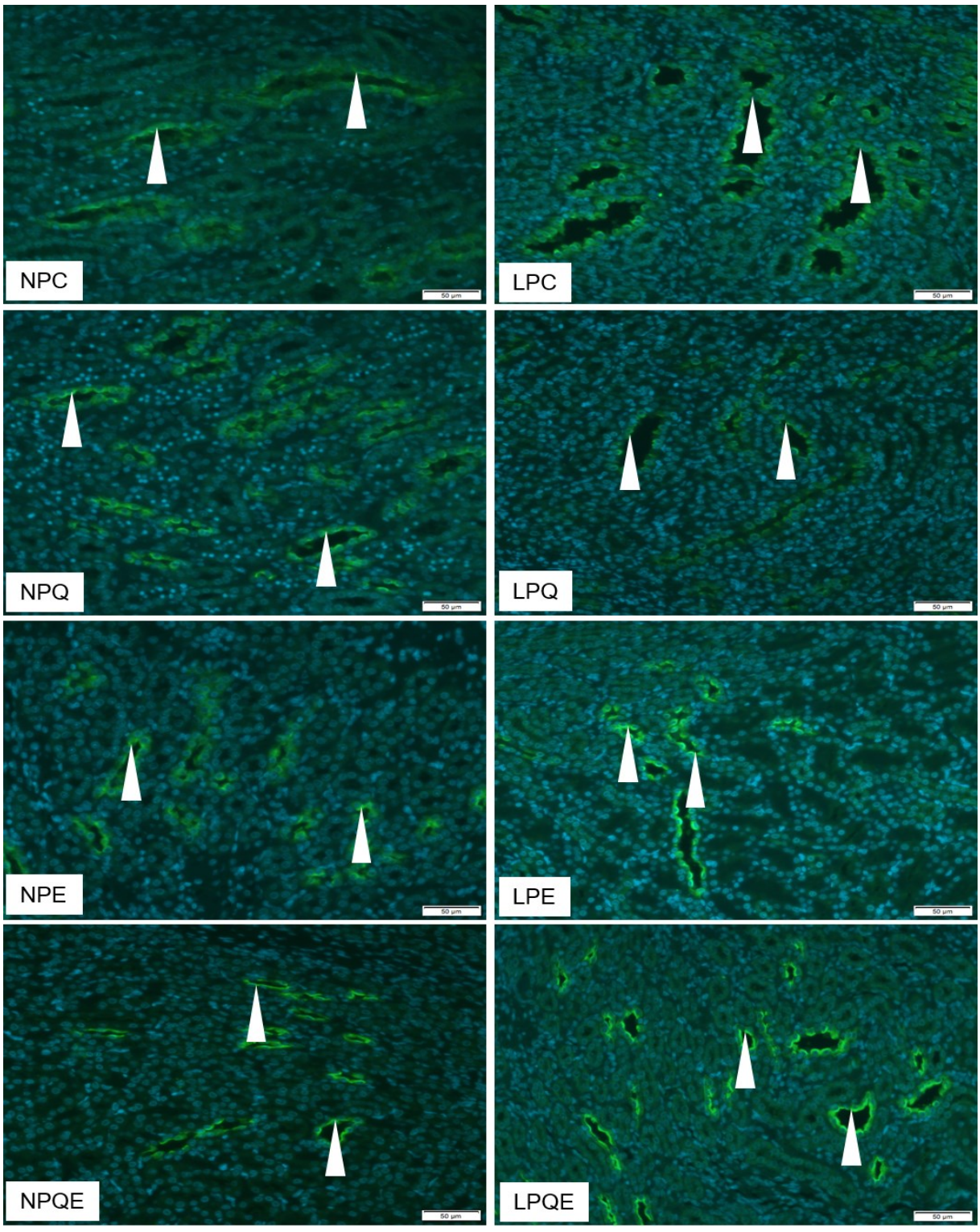

Figure 4.15: Immunofluorescence of the AQP2 water channels

Qualitative evaluation of the AQP2 water channels comparing NP-treated (left panel) and the LP-treated (right panel) using fluorescence intensity. White arrowhead indicates the apical membrane of the collecting duct. Scale bar=50µm. Key: NPC & LPC– Normal and Low protein controls, NPE & LPE- Normal and Low protein alcohol only, NPQ & LPQ- Normal and Low protein chloroquine only, NPEQ &LPQE –Chloroquine and alcohol concurrent treatment.

Figure 4.15 shows the comparison of the NP-treated and the LP-treated groups using the fluorescence intensity. The fluorescence intensity is highest in the LPQE, LPE and the NPQE compared to NPC, while LPQ has the lowest intensity compared to NPC. In addition, LPC, NPQ and NPE show no qualitative difference in the fluorescence intensity compared to NPC. In this regard, the high fluorescence intensity in the apical membrane indicates upregulation of the AQP2 water channels and signifies increased water reabsorption, while low fluorescence intensity indicates downregulation and reduced water reabsorption. Increased water reabsorption causes concentrated urine and a small urine output volume, whereas, reduced water reabsorption causes diluted urine and large urine output volume.

5 CHAPTER FIVE: DISCUSSION

This study aimed at investigating the renal effects of combined administration of alcohol and chloroquine in rats fed low protein. Subsequently, body weight, food intake and urine output of the experimental animals were monitored and recorded at different intervals of the experimental period. Kidney weight was measured and recorded and laboratory analyses were done to assess the kidney volume, relative medullary thickness and cortical thickness. Histological studies evaluated the microscopic pathological changes arising from the treatment using light microscopy and morphometry. Immunofluorescence assessment of the AQP2 water channel also clear the conundrum of interwoven ideas regarding the changes in urine volume output recorded. All the morphological analyses aimed at proving the deleterious renal problems of chloroquine, alcohol and low protein concurrent administration and finally, derangement of the serum urea and creatinine culminate the hypothesis and elicit the required functional correlate of the morphological distortions palpable in our experiment. The following paragraphs detailed the discussion of the results outcome of this study.

5.1 Body weight

Body weight changes are a vital tool for assessing health and disease status in an individual, being a critical indicator of a serious underlying health condition. Adequate quality protein is paramount to maintaining good health status and optimal body weight required for daily activities, while inadequate dietary protein is associated with many health problems including skeletal muscle wasting and weight loss (Wu, 2016). Thus, the significant loss in body weight of the low protein group as against the normal protein fed group is consistent with an earlier report (Mbajiorgu et al., 2008). This suggests physiological and biochemical homeostatic imbalance depicting the inability of the body to withstand the adverse effects of the treatments, indicating that therapeutic efficacy may be compromised in low protein dietary status, even with adequate energy intake.

The non-significant body weight loss following chloroquine and alcohol administration relative to control group contrasts progressive weight gain in rats administered alcohol combined with chloroquine previously report by Musabayane et al. (2000a)

alluding that calorie intake from alcohol was responsible for the weight gain since progressive weight loss was recorded in rats given chloroquine alone. However, the difference in our results could be due to the duration of alcohol administration and experimental design. While Musabayane et al. (2000a) treated the animals for four weeks, our result (after 8 weeks treatment) is in consonance with an earlier report with significant weight loss (Broulik et al., 2010) in which the animals were treated with alcohol for 12 weeks. Despite the significant weight loss in the low protein groups, no significant changes in food consumption were recorded in all the experimental groups, which is in line with the result reported by Rinaldi et al. (2013). This suggests that the weight loss in low protein group is not associated with lack of feeding but rather the quality of the food, which may have negatively affected the physiological and biochemical processes related to bodybuilding.

5.2 Organ weight

The organ weight in toxicity studies reveals invaluable insight alongside the microscopic changes (Bailey et al., 2004). In this study, the absolute kidney weight of the experimental rats at end of experiment was significantly lower in the low protein groups. However, report suggested that absolute organ weight can sometimes present less accurate interpretation of the actual toxicity of a xenobiotic (Nirogi et al., 2014), especially with significant body weight changes. Thus, for comparative purposes, relative organ weight (i.e. body weight percentage) is preferred (Nirogi et al., 2014).

The relative kidney weight was decreased in low protein groups compared to normal protein treated groups and control group. Separate chloroquine or alcohol treatment significantly decreased relative kidney weight in the low protein fed rats, but only slight changes were recorded when administered together, suggesting that possibly the drugs interactively negate the effects of each other. Furthermore, the significant reduction of kidney weight in LP-treated groups compared to NP- groups in both absolute and relative kidney weights, concurred with body weight results suggesting that adequate protein diet is vital for optimal functioning of normal biochemical and physiological processes that underpins maintenance of ideal body and organ weights, even against chemical insults.

5.3 Kidney volume

Kidney volume is arguably the most significant clinical indicator of kidney disease progression (Grantham and Torres, 2016). Several toxicity studies in human (Roseman et al., 2016) and animals (Mansouri et al., 2016; Deniz et al., 2017) on the kidney begins with total kidney volume assessment. In this study, kidney volume assessment and comparisons show there was significant kidney shrinkage in rats on low protein diet contrary to NP-treated groups and control group. This may be accounted for by general body weight loss in addition to kidney parenchymal contraction caused by increased collagen deposition (Hewitson, 2012). The results also showed a slight increase in kidney volume of chloroquine-treated rats in NP-treated groups compared to control group but recorded normal volume in the alcohol alone or in combination with chloroquine treated rats compared to control. However, the absence of change in kidney volume in ethanol-treated group is in contrast with a previous report which, associated alcohol treatment with kidney swelling in both human and rats (Epstein, 1997). Perhaps, because alcoholic liver cirrhosis linked with kidney enlargement (Epstein, 1997) did not occur in this study owing to the duration of the experiment since the two methods employed in the estimation of kidney volume yielded same results.

The two methods were used to ensure the accuracy of results relative to treatment effects. VGStudio kidney volume estimation is an automated, reliable software generated result, that helps validate the stereological method. A strong correlation between the two methods was observed validating the accuracy of the two methods and validity of our results.

5.4 Histology and morphometry

The histological and morphometry techniques employed to delineate the adverse effect of chloroquine and/or alcohol administration with normal or low protein dietary intake in kidney revealed some interesting results.

Histological examination revealed degeneration of apical brush border in proximal tubule cells, presence of vacuolation, necrosis and luminal deposits with chloroquine treatment but such were absent in the ethanol-treated rats in all the treatment groups

(i.e. NP- and LP-treated rats) relative to control group. But both chloroquine and alcohol treatments distinctly recorded degeneration of the distal tubule cells (evidenced by the bare nuclei within the lumen) and the narrowing of urinary space as previously reported by Musabayane et al. (2000b). Furthermore, combined treatments with chloroquine and alcohol also caused distortion of Bowman's capsule and glomeruli tuft in addition to all the above-mentioned features in both NP- and LP –treated groups compared to control group. These changes indicate a cellular response to stress and injury (Henics and Wheatley, 1999) and further suggest that chloroquine more adversely affected the renal morphology than alcohol in both dietary groups. Although more adversely in the LP-treated group, adequate protein intake will ameliorate the adverse renal effects of chloroquine and/or ethanol. However, inadequate protein intake with alcohol administration is just as detrimental as chloroquine. Additionally, it showed that adverse effects of alcohol treatment might require longer duration to become apparent since only mild distortion of distal tubule was observed.

The increased collagen deposition in the renal interstitium shown in LP-treated groups (more in LPQ than in LPE and infra-additively in LPEQ –treated group) was more than in NP-treated groups. This suggests a degree of adverse renal functional impairment and is consistent with a previous study that reported increased collagen deposition in prostate gland of rats following intrauterine exposure to 6% protein restriction (Rinaldi et al., 2013). However, to the best of our knowledge, the association between increased collagen deposition and LP-dietary intake in kidney tissue has not been reported.

The significantly decreased renal corpuscle diameter and slightly reduced glomeruli tuft diameter following alcohol and chloroquine treatments or both combined recorded in LP-treated groups compared to NP-treated groups and the control may be responsible for the narrowing of urinary space observed in morphometric measurements. Although the glomeruli tuft diameter only slightly changed, the number of glomeruli significantly reduced in the entire experimental groups compared to control except in NP-ethanol-treated rats. This reduction in glomeruli number points to renal functional derangements, which correlates with elevated serum creatinine and reduced urinal output recorded in this study, which suggests disposition to oliguria. Previous reports have associated chloroquine with obliteration and sclerosis of the glomeruli (Mũller-Hõcker et al., 2003; Albay et al., 2005) but

reduced glomeruli number was not reported. However, reduced nephron number was reported in rats exposed to intrauterine protein restriction (Siddique et al., 2014) and intrauterine alcohol exposure (Gray et al., 2010).

While the proximal tubules diameter was slightly decreased by alcohol or chloroquine independently, the diameter of the distal tubule was significantly decreased in LP-treated groups. However, in combination (i.e. LPEQ), both proximal and distal tubules were significantly reduced compared to the NP-groups and the control groups. Contrary to the results on the LP- groups, the proximal tubule diameter was slightly increased while the distal tubule was unaffected in the NP- groups compared to control group. However, the slight decrease observed in NPEQ- treated group in comparison with the control group as well as NPE- and NPQ- groups suggests the absence of synergistic action between alcohol and chloroquine. Despite changes in tubular diameter, the height of epithelial cells remained more or less unchanged except for a slight increase of proximal and distal tubule epithelial cell height in LPQ-treated group compared to control.

The renal cortical thickness is one of the reliable indicators of renal function (Yamashita et al., 2015). Therefore the slight reduction in NP-treated rats and significantly reduced cortical thickness in LP-treated rats in comparison to control group may explain decreased number of glomeruli observed in this study and as well the increased collagen deposition which possibly also resulted in a contraction of renal cortex.

The relative medullary thickness (RMT) is one of many factors that influence maximum urine concentrating ability of kidney. Other factors include presence of normal fornices in renal pelvis, structural organisation of collecting duct, dimensions of nephron and epithelial structure in renal corpuscle and tubules (Goodarzi and Akbari, 2016). Some studies have reported on relationship of RMT to body size and habitat (Beuchat, 1996; Laakkonen, 2002; Al-Kahtani et al., 2004; Tejo Riquelme et al., 2014). The present report considered the relationship of RMT and urine concentration ability as a marker of kidney adaptation in relation to the effects of chloroquine and alcohol administration in varying dietary protein intake. Abdellatif and Hassan (2013) reported a significantly increased RMT with compensated hypertrophy, following uninephrectomy of contralateral kidney in a goat suggesting that an increased workload on kidney will cause increased RMT. The non-significant

changes in RMT gross measurements in all the treatments groups (i.e. NP- and LP-treated rat groups) suggests that this parameter may not be subject to adverse effects of these treatments in both dietary conditions.

5.5 Aquaporin 2 water channel and urine volume

Aquaporin 2 water channel regulation is instrumental to urine concentrating mechanisms and kidney function in regulating body water and electrolytes homeostasis (Kwon et al., 2013). However, correlation between AQP2 activity regulation and urine volume, which is a marker of kidney function, was noticed. The AQP2 water channel helps further our understanding of the effects of chloroquine and/or alcohol with normal or low protein diet on normal renal function. Both Chloroquine and alcohol administration altered the regulation of AQP2 and urine production relative to dietary group. This is because reduced body mass and kidney shrinkage in low protein fed rats might affect the urine production processes and contribute significantly to urine output. The results show no obvious change of the AQP2 fluorescence intensity in normal protein due to chloroquine or alcohol administration. However, the urine production (i.e. urine production at termination) was slightly increased by chloroquine in NP-treated rats suggesting downregulation of AQP2 as previously reported (Von Bergen and Blount, 2012), in which the rats also developed polyuria. On the other hand, alcohol administration caused a slight decrease (in this experimental group) in urine production suggesting upregulation of AQP2 as previously reported (García-Delgado et al., 2004). The interactive effect of the treatments shows glaring upregulation of AQP2 intensity, possibly from the synergistic interaction between chloroquine and ethanol, which corresponds to almost half of the urine production in the control group, although statistically non-significant.

While low protein diet alone caused increased urine volume with no obvious change in AQP2 intensity, a previous report using western blot technique, reported reduced AQP2 protein and urine volume following two weeks low protein feeding (Sands et al., 1996). The scope of our study could not give a comprehensive molecular explanation to this difference, but it might suggest that prolonged duration in our study could have led to unique acclimatization, such that the fluorescence could not

detect an insignificant change in AQP2 channel. Secondly, the methodological approach employed differ in both studies and may lead to the differences in results outcome. Furthermore, LPQ-treated rats exhibited obvious downregulation of the AQP2 intensity, corresponding to slightly increased urine volume compared to low protein control (i.e. LPC). Contrarily, alcohol administration or concurrent with chloroquine cause obvious upregulation of AQP2, which correlates with half the urine volume compared to LPC. The interactive effect of chloroquine and alcohol on the regulation of AQP2 in both normal protein and low protein conditions is a novel finding from this study. In general, the urine volume began to decline in the LP-treated rats immediately after the one-week acclimatization, before the commencement of treatment. Moreover, the urine volume progressively declines in these groups mid-treatment and at termination compared to NP-treated and control.

5.6 Biochemical markers of kidney function

Clinically, urea and creatinine are commonly requested biochemical tests to assess renal function (Den Bakker et al., 2018). In this study, we assayed serum urea and creatinine to correlate the histological changes in the kidney to biochemical indicators of renal function.

Creatinine is the product of creatinine phosphate breakdown in the muscle and serum elevated values are associated with reduced glomerular filtration capacity to filter the waste product (Den Bakker et al., 2018). The slight and significant elevations due to chloroquine and alcohol respectively is consistent with a previous report by Todorovic et al. (2014) on chloroquine and Das et al. (2008) on ethanol, generally suggesting decline in renal function and as well in concomitant administration of chloroquine and alcohol which recorded elevated serum creatinine in both the dietary groups.

Serum urea level is significantly lower in low protein fed groups compared to control, but remain normal in the normal protein groups following chloroquine and/or alcohol administration. This is because urea is the product of amino acids metabolism and the amount of protein intake correlate with the amount of urea produced (Weiner et al., 2015). This pattern of decreased serum urea and increased serum creatinine attributed to low protein diet had been reported (Carrillo et al., 2014).

5.7 Conclusion

This study investigated the renal morphological changes caused by the interaction of chloroquine and alcohol in NP- and LP- dietary conditions. The findings of this study show the detrimental effect of chloroquine and/or alcohol administration in the kidney exacerbated by low protein than in normal protein. Moreover, low protein alone causes kidney damage and functional derangements, which is not surprising because low protein diet had previously been implicated in organ damage histologically (Norman et al., 2011).

Finally, this study is the first to show the interactive effects of chloroquine and alcohol concomitant administration in the kidney using morphometry among other novel findings in both normal and low protein conditions. Our results also indicated that adequate dietary protein could prevent, minimize and/or reverse the kidney histological distortions caused by alcohol and/or chloroquine.

5.8 Limitations and future research

Recovery phase not included due to time limitation for the study. Recovery phase could have clarify the healing/progression of kidney damages with chloroquine and alcohol withdrawal or by reinstituting adequate protein diet. Future research will seek to clarify this limitation and employ more analyses like the ADH hormonal assay, which correlates with AQP2 results. Serum/urine electrolytes to correlate with tubular function. Urine and plasma osmolality to correlate with maximum urine concentration and RMT.

5.9 Problems

Problem encountered in this research is the low protein diet formulation due to delay in getting the feed analysis results for the low protein formula.

6 REFERENCE LIST

1. Abdellatif, A. M. and Hassan, Y. (2013). Effects of uninephrectomy on morphological and histological measurements of the remnant kidney in a goat (*capra hircus*) model. *J Phys Pharm Adv,* 3(3)**,** 94-102. [doi:10.5455/jppa.20130322065835]

2. Adam, I. and Elbashir, M. I. (2004). Acute gluteal abscess due to chloroquine injection in sudanese pregnant woman. *Saudi Med J,* 25(7)**,** 963-964.

3. Adelusi, S. and Salako, L. (1982). The effect of protein-energy malnutrition on the absorption, distribution and elimination of chloroquine in the rat. *Gen Pharmacol-Vasc S* 13(6)**,** 505-509. [doi:10.1016/0306-3623(82)90025-8]

4. Ahmed, M. H., Ashton, N. and Balment, R. J. (2003). The effect of chloroquine on renal function and vasopressin secretion: A nitric oxide-dependent effect. *J Pharm Exp Ther,* 304(1)**,** 156-161. [doi:10.1124/jpet.102.042523]

5. Al-Bari, M. A. (2015). Chloroquine analogues in drug discovery: New directions of uses, mechanisms of actions and toxic manifestations from malaria to multifarious diseases. *J Antimicrob Chemother,* 70(6)**,** 1608-1621. [doi:10.1093/jac/dkv018]

6. Al-Kahtani, M. A., Zuleta, C., Caviedes-Vidal, E., et al. (2004). Kidney mass and relative medullary thickness of rodents in relation to habitat, body size and phylogeny. *Physiol Biochem Zool,* 77(3)**,** 346-365. [doi:10.1086/420941]

7. Albay, D., Adler, S. G., Philipose, J., et al. (2005). Chloroquine-induced lipidosis mimicking Fabry disease. *Mod Pathol,* 18(5)**,** 733-738. [doi:10.1038/modpathol.3800344]

8. Ashley, E. A., Dhorda, M., Fairhurst, R. M., et al. (2014). Spread of artemisinin resistance in *Plasmodium falciparum* malaria. *N Engl J Med,* 371(5)**,** 411-423. [doi:10.1056/NEJMoa1314981]

9. Augustijns, P. and Verbeke, N. (1993). Stereoselective pharmacokinetic properties of chloroquine and de-ethyl-chloroquine in humans. *Clin Pharmacokinet,* 24(3)**,** 259-269. [doi:10.2165/00003088-199324030-00007]

10. Bailey, S. A., Zidell, R. H. and Perry, R. W. (2004). Relationships between organ weight and body/brain weight in the rat: What is the best analytical endpoint? *Toxicol Pathol,* 32(4)**,** 448-466. [doi:10.1080/01926230490465874]

11. Bain, L. E., Awah, P. K., Geraldine, N., et al. (2013). Malnutrition in Sub–Saharan Africa: Burden, causes and prospects. *Pan Afr Med J,* 15(1)**,** 120-129. [doi:10.11604/pamj.2013.15.120.2535]

12. Berg, J. P. V. D., Vereecke, H. E. M., Proost, J. H., et al. (2017). Pharmacokinetic and pharmacodynamic interactions in anaesthesia: A review of current knowledge and how it can be used to optimize anaesthetic drug administration. *Br J Anaesth,* 118(1)**,** 44-57. [doi:10.1093/bja/aew312]

13. Beuchat, C. A. (1996). Structure and concentrating ability of the mammalian kidney: Correlations with habitat. *Am J Physiol Regul Integr Comp Physiol,* 271(1)**,** R157-R179.

14. Bhalekar, M. R., Upadhaya, P. G., Nalawade, S. D., et al. (2015). Anti-rheumatic activity of chloroquine-SLN gel on wistar rats using complete freund's adjuvant (CFA) model. *Indian J Rheumatol,* 10(2)**,** 58-64. [doi:10.1016/j.injr.2015.03.008]

15. Bijker, E. M., Bastiaens, G. J., Teirlinck, A. C., et al. (2013). Protection against malaria after immunization by chloroquine prophylaxis and sporozoites is mediated by preerythrocytic immunity. *Proc Natl Acad Sci U S A,* 110(19)**,** 7862-7867. [doi:10.1073/pnas.1220360110]

16. Broulik, P., Vondrova, J., Ruzicka, P., et al. (2010). The effect of chronic alcohol administration on bone mineral content and bone strength in male rats. *Physiol Res,* 59(4)**,** 599-604.

17. Browning, D. J. (2014). Pharmacology of chloroquine and hydroxychloroquine. *Hydroxychloroquine and chloroquine retinopathy.* Newyork: Springer, pp.35-63.

18. Caldwell, J., Gardner, I. and Swales, N. (1995). An introduction to drug disposition: The basic principles of absorption, distribution, metabolism, and excretion. *Toxicol Pathol,* 23(2)**,** 102-114.

19. Campisano, S. E., Echarte, S. M., Podaza, E., et al. (2017). Protein malnutrition during fetal programming induces fatty liver in adult male offspring rats. *J Physiol Biochem,* 73(2)**,** 275-285. [doi:10.1007/s13105-017-0549-1]

20. Carrillo, E., Jimenez, M. A., Sanchez, C., et al. (2014). Protein malnutrition impairs the immune response and influences the severity of infection in a hamster model of chronic visceral leishmaniasis. *PLOS one,* 9(2)**,** e89412. [doi:10.1371/journal.pone.0089412]

21. Casotti, G., Mancina, C. A. and Braun, E. J. (2006). Relationships between renal morphology and diet in 26 species of new world bats (suborder microchiroptera). *Zoology,* 109(3)**,** 196-207. [doi:10.1016/j.zool.2006.03.003]

22. Caterina, P., Antonello, D. P., Chiara, G., et al. (2013). Pharmacokinetic drug-drug interaction and their implication in clinical management. *J Res Med Sci,* 18**,** 600-609.

23. CDC. 2015. *Anopheles mosquitoes* [Online]. Atlanta, USA: CDC. Available: https://www.cdc.gov/malaria/about/biology/mosquitoes/index.html [Accessed 20 June 2018].

24. Cooper, R. and Magwere, T. (2008). Chloroquine: Novel uses and manifestations. *Indian J Med Res,* 127(4)**,** 305-316.

25. Costardi, J. V. V., Nampo, R. A., Silva, G. L., et al. (2015). A review on alcohol: From the central action mechanism to chemical dependency. *Rev Assoc Med Bras,* 61(4)**,** 381-387.

26. Cowman, A. F., Healer, J., Marapana, D., et al. (2016). Malaria: Biology and disease. *Cell,* 167(3)**,** 610-624. [doi:10.1016/j.cell.2016.07.055]

27. Das, S. K., Varadhan, S., Dhanya, L., et al. (2008). Effects of chronic ethanol exposure on renal function tests and oxidative stress in kidney. *Indian J Clin Biochem,* 23(4)**,** 341-344. [doi:10.1007/s12291-008-0075-6]

28. De Vries, P., Oosterhuis, B. and Van Boxtel, C. (1994). Single-dose pharmacokinetics of chloroquine and its main metabolite in healthy volunteers. *Drug Invest,* 8(3)**,** 143-149. [doi:10.1007/BF03259430]

29. Delanghe, J. R. and Speeckaert, M. M. (2011). Creatinine determination according to Jaffe—what does it stand for? *Nephrol Dial Transplant plus,* 4**,** 83–86. [doi:10.1093/ndtplus/sfq211]

30. Den Bakker, E., Gemke, R. J. and Bökenkamp, A. (2018). Endogenous markers for kidney function in children: A review. *Crit Rev Clin Lab Sci***,** 1-21. [doi:10.1080/10408363.2018.1427041]

31. Deniz, Ö. G., Kıvrak, E. G., Kaplan, A. A., et al. (2017). Effects of folic acid on rat kidney exposed to 900MHz electromagnetic radiation. *J Microsc Ultrastruct*. [doi:10.1016/j.jmau.2017.06.001]

32. Dos Santos, G. G., Batool, S., Hastreiter, A., et al. (2017). The influence of protein malnutrition on biological and immunomodulatory aspects of bone marrow mesenchymal stem cells. *Clin Nutr,* 36(4)**,** 1149-1157. [doi:10.1016/j.clnu.2016.08.005]

33. Drayer, D. E. (1974). Pathways of drug metabolism in man. *Med Clin North Am,* 58(5)**,** 927-944.

34. Ducharme, J. and Farinotti, R. (1996). Clinical pharmacokinetics and metabolism of chloroquine. *Clin Pharmacokinet,* 31(4)**,** 257-274.

35. Eckardt, M. J., File, S. E., Gessa, G. L., et al. (1998). Effects of moderate alcohol consumption on the central nervous system. *Alcohol Clin Exp Res,* 22(5)**,** 998-1040. [doi:10.1111/j.1530-0277.1998.tb03695.x]

36. El Shishtawy, M. A., Hassan, K. H., Ramzy, R., et al. (2015). Comparative toxicity study of chloroquine and hydroxychloroquine on adult albino rats. *Eur Sci J,* 1**,** 399-407.

37. Epstein, M. (1997). Alcohol's impact on kidney function. *Alcohol Health Res World,* 21(1)**,** 84-91.

38. Ezzeldin, E. (2012). Pharmacodynamic and pharmacokinetics of metronidazole in protein malnourished rats. *Afr J Pharm Pharmacol,* 6(43)**,** 2982-2993. [doi:10.5897/AJPP12.374]

39. Farahna, M., Bedri, S., Khalid, S., et al. (2010). Anti-plasmodial effects of *Azadirachta indica* in experimental cerebral malaria: Apoptosis of cerebellar Purkinje cells of mice as a marker. *North Am J Med Sci,* 2(11)**,** 518-525. [doi:10.4297/najms.2010.2518]

40. Ferreira-Borges, C., Rehm, J., Dias, S., et al. (2015). The impact of alcohol consumption on african people in 2012: An analysis of burden of disease. *Trop Med Int Health,* 21(1)**,** 52-60. [doi:10.1111/tmi.12618]

41. Foley, M. and Tilley, L. (1997). Quinoline antimalarials: Mechanisms of action and resistance. *Int J Parasitol,* 27(2)**,** 231-240. [doi:10.1016/S0020-7519(96)00152-X]

42. Fraser, A. G. (1997). Pharmacokinetic interactions between alcohol and other drugs. *Clin Pharmacokinet,* 33(2)**,** 79-90.

43. Frosch, A. E., Laufer, M. K., Mathanga, D. P., et al. (2014). The return of widespread chloroquine-sensitive *Plasmodium falciparum* to Malawi. *J Infect Dis,* 210(7)**,** 1110-1114. [doi:10.1093/infdis/jiu216]

44. Frosch, A. E., Venkatesan, M. and Laufer, M. K. (2011). Patterns of chloroquine use and resistance in Sub-Saharan Africa: A systematic review of household survey and molecular data. *Malar J,* 10(116). [doi:10.1186/1475-2875-10-116]

45. García-Delgado, M., Peral, M. J., García-Benítez, O., et al. (2004). Prolonged ethanol ingestion increases renal AQP2 and AQP3 expression in adult rats and in their offspring. *J Membrane Biol* 198(2)**,** 89-94. [doi:10.1007/s00232-004-0662-2]

46. Gately, I. (2008). The grain and the grape. *Drink: A cultural history of alcohol.* Newyork, USA: Penguin, pp.2-12.

47. Ginsburg, H., Famin, O., Zhang, J., et al. (1998). Inhibition of glutathione-dependent degradation of heme by chloroquine and amodiaquine as a possible basis for their antimalarial mode of action. *Biochem Pharmacol,* 56(10)**,** 1305-1313.

48. Glassock, R. J., Warnock, D. G. and Delanaye, P. (2017). The global burden of chronic kidney disease: Estimates, variability and pitfalls. *Nat Rev Nephrol,* 13(2)**,** 104-114. [doi:10.1038/nrneph.2016.163]

49. Goodarzi, N. and Akbari, M. (2016). Renal structure and its concentrating ability in the Persian squirrel (*Sciurus anomalus*). *Comp Clin Pathol,* 25(2)**,** 445-448. [doi:10.1007/s00580-015-2206-9]

50. Grantham, J. J. and Torres, V. E. (2016). The importance of total kidney volume in evaluating progression of polycystic kidney disease. *Nat Rev Nephrol,* 12(11)**,** 667-677. [doi:10.1038/nrneph.2016.135]

51. Gray, S. P., Denton, K. M., Cullen-Mcewen, L., et al. (2010). Prenatal exposure to alcohol reduces nephron number and raises blood pressure in progeny. *J Am Soc Nephrol* 21(11)**,** 1891-1902. [doi:10.1681/ASN.2010040368]

52. Gundersen, H. and Jensen, E. (1987). The efficiency of systematic sampling in stereology and its prediction. *J Microsc,* 147(3)**,** 229-263.

53. Gustafsson, L., Walker, O., Alvan, G., et al. (1983). Disposition of chloroquine in man after single intravenous and oral doses. *Br J clin Pharmac,* 15(4)**,** 471-479.

54. Hamberg, O., Ovesen, L., Dorfeldt, A., et al. (1990). The effect of dietary energy and protein deficiency on drug metabolism. *Eur J Clin Pharmacol,* 38**,** 567-570.

55. Harhaji-Trajkovic, L., Arsikin, K., Kravic-Stevovic, T., et al. (2012). Chloroquine-mediated lysosomal dysfunction enhances the anticancer effect of nutrient deprivation. *Pharm Res,* 29(8)**,** 2249-2263. [doi:10.1007/s11095-012-0753-1]

56. Henics, T. and Wheatley, D. N. (1999). Cytoplasmic vacuolation, adaptation and cell death: A view on new perspectives and features. *Biol Cell,* 91(7)**,** 485-498.

57. Hewitson, T. D. (2012). Fibrosis in the kidney: Is a problem shared a problem halved? *Fibrogenesis Tissue Repair,* 5(1)**,** S1-S14. [doi:10.1186/1755-1536-5-S1-S14]

58. Hines, R. N. and McCarver, D. G. (2002). The ontogeny of human drug-metabolizing enzymes: Phase I oxidative enzymes. *J Pharm Exp Ther,* 300(2)**,** 355-360. [doi:10.1124/jpet.300.2.355]

59. Hingson, R. W., Heeren, T. and Winter, M. R. (2006). Age at drinking onset and alcohol dependence: Age at onset, duration, and severity. *Arch Pediatr Adolesc Med,* 160(7)**,** 739-746. [doi:10.1001/archpedi.160.7.739]

60. Hlastala, M. P. (1998). The alcohol breath test: A review. *J Appl Physiol,* 84(2)**,** 401-408.

61. Hofstetter, J., Suckokw, M. A. and Hickman, D. L. (2005). Kidneys. *In:* Suckow, M. A., Weisbroth, S. & Franklin, C. (eds.) *The Laboratory Rat.* Second ed. USA: Elsevier Academic Press, pp.110-113.

62. Horak, E. and Sunderman, F. W. (1972). Measurements of serum urea nitrogen by conductivimetric urease assay. *Ann Clin Lab Sci,* 2(6)**,** 425-431.

63. Houzé, P., De Reynies, A., Baud, F., et al. (1992). Simultaneous determination of chloroquine and its three metabolites in human plasma, whole blood and urine by ion-pair high-performance liquid chromatography. *J Chromatogr B Biomed Sci Appl,* 574(2)**,** 305-312. [doi:10.1016/0378-4347(92)80044-Q]

64. Jha, V., Garcia-Garcia, G., Iseki, K., et al. (2013). Chronic kidney disease: Global dimension and perspectives. *Lancet,* 382(9888)**,** 260-272.

65. Kalia, S. and Dutz, J. P. (2007). New concepts in antimalarial use and mode of action in dermatology. *Dermatol Ther,* 20(4)**,** 160-174. [doi:10.1111/j.1529-8019.2007.00131.x]

66. Kato, R. (1977). Drug metabolism under pathological and abnormal physiological states in animals and man. *Xenobiotica,* 7(1-2)**,** 25-92. [doi:10.3109/00498257709036242]

67. Khosa, E., Kuonza, L. R., Kruger, P., et al. (2013). Towards the elimination of malaria in south africa: A review of surveillance data in mutale municipality, limpopo province, 2005 to 2010. *Malar J,* 12(7). [doi:10.1186/1475-2875-12-7]

68. Kirpich, I. A., Miller, M. E., Cave, M. C., et al. (2016). Alcoholic liver disease: Update on the role of dietary fat. *Biomolecules,* 6(1). [doi:10.3390/biom6010001]

69. Krafts, K., Hempelmann, E. and Skórska-Stania, A. (2012). From methylene blue to chloroquine: A brief review of the development of an antimalarial therapy. *Parasitol Res,* 111(1). [doi:10.1007/s00436-012-2886-x]

70. Krishna, S. and White, N. J. (1996). Pharmacokinetics of quinine, chloroquine and amodiaquine. *Clin Pharmacokinet,* 30(4)**,** 263-299. [doi:10.2165/00003088-199630040-00002]

71. Kumar Mishra, S., Singh, P. and Rath, S. K. (2013). Protective effect of quercetin on chloroquine-induced oxidative stress and hepatotoxicity in mice. *Malar Res Treat*. [doi:10.1155/2013/141734]

72. Kwon, T.-H., Frøkiær, J. and Nielsen, S. (2013). Regulation of aquaporin-2 in the kidney: A molecular mechanism of body-water homeostasis. *Kidney Res Clin Pract,* 32(3)**,** 96-102. [doi:10.1016/j.krcp.2013.07.005]

73. Laakkonen, J. (2002). Relative medullary thickness of shrews from arid environments: Intraspecific spatial analysis, and comparison to arctic shrews and tropical tenrecs. *Ann Zool Fennici,* 39(3)**,** 249-255.

74. Lieber, C. (2002). Relationships between nutrition, alcohol use, and liver disease. *Alcohol Res Health,* 27(3)**,** 220-231.

75. Lu, F., Culleton, R., Zhang, M., et al. (2017). Emergence of indigenous artemisinin-resistant *Plasmodium falciparum* in Africa. *N Engl J Med,* 376(10)**,** 991-993. [doi:10.1056/NEJMc1612765]

76. Mackenzie, A. H. (1983). Dose refinements in long-term therapy of rheumatoid arthritis with antimalarials. *Am J Med,* 75(1)**,** 40-45. [doi:10.1016/0002-9343(83)91269-X]

77. Mackenzie, P. I., Somogyi, A. A. and Miners, J. O. (2017). Advances in drug metabolism and pharmacogenetics research in Australia. *Pharmacol Res,* 116**,** 7-19. [doi:10.1016/j.phrs.2016.12.008]

78. Manary, M. (2013). Inadequate dietary protein intake: When does it occur and what are the consequences? *Food Nutr Bull,* 34(2)**,** 247-248.

79. Mansouri, E., Basgen, J. and Saremy, S. (2016). The effects of pomegranate extract on normal adult rat kidney: A stereological study. *Vet Res Forum,* 7(1)**,** 1-6.

80. May, P. A., De Vries, M. M., Marais, A.-S., et al. (2017). Replication of high fetal alcohol spectrum disorders prevalence rates, child characteristics and maternal risk factors in a second sample of rural communities in South Africa. *Int J Environ Res Public Health,* 14(5). [doi:10.3390/ijerph14050522]

81. Mbajiorgu, E. F., Aire, T. A., Volk, W., et al. (2008). Low protein diet enhances the toxicity of combined ethanol and chloroquine administration on gonadal weight, seminiferous tubular diameter and epithelial height of male Sprague-Dawley rats: A morphometric study. *Int J Health Sci,* 1(4)**,** 120-126.

82. McCarver, D. G. and Hines, R. N. (2002). The ontogeny of human drug-metabolizing enzymes: Phase II conjugation enzymes and regulatory mechanisms. *J Pharm Exp Ther,* 300(2)**,** 361-366. [doi:10.1124/jpet.300.2.361]

83. Mekonnen, S. K., Aseffa, A., Berhe, N., et al. (2014). Return of chloroquine-sensitive *Plasmodium falciparum* parasites and emergence of chloroquine-resistant *Plasmodium vivax* in Ethiopia. *Malar J,* 13(1)**,** 244-253. [doi:10.1186/1475-2875-13-244]

84. Meshnick, S. R. and Dobson, M. J. (2001). The history of antimalarial drugs. *In:* Rosenthal, P. J. (ed.) *Antimalarial chemotherapy.* Newyork: Humana press, pp.15-25.

85. Minker, E. and Ivan, J. (1990). Experimental and clinicopharmacological study of rectal absorption of chloroquine. *Acta Physiol Hung,* 77(3-4)**,** 237-248.

86. MMV. 2010. *Parasite lifecycle* [Online]. Available: http://www.mmv.org/malaria-medicines/parasite-lifecycle [Accessed 12 May 2016].

87. Moore, K. L. and Dalley, A. F. (2006). Kidneys, ureters and suprarenal glands. *Clinically Oriented Anatomy.* 5th ed. Philadelphia: Lippincott Williams & Wilkins, pp.308-311.

88. Motamedi, M. K., Barzin, M., Ebrahimi, M., et al. (2017). Severe fatal protein malnutrition and liver failure in a morbidly obese patient after mini-gastric bypass surgery: Case report. *Int J Surg Case Rep,* 33**,** 71-74. [doi:10.1016/j.ijscr.2017.02.033]

89. Motawi, T. K., Abd-Elgawad, H. M. and Shahin, N. N. (2013). Effect of protein malnutrition on the metabolism and toxicity of cisplatin, 5-fluorouracil and mitomycin C in rat stomach. *Food Chem Toxicol,* 56**,** 467-482. [doi:10.1016/j.fct.2013.02.042]

90. Mukherjee, S. (2013). Alcoholism and its effects on the central nervous system. *Curr Neurovasc Res,* 10(3)**,** 256-262.

91. Mũller-Hõcker, J., Schmid, H., Weiss, M., et al. (2003). Chloroquine-induced phospholipidosis of the kidney mimicking Fabry's disease: Case report and review of the literature. *Hum Pathol,* 34(3)**,** 285-289. [doi:10.1053/hupa.2003.36]

92. Musabayane, C., Cooper, R., Osim, E., et al. (2000a). Renal electrolyte and fluid handling in the rat following chloroquine and/or ethanol administration. *Gen Pharmacol-Vasc S* 34(1)**,** 43-51. [doi:10.1016/S0306-3623(00)00045-8]

93. Musabayane, C. T., Cooper, R. G., Rao, P. V. V. P., et al. (2000b). Effects of ethanol on the changes in renal fluid and electrolyte handling and kidney morphology induced by long-term chloroquine administration to rats. *Alcohol,* 22(3)**,** 129-138. [doi:10.1016/S0741-8329(00)00110-5]

94. Mwanza, S., Joshi, S., Nambozi, M., et al. (2016). The return of chloroquine-susceptible *Plasmodium falciparum* malaria in Zambia. *Malar J,* 15(1). [doi:10.1186/s12936-016-1637-3]

95. Mwanza, S., Nambozi, M., Chileshe, J., et al. (2017). Chloroquine-sensitive *plasmodium falciparum* in a high-burden malaria area after over a decade of its withdrawal as first-line antimalarial medicine: Case of nchelenge district. *BMJ Glob Health,* 2(Suppl 2)**,** A17-A17. [doi:10.1136/bmjgh-2016-000260]

96. Naicker, S. (2013). End-stage renal disease in Sub-Saharan Africa. *Kidney Int Suppl,* 3(2)**,** 161-163.

97. Ndam, N. T., Basco, L. K., Ngane, V. F., et al. (2017). Reemergence of chloroquine-sensitive *pfcrt* K76 *Plasmodium falciparum* genotype in southeastern Cameroon. *Malar J,* 16(1). [doi:10.1186/s12936-017-1783-2]

98. Niemelä, O., Niemelä, M., Bloigu, R., et al. (2017). Where should the safe limits of alcohol consumption stand in light of liver enzyme abnormalities in alcohol consumers? *PloS one,* 12(12)**,** e0188574. [doi:10.1371/journal.pone.0188574]

99. Nirogi, R., Goyal, V. K., Jana, S., et al. (2014). What suits best for organ weight analysis: Review of relationship between organ weight and body/brain weight for rodent toxicity studies. *Int J Pharm Sci Res,* 5(4)**,** 1525-1532. [doi:10.13040/IJPSR.0975-8232.5(4).1525-32]

100. Nogueira, L. C., Do Rio, R. F., Lollo, P. C., et al. (2017). Moderate alcoholic beer consumption: The effects on the lipid profile and insulin sensitivity of adult men. *J Food Sci,* 82(7)**,** 1720-1725. [doi:10.1111/1750-3841.13746]

101. Norman, K., Stobäus, N., Gonzalez, M. C., et al. (2011). Hand grip strength: Outcome predictor and marker of nutritional status. *Clin Nutr,* 30(2)**,** 135-142. [doi:10.1016/j.clnu.2010.09.010]

102. Nyengaard, J. R. (1999). Stereologic methods and their application in kidney research. *J Am Soc Nephrol,* 10(5)**,** 1100-1123.

103. O'keefe, J. H., Bhatti, S. K., Bajwa, A., et al. Alcohol and cardiovascular health: The dose makes the poison or the remedy. Mayo Clinic Proceedings, 2014. Elsevier, 382-393.

104. Olafson, K. N., Ketchum, M. A., Rimer, J. D., et al. (2015). Mechanisms of hematin crystallization and inhibition by the antimalarial drug chloroquine. *Proc Natl Acad Sci U S A,* 112(16)**,** 4946-4951. [doi:10.1073/pnas.1501023112]

105. Oluleye, T., Babalola, Y. and Ijaduola, M. (2015). Chloroquine retinopathy: Pattern of presentation in Ibadan, Sub-Sahara Africa. *Eye,* 30**,** 64–67. [doi:10.1038/eye.2015.185]

106. Oscar-Berman, M. and Marinković, K. (2007). Alcohol: Effects on neurobehavioral functions and the brain. *Neuropsychol Rev,* 17(3)**,** 239-257. [doi:10.1007/s11065-007-9038-6]

107. Park, E. J. and Kwon, T. H. (2015). A minireview on vasopressin-regulated aquaporin-2 in kidney collecting duct cells. *Electrolyte Blood Press* 13. [doi:10.5049/EBP.2015.13.1.1]

108. Park, G. (2001). Drug metabolism. *Br J Anaesth,* 1(6)**,** 185-188.

109. Phillips, M. A., Burrows, J. N., Manyando, C., et al. (2017). Malaria. *Nat Rev Dis Prim,* 3. [10.1038/nrdp.2017.50]

110. Pinheiro, P. P., Alencar, D. M. D., Pimentel, J. V. C., et al. (2015). Impacts of alcoholism in public health, a systematic review. *Int Arch Med,* 8(127). [doi:10.3823/1726]

111. Pisa, P. T., Loots, D. T. and Nienaber, C. (2010). Alcohol metabolism and health hazards associated with alcohol abuse in a South African context: A review. *S Afr J Clin Nutr,* 23(3)**,** 4-10.

112. Popova, S., Lange, S., Probst, C., et al. (2017). Estimation of national, regional and global prevalence of alcohol use during pregnancy and fetal alcohol syndrome: A systematic review and meta-analysis. *Lancet Glob Health,* 5(3)**,** e290-e299. [doi:10.1016/S2214-109X(17)30021-9]

113. Projean, D., Baune, B., Farinotti, R., et al. (2003). In vitro metabolism of chloroquine: identification of CYP2C8, CYP3A4 and CYP2D6 as the main isoforms catalyzing N-desethylchloroquine formation. *Drug Metab Dispos,* 31(6)**,** 748-754.

114. Rainsford, K., Parke, A. L., Clifford-Rashotte, M., et al. (2015). Therapy and pharmacological properties of hydroxychloroquine and chloroquine in treatment of systemic lupus erythematosus, rheumatoid arthritis and related diseases. *Inflammopharmacol,* 23(5)**,** 231-269. [doi:10.1007/s10787-015-0239-y]

115. Ramchandani, V., Bosron, W. and Li, T. (2001). Research advances in ethanol metabolism. *Pathol Biol,* 49(9)**,** 676-682. [doi:10.1016/S0369-8114(01)00232-2]

116. Ridley, R. G. (1998). Malaria: Dissecting chloroquine resistance. *Curr Biol,* 8(10)**,** 346-349. [doi:10.1016/S0960-9822(98)70218-0]

117. Rinaldi, J. C., Justulin Jr, L. A., Lacorte, L. M., et al. (2013). Implications of intrauterine protein malnutrition on prostate growth, maturation and aging. *Life Sci,* 92(13)**,** 763-774. [doi:10.1016/j.lfs.2013.02.007]

118. Roseman, D. A., Hwang, S.-J., Oyama-Manabe, N., et al. (2016). Clinical associations of total kidney volume: The Framingham heart study. *Nephrol Dial Transplant*. [doi:10.1093/ndt/gfw237]

119. Ross, M. H. and Pawlina, W. (2011). Urinary system. *Histology a text and atlas with correlated cell and molecular biology.* 6th ed. Philadelphia: Lippincott Williams & Wilkins,, pp.698-723.

120. Rougemont, M., Van Saanen, M., Sahli, R., et al. (2004). Detection of four *Plasmodium spp* in blood from humans by 18S rRNA gene subunit-based and species-specific real-time PCR assays. *J Clin Microbiol,* 42(12)**,** 5636-5643. [doi:10.1128/JCM.42.12.5636–5643.2004]

121. Rundio, A. (2013). Understanding alcoholism. *Nurs Clin N Am,* 48**,** 385–390. [doi:10.1016/j.cnur.2013.05.001]

122. Sands, J. M., Naruse, M., Jacobs, J. D., et al. (1996). Changes in aquaporin-2 protein contribute to the urine concentrating defect in rats fed a low-protein diet. *J Clin Invest,* 97(12)**,** 2807-2814. [doi:10.1172/JCI118736]

123. Santolaria, F. and González-Reimers, E. (2013). Alcohol and nutrition: An overview. *In:* Watson, R. R., Preedy, V. R. & Zibadi, S. (eds.) *Alcohol, nutrition, and health consequences.* Newyork: Humana Press, pp.3-14.

124. Savarino, A., Boelaert, J. R., Cassone, A., et al. (2003). Effects of chloroquine on viral infections: An old drug against today's diseases. *Lancet Infect Dis,* 3(11)**,** 722-727.

125. Savarino, A., Di Trani, L., Donatelli, I., et al. (2006). New insights into the antiviral effects of chloroquine. *Lancet Infect Dis,* 6(2)**,** 67-69.

126. Schönfeldt, H. C. and Hall, N. G. (2012). Dietary protein quality and malnutrition in Africa. *Br J Nutr,* 108(2)**,** 69-76. [doi:10.1017/S0007114512002553]

127. Seki, E. (2016). Acrolein, a new villain in the development of alcoholic liver disease. *Cell Mol Gastroenterol Hepatol,* 2(5)**,** 544-545. [doi:10.1016/j.jcmgh.2016.06.005]

128. Shiryaev, S. A., Mesci, P., Pinto, A., et al. (2017). Repurposing of the anti-malaria drug chloroquine for Zika Virus treatment and prophylaxis. *Sci Rep,* 7. [doi:10.1038/s41598-017-15467-6]

129. Siddique, K., Guzman, G. L., Gattineni, J., et al. (2014). Effect of postnatal maternal protein intake on prenatal programming of hypertension. *Reprod Sci,* 21(12)**,** 1499-1507. [doi:10.1177/1933719114530186]

130. Singh, V. P., Singh, N. and Jaggi, A. S. (2013). A review on renal toxicity profile of common abusive drugs. *Korean J Physiol Pharmacol,* 17(4)**,** 347-357. [doi:10.4196/kjpp.2013.17.4.347]

131. Slater, A. F. (1993). Chloroquine: mechanism of drug action and resistance in *Plasmodium falciparum*. *Pharmac Ther,* 57(2)**,** 203-235.

132. Snyder, B. D., Polasek, T. M. and Doogue, M. P. (2012). Drug interactions: Principles and practice. *Aust Prescr,* 35**,** 85-88. [doi:10.18773/austprescr.2012.037]

133. Spies, C. D., Sander, M., Stangl, K., et al. (2001). Effects of alcohol on the heart. *Curr Opin Crit Care,* 7(5)**,** 337-343.

134. Stanifer, J. W., Jing, B., Tolan, S., et al. (2014). The epidemiology of chronic kidney disease in Sub-Saharan Africa: A systematic review and meta-analysis. *Lancet Glob Health,* 2(3)**,** e174-e181.

135. Sullivan, D. J. (2002). Theories on malarial pigment formation and quinoline action. *Int J Parasitol,* 32(13)**,** 1645-1653. [doi:10.1016/S0020-7519(02)00193-5]

136. Tejo Riquelme, P. A., Diaz Isenrath, G. B., Andino, N., et al. (2014). Renal intraspecific variation along an aridity gradient detected by new renal indices

in a desert herbivorous rodent. *J Exp Zool,* 321(6)**,** 348-356. [doi:10.1002/jez.1863]

137. Temba, M. C., Njobeh, P. B., Adebo, O. A., et al. (2016). The role of compositing cereals with legumes to alleviate protein energy malnutrition in Africa. *Int J Food Sci Technol,* 51(3)**,** 543-554. [doi:10.1111/ijfs.13035]

138. Tenenbaum, A., Wexler, I. and Merrick, J. (2016). Fetal alcohol syndrome. *In:* Rubin, I. L., Merrick, J., Greydanus, D. E. & Patel, D. R. (eds.) *Health care for people with intellectual and developmental disabilities across the lifespan.* Switzerland: Springer, pp.873-880.

139. Titus, E. O. (1989). Recent developments in the understanding of the pharmacokinetics and mechanism of action of chloroquine. *Ther Drug Monit,* 11(4)**,** 369-379.

140. Todorovic, Z., Medic, B., Basta-Jovanovic, G., et al. (2014). Acute pretreatment with chloroquine attenuates renal I/R injury in rats. *PloS One,* 9(3)**,** 1-10.

141. Tönnesmann, E., Kandolf, R. and Lewalter, T. (2013). Chloroquine cardiomyopathy–a review of the literature. *Immunopharmacol Immunotoxicol,* 35(3)**,** 434-442. [doi:10.3109/08923973.2013.780078]

142. Trape, J.-F. (2001). The public health impact of chloroquine resistance in Africa. *Am J Trop Med Hyg,* 64(1 suppl)**,** 12-17.

143. Unekwuojo, E. G., Omale, J. and Aminu, R. O. (2011). Suppressive, curative and prophylactic potentials of Morinda lucida (Benth) against erythrocytic stage of mice infective chloroquine sensitive Plasmodium berghei NK-65. *Br J Appl Sci Technol,* 1(3)**,** 131-140.

144. Von Bergen, T. N. and Blount, M. A. (2012). Chronic use of chloroquine disrupts the urine concentration mechanism by lowering cAMP levels in the inner medulla. *Am J Physiol Renal Physiol,* 303(6)**,** F900-F905. [doi:10.1152/ajprenal.00547.2011]

145. Wallace, D. J., Gudsoorkar, V. S., Weisman, M. H., et al. (2012). New insights into mechanisms of therapeutic effects of antimalarial agents in SLE. *Nat Rev Rheumatol,* 8(9)**,** 522-533.

146. Webb, J. L. (2011). Malaria in Africa. *Hist Compass,* 9(3)**,** 162-170. [doi:10.1111/j.1478-0542.2010.00757.x]

147. Weiner, I. D., Mitch, W. E. and Sands, J. M. (2015). Urea and ammonia metabolism and the control of renal nitrogen excretion. *Clin J Am Soc Nephrol,* 10(8)**,** 1444-1458.

148. Wellems, T. E. and Plowe, C. V. (2001). Chloroquine-resistant malaria. *J Infect Dis,* 184(6)**,** 770-776. [doi:10.1086/322858]

149. WHO (2014). *Global status report on alcohol and health 2014*. Geneva, pp: 48-50.

150. WHO (2017). *World Malaria Report 2016*. Geneva, pp: 41-43.

151. Wilson, J. L. L., Miranda, C. A. and Knepper, M. A. (2013). Vasopressin and the regulation of aquaporin-2. *Clin Exp Nephrol,* 17**,** 751–764. [doi:10.1007/s10157-013-0789-5]

152. Wood, G. C. and Woodcock, B. G. (1970). Effects of dietary protein deficiency on the conjugation of foreign compounds in rat liver. *J Pharm Pharmac,* 22**,** 60S-63S.

153. Wu, G. (2016). Dietary protein intake and human health. *Food Funct,* 7(3)**,** 1251-1265. [doi:10.1039/c5fo01530h]

154. Yamashita, S. R., Atzingen, A. C. V., Iared, W., et al. (2015). Value of renal cortical thickness as a predictor of renal function impairment in chronic renal disease patients. *Radiol Bras,* 48(1)**,** 12-16. [doi:10.1590/0100-3984.2014.0008]

155. Young, B., Lowe, J. S., Stevens, A., et al. (2006). Urinary system. *Wheater's functional histology: A text and colour atlas.* 5th ed. Philadelphia: Elsevier, pp.302-327.

156. Zakhari, S. (2006). Overview: How is alcohol metabolized by the body? *Alcohol Res Health,* 29(4)**,** 245-255.

157. Zha, Y. and Qian, Q. (2017). Protein Nutrition and Malnutrition in CKD and ESRD. *Nutrients,* 9(3). [doi:10.3390/nu9030208]

7 APPENDICES

7.1 Appendix 1: Turnitin report

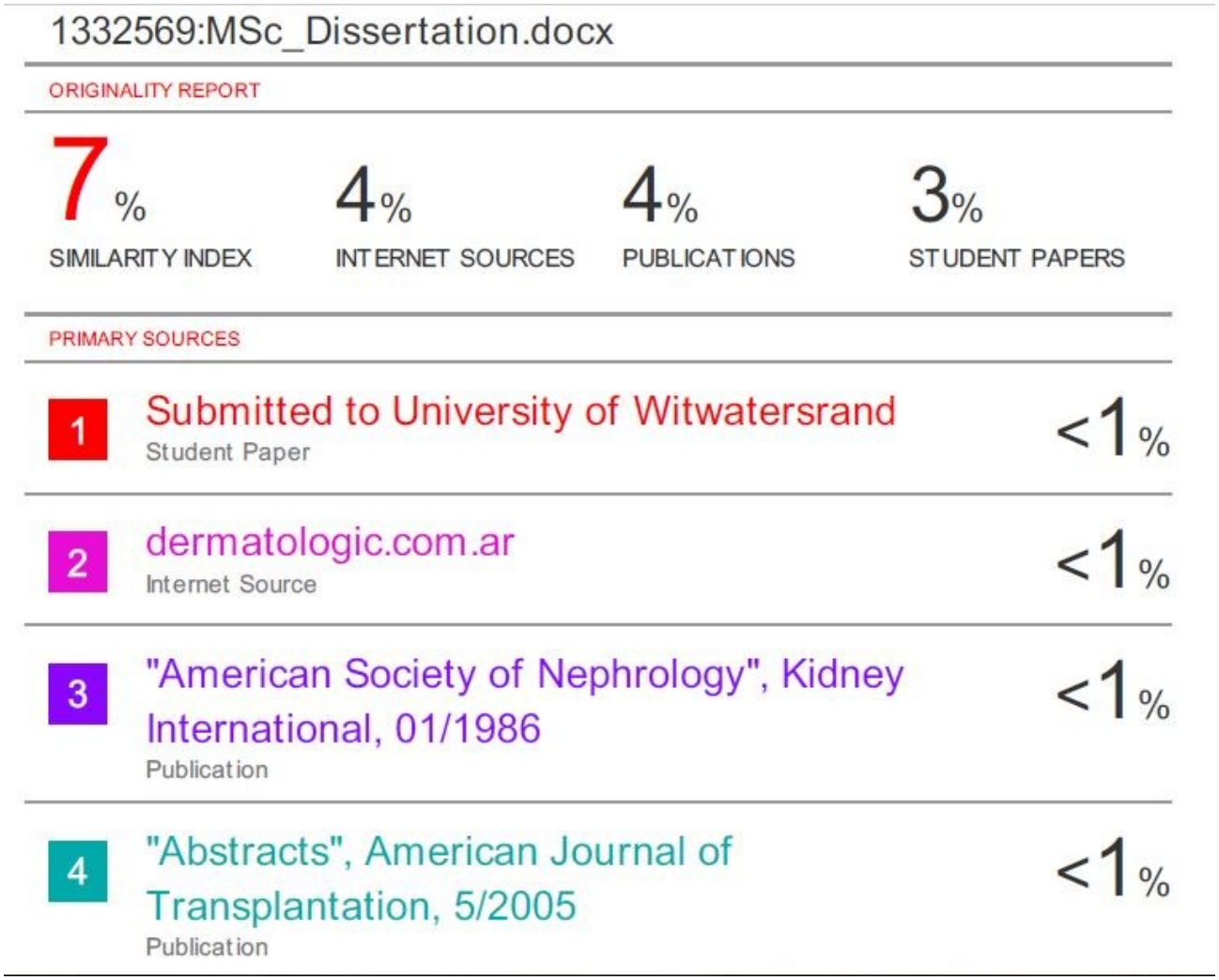

1332569:MSc_Dissertation.docx

ORIGINALITY REPORT

7%	4%	4%	3%
SIMILARITY INDEX	INTERNET SOURCES	PUBLICATIONS	STUDENT PAPERS

PRIMARY SOURCES

1	Submitted to University of Witwatersrand Student Paper	<1%
2	dermatologic.com.ar Internet Source	<1%
3	"American Society of Nephrology", Kidney International, 01/1986 Publication	<1%
4	"Abstracts", American Journal of Transplantation, 5/2005 Publication	<1%

7.2 Appendix 2: Ethics approval

STRICTLY CONFIDENTIAL

ANIMAL ETHICS SCREENING COMMITTEE (AESC)

CLEARANCE CERTIFICATE NO. 2015/11/54/C

APPLICANT: Mr A Abdurrahman

SCHOOL: Anatomical Sciences
DEPARTMENT:
LOCATION:

PROJECT TITLE: Interactions of chloroquine and/or ethanol on renal morphology of normal or low protein fed male Sprague Dawley Rats

Number and Species

80 Male Sprague Dawley Rats

Approval was given for the use of animals for the project described above at an AESC meeting held on 2015/11/24. This approval remains valid until 2018/02/15.

The use of these animals is subject to AESC guidelines for the use and care of animals, is limited to the procedures described in the application form and is subject to any additional conditions listed below:

None

Signed: _____ (Chairperson, AESC) Date: 18th Feb 2016

I am satisfied that the persons listed in this application are competent to perform the procedures therein, in terms of Section 23 (1) (c) of the Veterinary and Para-Veterinary Professions Act (19 of 1982)

Signed: _____ (Registered Veterinarian) Date: 19/2/16

cc: Supervisor: Professor E F Mbajiorgu
Director: CAS

Works 2000/lain0015/AESCCert.wps

7.3 Appendix 3: Modifications of ethics approval

AESC 2012 M&E

Please note that only typewritten applications will be accepted.

UNIVERSITY OF THE WITWATERSRAND

ANIMAL ETHICS SCREENING COMMITTEE
MODIFICATIONS AND EXTENSIONS TO EXPERIMENTS

a. Name: Abdurrahman Abdulkadir

b. School and email address: Anatomical sciences 1332569@students.wits.ac.za

c. Experiment to be modified / extended

		AESC NO	
Original AESC number	2015	11	54/C
Other M&Es :			Nil

d. Project Title: Interaction of chloroquine and/or ethanol on the kidney morphology of normal or low protein fed male Sprague dawley rats.

		No.	Species
e.	Number and species of animals originally approved:	80	*Sprague dawley*
f.	Number of additional animals previously allocated on M&Es:	Nil	
g.	Total number of animals allocated to the experiment to date:	Nil	
h.	Number of animals used to date:	Nil	

i. Specific modification / extension requested:
I request the addition of Dr Hassan Sani Yauri (Person Number 1332558), Miss Lynette Sena (Person Number 493688) and Mr Trust Nyirenda (Person Number 1222576) to be co-workers in the study for technical support.

j. Motivation for modification / extension:

The procedures during receipt and termination of the experimental animals are labour intensive and require help from co-workers.

Date: 10/03/2016 Signature:

RECOMMENDATIONS: Approved.

Inclusion of Miss L Sena, Mr T Nyirenda and Dr H S Yauri as co-workers.
The abovementioned should attend a CAS first-time user's session before working with the rats.

Date: 10th March 2016 Signature:
Chairman AESC

AESC 2012 M&E

Please note that only typewritten applications will be accepted.

UNIVERSITY OF THE WITWATERSRAND

ANIMAL ETHICS SCREENING COMMITTEE

MODIFICATIONS AND EXTENSIONS TO EXPERIMENTS

a. Name: Abdurrahman Abdulkadir

b. School and email address: Anatomical sciences 1332569@students.wits.ac.za

c. Experiment to be modified / extended **AESC NO**

Original AESC number	**2015**	**11**	**54/C**
Other M&Es :	Inclusion of Co-workers		

d. Project Title: Interaction of chloroquine and/or ethanol on the kidney morphology of normal or low protein fed male Sprague dawley rats.

		No.	**Species**
e.	Number and species of animals originally approved:	80	*Sprague dawley*
f.	Number of additional animals previously allocated on M&Es:	Nil	
g.	Total number of animals allocated to the experiment to date:	33	
h.	Number of animals used to date:	33	

i. Specific modification / extension requested:

I kindly request to take photographs of some organs and procedures at termination that will be included in dissertation write up.
In addition I would like to also harvest more organs than initially specified.

j. Motivation for modification / extension:

Photographs will be used as illustrations in the dissertation. The treatments are likely to affect more tissues than the target organs for the study. Thus in order to expand our study and make full use of the animals to avoid repeating treatments for further studies in future we would like to collect more organs and tissues at euthanasia. The organs that will be removed are going to be processed for H&E staining and light microscopy. These include Liver, heart, stomach, brain, spleen, adrenal glands, testes and epididymis.

Date: 21/07/2016 Signature:

RECOMMENDATIONS: Approved.
-Photography of organs and procedures (ensure that the photos are aesthetic and not of a nature that will bring the University into disrepute).
-Collection of additional organs as detailed above.

Date: 26th July 2016

Signature:

Chairman, AESC

7.4 Appendix 4: Feed analysis results

Analysis	Dry matter	Moisture	Ash	Fat (ether extraction)	Fibre (crude)	* Protein (N x 6.25)	Calcium	Phosphorous	Gross energy
Method Number	ASM 013	ASM 013	ASM 048	ASM 044	ASM 059	ASM 078	ASM 042	ASM 045	ASM 053
Unit	%	%	%	%	%	%	%	%	MJ/kg
Sample Number									
1 : Concentrate feed	91.11	8.89	6.99	3.34	2.60	21.19	1.32	0.62	16.40

Sample	Sample type	Date analysis commenced
1	Animal feed (unspecified)	29/04/2016

* For the conversion of nitrogen content to protein content the factor 6.25 was used.

TEST REPORT 2016-F-355

This laboratory holds SANAS accreditation for analyses with an ASM number.
Results are expressed on a wet basis, therefore as samples were received.

Analysis	Method Number	Unit	Sample Number 1 : Cassava : Casfeed 5:1	Sample Number 2 : Cassava : Casfeed 6:1
Dry matter	ASM 013	%	92.94	92.78
Moisture	ASM 013	%	7.06	7.22
Ash	ASM 048	%	3.39	3.35
*Protein (N x 6.25)	ASM 078	%	6.42	5.57
Fat (ether extraction)	ASM 044	%	6.49	3.25
Fibre (crude)	ASM 059	%	3.70	3.74
Calcium	ASM 042	%	3.41	2.95
Phosphorous	ASM 045	%	0.16	0.15

Sample	Sample type	Date analysis commenced
1-2	Animal feed (unspecified)	19/10/2016

* For the conversion of nitrogen content to protein content the factor 6.25 was used.

UNIVERSITY OF THE FREE STATE
UNIVERSITEIT VAN DIE VRYSTAAT
YUNIVESITHI YA FREISTATA
UFS·UV
NATURAL AND AGRICULTURAL SCIENCES
NATUUR- EN LANDBOUWETENSKAPPE
Department of Animal, Wildlife and Grassland Sciences

Nyirenda, Trust

MSc Medicine Student
School of Anatomical Sciences, Faculty of Health Sciences,
University of the Witwatersrand

RESULTS

VAT No :

30-10-2017

The following samples were analysed :

Client	DM	OM	CP	GE	NDF	ADF	ADL	Fat
Sample	g / kg sample	g / kg DM	g / kg DM	MJ / kg DM	g / kg DM	g / kg DM	g / kg DM	g / kg DM
Cas Feed 1:6	934.35	949.18	58.65	15.97	152.30	51.38		7.35
Cas Feed	928.47	909.88	243.13	16.76	146.40	63.86		23.83

Please note that the information are not for commercial or advertising purposes.

Please contact us for any further enquiries.

Kind regards

* DM = droë materiaal / dry matter; OM = organiese materiaal / organic matter; RP/CP = ruproteïen / crude protein; BE/GE = bruto energie / gross energy; NBV/NDF = neutraalbestande vesel / neutral-detergent fibre; SBV/ADF = suurbestande vesel / acid-detergent fibre; SBL/ADL = suurbestande lignien / acid-detergent lignin; Minerale / Minerals (Ca,Mg,Na,K,P,pH)

205 Nelson Mandela Drive/Rylaan, Park West/Parkwes, Bloemfontein 9301, South Africa/Suid-Afrika
P.O. Box/Posbus 339, Bloemfontein 9300, South Africa/Suid-Afrika,
Tel : 051-4019712, E-Pos/E-mail : vandermerwejam@ufs.ac.za

7.5 Appendix 5: Recipes

A. Schedule for the Citadel 1000 automatic tissue processor

A. 70% Alcohol	1h30min x 1 change
B. 95% Alcohol	1h30min x 3 changes
C. Absolute Alcohol	1h30min x 3 changes
D. Chloroform	1h30min x 2 changes
E. Waxing	2h x 2 changes

B. Dewaxing and Hydration of paraffin wax sections

A. Place the slides required into staining rack.	
B. Immerse slides in xylene	5min x 2 changes
C. Transfer to absolute alcohol	10 dips x 2 changes
D. Transfer to 95% alcohol	10 dips x 2 changes
E. Transfer to 70% alcohol	10 dips x 1 change
F. Rinse in running water	

C. Dehydration of the sections

A. After staining the sections	
B. Immerse in 70% alcohol	10 dips x 1 change
C. Transfer to 95% alcohol	10 dips x 2 changes
D. Transfer to absolute alcohol	10 dips x 2 changes
E. Transfer to xylene	30 sec x 2 changes
F. Mount and coverslip with Entellen®	

D. Mayer's Haematoxylin and Eosin staining technique

A. Dewax and hydrate the sections
B. Stain in Mayer's Haematoxylin 5min
C. Wash in running water 5min
D. Differentiate with 1% acid alcohol 2-3 dips
E. Wash in running water 5min
F. Counterstain in Eosin 30sec
G. Wash briefly in running water
H. Dehydrate, clear in xylene, mount and coverslip

Haematoxylin solution (1000ml)

Haematoxylin	4g
Distilled water	1000ml
Sodium Iodate	0.3g
Potassium Alum	50g
Citric Acid	1.5g
Chloral Hydrate	75g

Eosin solution (1000ml)

Stock Eosin	250ml
Calcium chloride	20g
Distilled water	750ml

Stock Eosin (1000ml)

Eosin Y	8g
Erythrocin	2g
Distilled water	1000ml

E. Masson's trichrome staining technique

A. Dewax and hydrate sections
B. Stain in Celestine blue 5min
C. Rinse in distilled water
D. Stain in Mayer's Haematoxylin 5min
E. Wash in running water 5min
F. Differentiate with 1% acid alcohol 3 dips
G. Wash in running water 5min
H. Stain in acid fuchsin 5min
I. Rinse in distilled water
J. Treat with phosphomolybdic acid 5min
K. Drain sections
L. Stain with light green 5min
M. Rinse in distilled water
N. Treat with 1% acetic acid 2min
O. Dehydrate, clear in xylene, mount and coverslip

Celestin blue solution (100ml)

5% ammonium ferric sulphate	100ml
Celestin Blue (CI 51050)	0.5g

Boil for 3min, filter when cool and store refrigerated

Acid fuchsin solution (100ml)

Acid fuchsin	0.5g
Glacial acetic acid	0.5ml
Distilled water	100ml

Phosphomolybdic acid solution (100ml)

Phosphomolybdic acid	1g
Distilled water	100ml

Light green solution (100ml)

Light green	2g
Glacial acetic acid	2.5ml
Distilled water	100ml

F. Immunofluorescence of paraffin section for AQP2 channel

A. Dewax and hydrate the sections
B. Heat antigen retrieval in citrate buffer pH 6 10 min
C. Allow to cool at room temperature 20 min
D. Wash in PBS/0.2% Triton-X 100 5 min x 3 changes
E. Block with 10% normal goat serum 1 hour at room temp.
F. Incubate with primary antibody in humid chamber 1:1000 dilution overnight at 4^0C
G. Wash in PBS 5 min x 3 changes
H. Incubate with secondary antibody in the dark room 1:500 dilution 1h at room temp.
I. Wash in PBS 5 min x 3 changes
J. Mount with fluoromount® and store in the dark at 4^0C until viewing

Citrate buffer solution pH 6.0 with 0.05% tween 20 (1000ml)

Tri-sodium citrate di-hydrate	2.9g
Distilled water	1000ml
Adjust pH to 6.0	
Tween 20	0.5ml

1M Phosphate buffer solution (PBS) pH 7.4 (2000ml)

Sodium chloride	16g
di-Sodium hydrogen phosphate	3.5g
Potassium chloride	0.4g
Potassium di-hydrogen phosphate	0.4g
Distilled water	2000ml

Antibody diluent (100ml)

PBS	100ml
Triton X 100	0.2ml

G. Gelatin coated slides

A. Heat distilled water to 60^0C and dissolve gelatine
B. Stir in chromium potassium sulphate
C. Allow to cool (40-50^0C) and dip racks of slides into it
D. Drain slides and allow to dry overnight at 42^0C in an incubator

Chrome alum gelatin solution (500ml)

Gelatin	1.5g
Chromium potassium sulphate	0.25g
Distilled water	500ml

H. Silane coated slides

A. Immerse racks of slide in 2% APES	30min x 1 change
B. Rinse in acetone	10 dips x 2 changes
C. Rinse in distilled water	10 dips x 1 change
D. Dry overnight at 37^0C in an incubator	

2% aminopropyltriethoxysilane (APES) in acetone solution (100ml)

Aminopropyltriethoxysilane	2ml
Acetone	98ml

I. 10% neutral buffered formalin solution (100ml)

Distilled water	90ml
Formaldehyde 37-40%	10ml
Sodium di-hydrogen phosphate	0.35g
Di-sodium hydrogen phosphate	0.65g

7.6 Appendix 6: Methodology

A. Representative photograph of the metabolic cages

This figure represents the method of 24-hour urine collection using metabolic cages. It shows the metabolic cages with rats in situ and urine collected. Photo: Abdurrahman Abdulkadir.

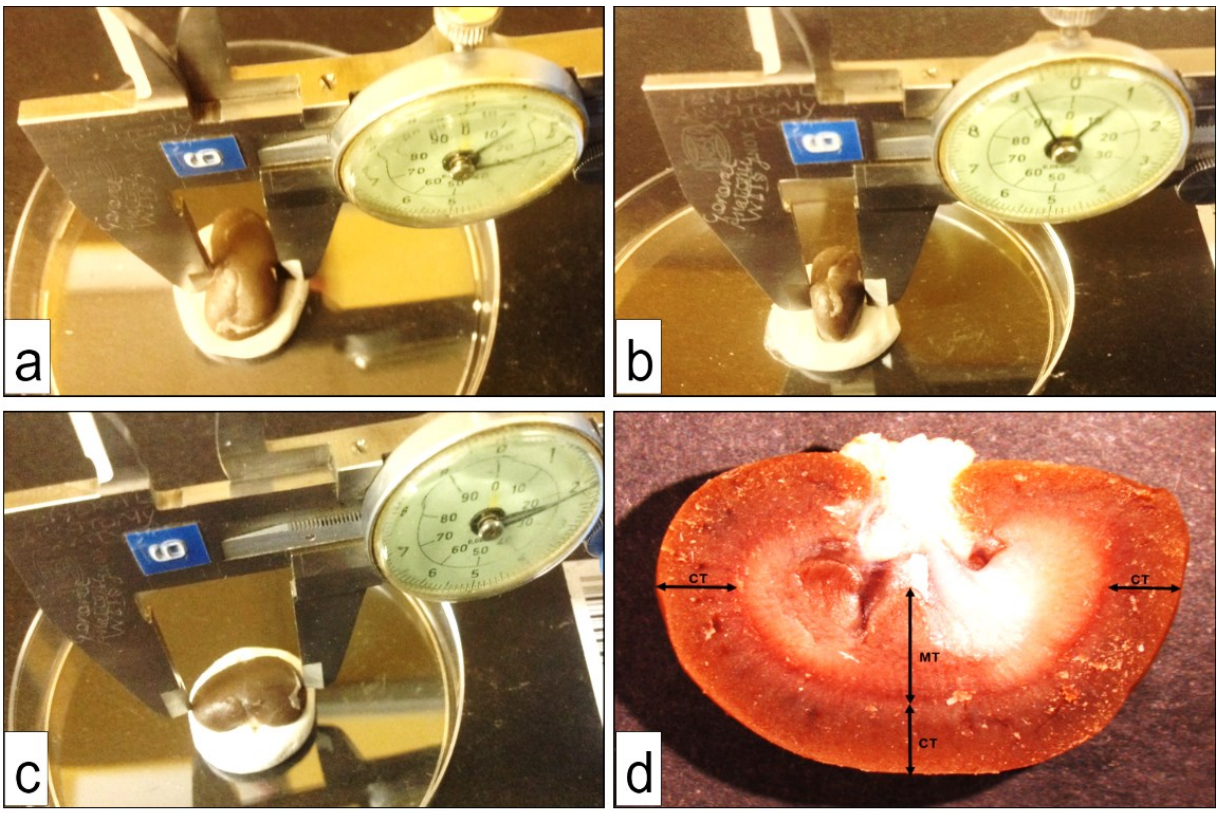

B. Photographs of the methods of RMT measurements

This figure shows the methods for measurement of (a) width, (b) thickness and (c) length of the kidney using the dial vernier calliper. The black arrows on the (d) illustrate the measurement of cortical thickness (CT) and medullary thickness (MT) using ImageJ. Photo: Abdurrahman Abdulkadir.

7.7 Appendix 7: Supplementary data

Normality test – Shapiro wilk test

Shapiro wilk test	Terminal weight	Weight gain	Food consumption	1st urine volume	2nd urine volume	3rd urine volume	Basal weight	Creatinine	Urea
NPC	0.4031	0.9668	0.3237	0.3512	0.1786	0.9324	0.0139	0.4183	0.31549
NPQ	0.4755	0.9458	0.0243	0.6133	0.1026	0.1507	0.0744	0.4443	0.89651
NPE	0.4913	0.4457	0.1991	0.5028	0.9341	0.1112	0.4641	0.0152	0.06388
NPQE	0.9219	0.3779	0.3909	0.2415	0.1417	0.238	0.0469	0.4473	0.04424
LPC	0.4197	0.0686	0.381	0.1401	0.0101	0.0607	0.5486	0.6236	0.64391
LPQ	0.913	0.16	0.9588	0.6283	0.7113	0.9179	0.6579	0.6615	0.77060
LPE	0.0221	0.7566	0.5834	0.7676	0.0857	0.939	0.235	0.9272	0.45078
LPQE	0.2033	0.1912	0.2642	0.9906	0.6895	0.9333	0.6051	0.8991	0.61478

Shapiro wilk test	Kidney weight	Relative kidney weight	Relative medullary thickness	Cortical thickness	Kidney volume VGStudio	Kidney volume stereology	Glomerular count	Collagen area fraction
NPC	0.8798	0.0466	0.4061	0.0178	0.4133	0.4020	0.87137	0.99944
NPQ	0.0801	0.7568	0.2469	0.0616	0.7847	0.6764	0.80607	0.04097
NPE	0.0599	0.0898	0.9254	0.4661	0.6554	0.3763	0.94624	0.42307
NPQE	0.9073	0.5676	0.4761	0.1606	0.8033	0.9092	0.30564	0.08433
LPC	0.1657	0.6530	0.3800	0.6924	0.3136	0.3732	0.99755	0.9228
LPQ	0.1835	0.8613	0.6666	0.9049	0.7473	0.2938	0.94995	0.14207
LPE	0.7006	0.2131	0.3798	0.9464	0.0125	0.1142	0.03309	0.20623
LPQE	0.0016	0.7001	0.5505	0.8671	0.2101	0.8794	0.45039	0.20967

Shapiro wilk test	Glomerular diameter	Renal corpuscle diameter	Bowman's space diameter	Distal convoluted tubule diameter	Proximal convoluted tubule diameter	Distal convoluted tubule epithelial height	Proximal convoluted tubule epithelial height
NPC	0.0000	0.0000	0.0139	0.1027	0.4702	0.0061	0.8291
NPQ	0.1389	0.2330	0.0014	0.0340	0.9022	0.0183	0.7121
NPE	0.0000	0.0000	0.0000	0.0559	0.6110	0.0006	0.9996
NPQE	0.0113	0.0005	0.0025	0.1198	0.7844	0.5315	0.9919
LPC	0.8320	0.8222	0.0014	0.7545	0.7698	0.0319	0.0045
LPQ	0.0001	0.0005	0.7720	0.0000	0.0000	0.0000	0.0073
LPE	0.1883	0.0421	0.0241	0.4060	0.7672	0.3625	0.0908
LPQE	0.7365	0.9598	0.0667	0.7908	0.7304	0.5149	0.0005

One-way ANOVA and Kruskal Wallis tests

	One-way ANOVA	**p-value**
1	Total weight gain	0.00001
2	1st urine volume	0.0003
3	3rd Urine volume	0.00001
4	Relative medullary thickness	0.2712
5	Kidney volume using stereology	0.00001
6	Kidney size	0.00001
7	Absolute medullary thickness	0.0033

	Kruskal-Wallis test	**p-value**
1	Cortical thickness	0.0004
2	Food consumption	0.4618
3	2nd Urine volume	0.0001
4	Terminal mass	0.0001
5	Basal weight	0.4365
6	Relative kidney weight	0.0208
7	Kidney weight	0.0001
8	Kidney volume using VGStudio	0.0001
9	Glomerular diameter	0.4612
10	Renal corpuscle diameter	0.0288
11	Urinary space diameter	0.0001
12	Glomerular count	0.0195
13	Distal convoluted tubule diameter	0.0001
14	Proximal convoluted tubule diameter	0.0001
15	Proximal tubule epithelial height	0.2172
16	Distal tubule epithelial height	0.3284
17	Collagen area fraction	0.2099
18	Urea	0.0001
19	Creatinine	0.0559

Pairwise mean comparison – Bonferroni

Weight gain	NPC	NPQ	NPE	NPQE	LPC	LPQ	LPE
NPQ	1.000						
NPE	1.000	1.000					
NPQE	1.000	1.000	1.000				
LPC	0.000	0.000	0.000	0.000			
LPQ	0.000	0.000	0.000	0.000	1.000		
LPE	0.000	0.000	0.000	0.000	1.000	1.000	
LPQE	0.000	0.000	0.000	0.000	1.000	1.000	1.000

1st Urine volume	NPC	NPQ	NPE	NPQE	LPC	LPQ	LPE
NPQ	1.000						
NPE	1.000	1.000					
NPQE	1.000	1.000	1.000				
LPC	0.122	0.013	0.010	0.755			
LPQ	0.281	0.033	0.025	1.000	1.000		
LPE	1.000	0.405	0.326	1.000	1.000	1.000	
LPQE	0.575	0.075	0.059	1.000	1.000	1.000	1.000

3rd Urine volume	NPC	NPQ	NPE	NPQE	LPC	LPQ	LPE
NPQ	1.000						
NPE	1.000	1.000					
NPQE	0.081	0.003	0.341				
LPC	0.000	0.000	0.001	1.000			
LPQ	0.009	0.002	0.045	1.000	1.000		
LPE	0.000	0.000	0.000	0.009	1.000	0.081	
LPQE	0.000	0.000	0.000	0.005	1.000	0.045	1.000

Kidney volume stereology	NPC	NPQ	NPE	NPQE	LPC	LPQ	LPE
NPQ	1.000						
NPE	1.000	1.000					
NPQE	1.000	1.000	1.000				
LPC	0.001	0.000	0.000	0.000			
LPQ	0.001	0.000	0.000	0.000	1.000		
LPE	0.000	0.000	0.000	0.000	1.000	1.000	
LPQE	0.000	0.000	0.000	0.000	1.000	1.000	1.000

Pairwise mean comparison – Dunns

Cortical thickness	NPC	NPQ	NPE	NPQE	LPC	LPQ	LPE
NPQ	0.4786						
NPE	0.4946	0.4732					
NPQE	0.3264	0.3073	0.3313				
LPC	0.0108	0.0112	0.0112	0.0324			
LPQ	0.0027	0.0023	0.0028	0.0097	0.3120		
LPE	0.0016	0.0014	0.0017	0.0064	0.2596	0.4386	
LPQE	0.0058	0.0050	0.0060	0.0190	0.4097	0.3967	0.3386

2nd Urine volume	NPC	NPQ	NPE	NPQE	LPC	LPQ	LPE
NPQ	0.4652						
NPE	0.3608	0.3286					
NPQE	0.0512	0.061	0.0233				
LPC	0.0045	0.0057	0.0015	0.1632			
LPQ	0.0067	0.0085	0.0023	0.2003	0.4439		
LPE	0.00001	0.00001	0.00001	0.0085	0.08	0.061	
LPQE	0.0001	0.0001	0.00001	0.0122	0.1019	0.079	0.4465

Terminal weight	NPC	NPQ	NPE	NPQE	LPC	LPQ	LPE
NPQ	0.2684						
NPE	0.2445	0.4706					
NPQE	0.4123	0.3460	0.3192				
LPC	0.0014	0.0002	0.0001	0.0007			
LPQ	0.0020	0.0002	0.0002	0.0010	0.4599		
LPE	0.0004	0.0000	0.0000	0.0002	0.3635	0.3264	
LPQE	0.0017	0.0002	0.0002	0.0008	0.4759	0.4839	0.3410

Kidney weight	NPC	NPQ	NPE	NPQE	LPC	LPQ	LPE
NPQ	0.4492						
NPE	0.4813	0.4679					
NPQE	0.4202	0.4706	0.4386				
LPC	0.0003	0.0002	0.0003	0.0002			
LPQ	0.0005	0.0003	0.0004	0.0002	0.4626		
LPE	0.0000	0.0000	0.0000	0.0000	0.2864	0.2553	
LPQE	0.0038	0.0026	0.0033	0.0020	0.2301	0.2596	0.0964

Relative kidney weight	NPC	NPQ	NPE	NPQE	LPC	LPQ	LPE
NPQ	0.3535						
NPE	0.3049	0.4466					
NPQE	0.4519	0.3097	0.264				
LPC	0.0158	0.0382	0.0507	0.0116			
LPQ	0.0125	0.031	0.0416	0.0091	0.4626		
LPE	0.0048	0.0134	0.0187	0.0033	0.3288	0.3635	
LPQE	0.1988	0.3192	0.3686	0.1668	0.0964	0.0813	0.0404

Kidney volume VGStudio	NPC	NPQ	NPE	NPQE	LPC	LPQ	LPE
NPQ	0.2667						
NPE	0.4029	0.3531					
NPQE	0.4935	0.2614	0.3966				
LPC	0.0096	0.0015	0.0048	0.0100			
LPQ	0.0084	0.0013	0.0042	0.0087	0.4804		
LPE	0.0008	0.0001	0.0003	0.0009	0.2110	0.2255	
LPQE	0.0031	0.0004	0.0014	0.0033	0.3471	0.3654	0.3410

Urea	NPC	NPQ	NPE	NPQE	LPC	LPQ	LPE
NPQ	0.4838						
NPE	0.4409	0.4569					
NPQE	0.4677	0.4516	0.4091				
LPC	0.0020	0.0023	0.0031	0.0015			
LPQ	0.0001	0.0002	0.0002	0.0001	0.2244		
LPE	0.0128	0.0142	0.0186	0.0104	0.2581	0.0797	
LPQE	0.0147	0.0163	0.0212	0.0119	0.2409	0.0720	0.4784

Creatinine	NPC	NPQ	NPE	NPQE	LPC	LPQ	LPE
NPQ	0.2399						
NPE	0.0485	0.1702					
NPQE	0.0916	0.2661	0.3712				
LPC	0.0025	0.0181	0.1267	0.0707			
LPQ	0.1014	0.2854	0.3497	0.4771	0.0632		
LPE	0.0133	0.0653	0.2882	0.1874	0.2798	0.1723	
LPQE	0.0024	0.0170	0.1216	0.0674	0.4902	0.0602	0.2716

Bowman's space diameter	NPC	NPQ	NPE	NPQE	LPC	LPQ	LPE
NPQ	0.0000						
NPE	0.0001	0.0200					
NPQE	0.0014	0.0036	0.2640				
LPC	0.0000	0.3956	0.0368	0.0077			
LPQ	0.0000	0.3855	0.0095	0.0015	0.2892		
LPE	0.0000	0.0220	0.0000	0.0000	0.0113	0.0424	
LPQE	0.0000	0.0107	0.0000	0.0000	0.0052	0.0223	0.3878

Renal corpuscle diameter	NPC	NPQ	NPE	NPQE	LPC	LPQ	LPE
NPQ	0.1577						
NPE	0.4702	0.1404					
NPQE	0.2945	0.3214	0.2693				
LPC	0.4487	0.1908	0.4193	0.3405			
LPQ	0.0099	0.0924	0.0081	0.0368	0.0139		
LPE	0.0253	0.1707	0.0212	0.0785	0.0339	0.3540	
LPQE	0.0077	0.0781	0.0063	0.0299	0.0109	0.4633	0.3203

Proximal tubule diameter	NPC	NPQ	NPE	NPQE	LPC	LPQ	LPE
NPQ	0.0766						
NPE	0.0699	0.4805					
NPQE	0.0152	0.2309	0.2460				
LPC	0.4569	0.0622	0.0565	0.0115			
LPQ	0.0916	0.0029	0.0025	0.0002	0.1107		
LPE	0.1379	0.0059	0.0051	0.0006	0.1631	0.4048	
LPQE	0.0224	0.0003	0.0002	0.0000	0.0288	0.2494	0.1795

Distal tubule diameter	NPC	NPQ	NPE	NPQE	LPC	LPQ	LPE
NPQ	0.4750						
NPE	0.1986	0.2165					
NPQE	0.3457	0.3229	0.1068				
LPC	0.0007	0.0006	0.0000	0.0026			
LPQ	0.0000	0.0000	0.0000	0.0000	0.0462		
LPE	0.0000	0.0000	0.0000	0.0001	0.1384	0.2758	
LPQE	0.0000	0.0000	0.0000	0.0000	0.0059	0.2023	0.0765

Glomerular Count	NPC	NPQ	NPE	NPQE	LPC	LPQ	LPE
NPQ	0.0351						
NPE	0.1226	0.2582					
NPQE	0.0394	0.4788	0.2757				
LPC	0.0469	0.4461	0.3039	0.4672			
LPQ	0.0002	0.0419	0.0087	0.0374	0.0311		
LPE	0.0022	0.1489	0.0455	0.1369	0.1197	0.2459	
LPQE	0.0035	0.1878	0.0624	0.1738	0.1535	0.1997	0.4384

Chemicals used in the experiment

S/No	Chemical	Manufacturer
1	Haematoxylin	Merck, Germany
2	Sodium Iodate	BDH chemicals, England
3	Potassium alum	ACE, South Africa
4	Citric acid	Reidel-De haen, Germany
5	Calcium chloride	Reidel-De haen, Germany
6	Eosin Y	Merck, Germany
7	Erythrocin	Merck, Germany
8	Ammonium ferric sulphate	Merck, Germany
9	Acid fuchsin	Merck, Germany
10	Glacial acetic acid	ACE, South Africa
11	Phosphomolybdic acid	Merck, Germany
12	Light green	BDH chemicals, England
13	Tri-sodium citrate di-hydrate	ACE, South Africa
14	Tween 20	Merck, Germany
15	Sodium chloride	ACE, South Africa
16	di-Sodium hydrogen phosphate	ACE, South Africa
17	Potassium chloride	ACE, South Africa
18	Potassium di-hydrogen phosphate	ACE, South Africa
19	Triton X-100	Sigma Aldrich, USA
20	Gelatine	Hopkin &Williams, England
21	Chromium potassium sulphate	BDH chemicals, England
22	Formaldehyde 37-40%	ACE, South Africa
23	Sodium di-hydrogen phosphate	ACE, South Africa